POLYMERIZATON OF POLAR MONOMERS VIA DIMETHYL ZIRCONOCENES AND TRIS(PENTAFLUOROPHENYL)BORANE

by

Jun Wang

A dissertation submitted to the Graduate Faculty in Chemistry in partial fulfillment of the requirements for the degree of Doctor of Philosophy, The City University of New York

2003

This manuscript has been read and accepted for the Graduate Faculty in Chemistry in satisfaction of the dissertation requirement for the degree of Doctor of Philosophy.

1/27/2003 George Odian

Date Chair of Examining Committee

1/28/2003 Gerald Koppel

Date Executive Officer

Professor William F. Berkowitz William F Berkowitz

Professor George Odian George Odian

Professor Howard Haubenstock Howard Haubenstock

Supervisory Committee

Abstract

POLYMERIZATON OF POLAR MONOMERS VIA DIMETHYL ZIRCONOCENES AND TRIS(PENTAFLUOROPHENYL)BORANE

by

Jun Wang

Advisers: Professor George Odian, Professor Howard Haubenstock

Group 4 metallocene initiation systems were discovered for efficient polymerization of methyl methacrylate (MMA). The initiation systems consisted of a dimethyl zirconocene (initiator) and $B(C_6F_5)_3$ (coinitiator). The molar ratio of the dimethyl zirconocene to $B(C_6F_5)_3$ was found crucial for efficient polymerization. Instead of a slow polymerization (or no polymerization) with a 1:1 molar ratio, a 2:1 molar ratio gave a 20-fold (or more) rate increase. The quantitative conversion of MMA was obtained in less than 1 h. A further increase of the molar ratio did not result in additional acceleration. Two representative initiation systems, in which Cp_2ZrMe_2 (**1**) and *rac*-$Me_2Si(IndH_4)_2ZrMe_2$ (**2**) were used as the initiator respectively, were prepared. The kinetics, stereochemical control, and living characteristics of these polymerization systems were studied. System 2, in which **2** was used, produced a living polymerization: the continuation of polymerization after the addition of a second batch of monomer, a narrow molecular weight distribution (MWD) throughout the whole polymerization ($\bar{M}_w/\bar{M}_n$ = 1.2) and a linear increase of $\bar{M}_n$ versus conversion in both the first and second

polymerization batches were obtained. Highly isotactic ([rr] ≥ 88%) polymer was produced and an enantiomorphic site-control mechanism for the chain propagation was shown by ^{13}C. However, System 1, in which **1** was used, showed a chain termination (or transfer) process and new active species were generated during the polymerization. Moderately syndiotactic polymer ([rr] = 55%) was obtained. The chain propagation followed neither an enantiomorphic site-control mechanism nor a chain-end control mechanism. The kinetics of these two systems were also different. For System 2, the polymerization rate was first order in the monomer concentration and second order in the initiation system; while for System 1, they were zero order and third order respectively. A mechanism is proposed to accommodate the kinetic results and the ratio effect.

In addition, preliminary experiments for polymerization of methyl acrylate, 1-hexene, ε-caprolactone, propylene oxide, vinyl acetate and copolymerization of MMA with ε-caprolactone, MMA with 1-pentene were also performed.

Acknowledgments

I wish to express my appreciation to the many people who aided me in completing this thesis. This thesis and the research work in it were completed under the guidance of my mentors: Professor George Odian and Professor Howard Haubenstock. I am grateful to the time and effort they gave to direct me through the past five years on how to accomplish the scientific research work. Their advice to me and their philosophy of science will always accompany me. Helpful suggestions on the research direction of the thesis from the thesis committee member, Professor William F. Berkowitz are gratefully acknowledged. I also appreciate Professor Berkowitz's time for reading my research reports, thesis and attending the committee meetings. Great help were obtained from Dr. Hsin Wang, the NMR manager at College of Staten Island. Dr. Wang's expertise on NMR improved the NMR work in this thesis and is sincerely appreciated. I also want to thank Mr. Tai Park, who helped me solve a lot of problems on computers and work stations, which saved me much time. The various helps from my fellow students in the Ph.D polymer program, Shiying Tian, Chong Cheng, Chang Xu and Yong Chen are also acknowledged. Last, but not least, I thank, from the bottom of my heart, my family for their patience, understanding and support.

I also thank the department of Chemistry, College of Staten Island for providing me teaching assistant position. The financial support from the PSC-BHE Research Program of the City University of New York is gratefully acknowledged as well.

Table of Contents:

List of Tables:

List of Schemes:

List of Figures:

1. Introduction

1.1 Metallocene Initiation Systems

Initiation systems containing the metallocenes of early transition metals, i.e., Group 3 and Group 4 metals, have been extensively studied. They are highly active for the polymerization of olefinic hydrocarbons and give good control of the stereochemistry of the polymers produced[1-5]. In general, an initiation system of Group 3 metals consists of only one component, the metallocene itself. An initiation system of Group 4 metals, however, contains two components, an initiator and a coinitiator. The initiator is the metallocene compound and the initiator is a strong Lewis acid that aids the formation of the real active polymerization species. In these two-component systems, the metallocenes are also sometimes called catalyst precursors. The active center for the polymerization formed from Group 3 metallocene is neutral, while the active center formed from Group 4 metallocene is cationic, which coordinates better with the nucleophilic moiety in the monomer, e.g., C=C double bonds, carbonyl groups in acrylates.

1.1.1 Metallocenes

1.1.1.1 Definition

Metallocenes have been developed for most transition metals. According to the definition in the book "Metallocenes, Synthesis, Reactivity, Applications", edited by Togni and Halterman[6], "a metallocene, strictly speaking, is a 'sandwiched' bis(cyclopentadienyl) metal derivative which is expressed by the formula $[M(\eta^5\text{-}C_5R_5)_2]$. However, it is currently accepted to designate as metallocenes also compounds containing, for instance, other ligands, e.g., the so-called bent metallocenes, such as Cp_2WH_2; or complexes in which one of the Cp fragments has been replaced by an

anionic ligand fulfilling similar coordination-chemical purposes", the so-called "half-sandwiched" metallocenes, such as $CpZrCl_3$.

In the area of polymerization, studies of metallocenes have been mostly focused on the Group 3 and Group 4 metals, especially the Group 4 metals, i.e. titanium (Ti), zirconium (Zr) and hafnium (Hf). The concept of cyclopentadienyl ligand has been extended to include, besides Cp, some cyclopentadienes with additional fused, such as indenyl (Ind) and fluorenyl (Flu). All these ligands have their 5-membered rings coordinated to the metal center through a π-bond with the hapticity (a value indicating that how many elements in a species coordinate to metal) of 5 (η^5). The upper and lower rings (if there are two) can be connected by some short bridging groups, e.g. Me_2Si=, Me_2C=, or $-CH_2CH_2-$ groups, forming the bridged or ansa-metallocenes. Scheme 1 shows the general topological structure of the metallocenes used in this area.

Scheme 1

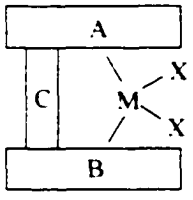

A: η^5-carbocyclic π-ligand, such as Cp, Ind, Flu;

B: a structure of A (sandwiched structure) or other single functional groups, such as amine, halogen, alkyl, etc. (half-sandwiched structure).

C: an optional bridge, e.g. $-Me_2Si-$, $-Me_2C-$, or $-CH_2CH_2-$.

M: transition metal

X: hydrogen, halogen, alkyl, alkoxy, etc

1.1.1.2 Variations and Properties of Metallocenes.

Though the general structure of the metallocenes is shown in Scheme 1, the variations possible are very large; the parameters of the metallocene structure that can be changed are listed as follows:

1.1.1.2.1 π-Ligands Variations

The most-used π-ligands are of three general types, as shown in Scheme 2.

Scheme 2

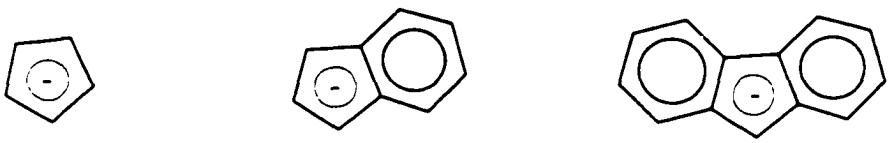

Cyclopentadienyl (Cp) | Indenyl (Ind) | Fluorenyl (Flu)

Besides these basic forms, several substituted forms of each type are also used in the metallocene initiation systems. The most-used substituted forms are shown in Scheme 3.

Scheme 3

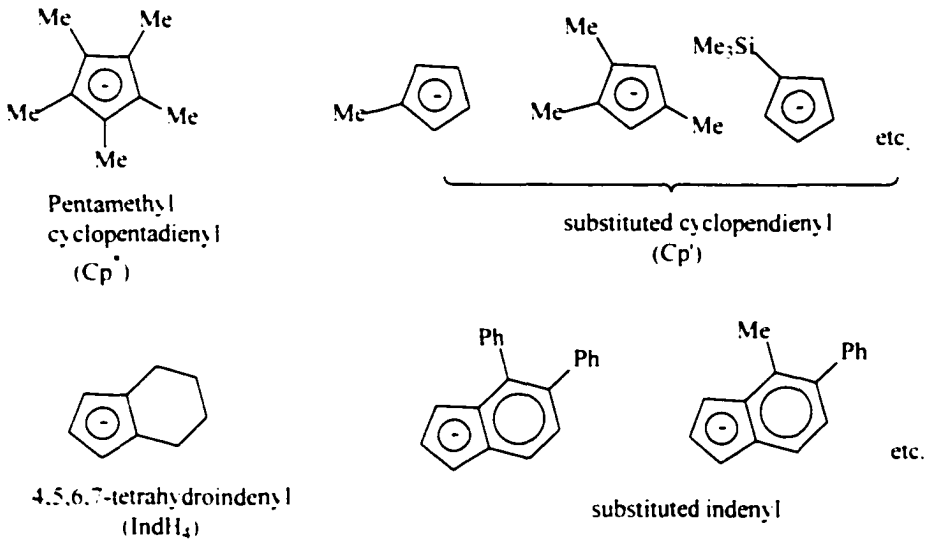

Some general trends exist in the variation of these π-ligands.

- All of these π-ligands form the metallocenes with higher stability than those of the organometallic compounds with merely metal-carbon bonds. This is due to the coordination of the π-ligands to the central metal, which delocalizes the electron density; and the bulky size of Cp around the central metal, which sterically shields the central metal from being attacked.
- Ind type ligands stabilize the central metal more than Cp type ligands do. This is because Ind has longer conjugated bonds, which delocalizes the electron density further, and a larger size, which provides more steric shielding, than Cp.
- Alkyl substitution stabilizes metallocenes.

  In general, substitution of methyls for hydrogens on the cyclopentadienyl ligand results in a significant electronic effect. For example, the substitution of two pentamethylcyclopentadienyl (Cp^*) groups for the cyclopentadienyl (Cp) ligands is approximately equivalent to a one-electron reduction of the complexed metal, which is due to:

  - The inductive and hyperconjugation effects of the methyl group toward the central metal.
  - The increased steric shielding of the coordination space around the central metal.

  The trialkylsilyl group was found to be slightly more electron-donating than methyl
- The substituents on the π-ligands also have effects on the coordination-gap aperture (the largest possible angle spanned by two ring planes through the metal center in a bent metallocene) of the metallocenes, which is shown as angle α and

β in the examples of Scheme 4. The substitution lowers the coordination-gap apertures, which will affect the insertion mode of the growing chain.

Scheme 4

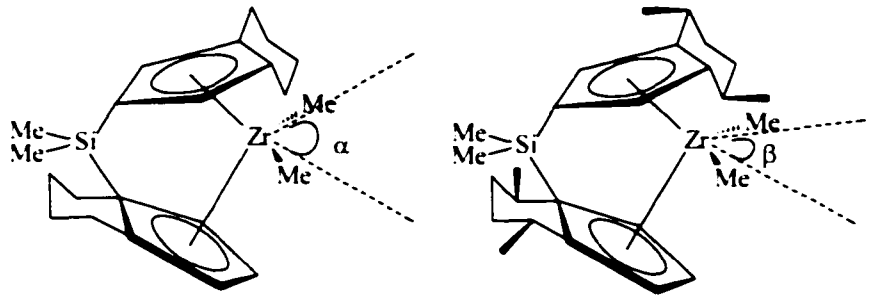

α, β are coordination-gap apertures

1.1.1.2.2 "Sandwich" and "Half-sandwich" Variation:

Originally, only the sandwiched metallocenes were studied as the initiator for the olefin polymerizations. Recently, half-sandwiched metallocenes were also found active to the polymerization of olefins. A significant discovery was that half-sandwiched metallocenes, e.g. $CpTiCl_3$, when combined with a coinitiator, can produce syndiotactic polystyrene. Another reason for the study of half-sandwiched metallocenes is due to their different steric structure compared to the sandwiched counterparts. The bridged half-sandwich metallocenes, e.g. *ansa*-monocyclopentadienyl-amido (CpA, e.g., $Me_2SiCp(NBu^t)MCl_2$) are considered to have a more open initiator active site, which allows them to incorporate other olefins into polyethylene. The coordination sphere of the metal center of the initiator opens because of the lack of one Cp ring, and enables copolymerization of ethylene with common monomers such as propylene, butene, hexene, as well as sterically hindered α-olefins such as styrene and 4-vinylcyclohexene.

1.1.1.2.3 Bridged and Non-bridged Variation:

Without a bridge that connects the two π–ligands in a metallocene compound, each π–ligand is free to rotate around the axis passing through the center of its 5-member ring and the metal center. Therefore the active species formed by this metallocene do not have a unique steric conformation. Several possible special sites exist from which a monomer can insert into the M – P bond (M, the central metal; P, the polymer chain that already grows). Or a monomer can insert into the M – P bond with more than one possible orientation. Hence, chain growth process generally does not follow an enantiomorphic site-control mechanism (the stereoregularity of the polymer chain is controlled by the chirality of the metallocene initiator). In most cases, the chain growth in the polymerization system initialized by a non-bridged metallocene system follows a chain-end control mechanism: the stereoregularity of the polymer chain is controlled by the asymmetry of the last inserted monomer unit, and is caused by the steric hindrance between the monomer and the chain unit next to the growth site. However, in some special situations, when some spacious groups exist on the π–ligands of the metallocene compounds, the rotation around the axis passing through the center of π-ligand's 5-member ring and the metal center will be severely restricted by steric hindrance. Therefore only one or two special sites will be largely preferred, or only one or two monomer orientations will be preferred while insertion occurs. Under these circumstances, the restricted conformation of the metallocene may act as a template for the monomer insertion and consequently an enantiomorphic site-control mechanism is enforced. The polymer produced will have some controlled tacticity (isotacticity or syndiotacticity).

If a metallocene has a bridge connecting its two π–ligands, an *ansa*-metallocene, the rotation of its π–ligands is restricted. The structure of the metallocene is restrained and it may act as a template for the insertion of monomer, only allowing a restricted number of favorable monomer orientations to be taken at some well defined sites. This process generally facilitates an enantiomorphic site-control mechanism and the stereochemistry of the final polymer is well controlled. Generally, when a chiral *ansa*-metallocene with C_2-symmetry (i.e., the *racemic* form of the metallocene which has only a C_2 axis of symmetry, e.g., *rac*-$Me_2Si(Ind)_2ZrCl_2$) is used for the polymerization of α–olefins, isotactic polymers will be obtained.

1.1.1.2.4 Variation of the Bridging Moieties:

The major effect of the bridge moieties on the structure of the metallocenes is concerned with the coordination-gap aperture. A shorter bridge such as $-(CH_3)_2C-$ gives a more bent structure with an wider aperture, while a longer one, such as $-CH_2CH_2-$, puts less geometrical strain on the sandwiched structures.

Another change on the bridge involves the substitution of the hydrogen atoms in the ethanediyl ($-CH_2CH_2-$) or the methyl groups in the dimethylsilyl ($-SiMe_2-$) bridge by some groups with chiral centers. However, this effect is less pronounced compared to that of the substitutions occurred directly on the Cp or Ind moieties.

1.1.1.2.5 Variation of the Central Metals:

The widely studied metallocenes for the polymerization of olefins are mostly from Group 3 (including rare earth metals) and Group 4 metals. For Group 3 and rare earth metals, metallocenes of both scandium (Sc) and yttrium (Y) (both are Group 3 metals) have been found active toward the polymerization of olefins; metallocenes from lanthanoid series metals, such as Samarium (Sm), Ytterbium (Yb), Lutetium (Lu), show a

better polymerization capability and intensive work has been done to study these initiation systems.[7]

One big advantage for developing Group 4 metallocenes is that metals in this group are less expensive: Ti and Zr occur to the extent of 0.63% and 0.022% (which is roughly as abundant as carbon) in the lithosphere, respectively. They are two of the several least expensive transition metals along with Fe, Cu, Mn. Furthermore, since the metallocenes of Ti and Zr exhibit high activity and stereospecificity for the polymerization of olefins, immense research work has been carried out on their catalytic applications. Though Hf in this group has also been studied as a metallocene initiator, the main purpose of this research was for comparison with the other two elements. No practical interest has been paid to Hf due to its high cost. Comparing Ti and Zr, the titanocene initiators are unstable at conventional polymerization temperature (0 – 40 °C) because Ti (IV) is readily reduced to Ti (III), causing the reduction of the activity of the titanocene initiator. Hence, the so called "metallocene initiators" are mostly zirconocene derivatives.

1.1.2 Coinitiators

Metallocene initiation systems of Group 3 and Group 4 metals used for the polymerization of olefins are different in their composition. With the Group 3 metallocene initiation systems, the metallocenes themselves are the active species for the polymerizations; while with the Group 4 metallocene initiation systems, the coinitiators, which are strong Lewis acids, are needed for the formation of the active species.

1.1.2.1 Functions of the Coinitiator

In the olefin polymerizations via the metallocene initiation systems, the major function of the coinitiators is to break (or weaken) the M – C bond in the metallocenes and to abstract the anionic (or partially negative charged) moiety away from the cationic

(or partially cationic) metallocene species, which are believed to be the real active centers for the polymerizations. This process, which is shown in Scheme 5, is sometimes called the activation process[8,9] of the metallocenes. The cationic (or partially cationic) metallocene species thereby formed have the space and molecular orbitals that are necessary for the σ interaction from the incoming olefin monomers.

Scheme 5

initiator coinitiator active center

R is methyl in most cases.

When a dihalogenated metallocene, e.g. Cp_2ZrCl_2, is used instead of dimethyl metallocene, e.g Cp_2ZrMe_2, a methylation step before the above activation step is needed. Some coinitiators provide this function as well as the activation. An example of these coinitiators is methylaluminoxane (MAO) (see Section 1.1.2.3.1)

1.1.2.2 Requirements for the Coinitiators

In order to form the active sites for the polymerizations of the olefins, the following requirements for the coinitiators must be satisfied:

- Strong Lewis acid.

  In order to activate the Group 4 metallocenes, the coinitiators need to be adequately eletrophilic, and tend to abstract the methyl group from metallocene and form the cationic active centers.

- Sufficiently non-coordination to the cationic active centers

After the abstraction has taken place, cationic and anionic (or partially charged) species are formed. Competitive coordination to the (partially) cationic active species will occur with all kinds of the nucleophilic species in the system. These nucleophilic species include the (partially) anionic species, the solvent, and the monomer. Because in most cases, the polymerizations occur only in nonpolar solvents (e.g. toluene) or in bulk, competition from the solvent is minor. Therefore, in order to provide more chances for the monomer to coordinate with the (partially) cationic species, i.e., the active centers of the polymerization, it is crucial to make the (partially) anionic species less coordinative than the monomer. Otherwise, the (partially) cationic active centers would coordinate more preferably with the (partially) anionic species, whose major part is derived from the coinitiators, and the monomer's coordination to the active centers would be impeded. No polymerization would occur. An example of such a poor coinitiator is the borate salt (BPh_4^-). In earlier searching for coinitiators, trityl borate ($[Ph_3C]^+[BPh_4]^-$) was tried, since this compound can activate the dimethyl zirconocene readily due to the high electrophilicity of the $[Ph_3C]^+$. For example:

$$Cp_2ZrMe_2 + [Ph_3C]^+[BPh_4]^- \rightarrow [Cp_2ZrMe]^+[BPh_4]^- + [Me]^-[Ph_3C]^+$$

However, no polymerization of olefins was found, due to the reactions between BPh_4^- and the cationic center. Several such reactions are listed as follows:

- Metalation, in which a covalent bond is formed between the cationic metal part and BPh_4^-.
- Phenyl group transfer; in which a phenyl group is combined with the cationic metal, forming a covalent bond and a BPh_3 is released.

- Electron transfer: in which coordination of phenyl to cationic center exists, e.g., through hydrogen bonding.

Such coordinations are shown in Scheme 6.

Scheme 6

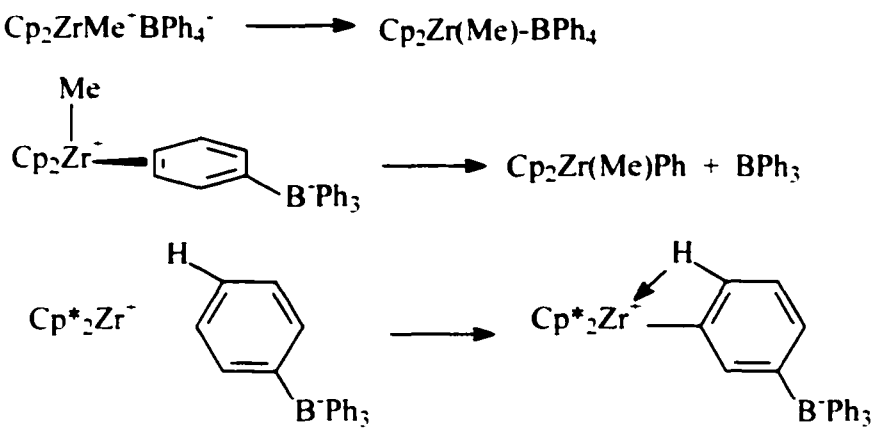

In addition BPh_4^- is susceptible to photochemical decomposition. All of these reactions limit the use of this anion and render it less than ideal for the application as a coinitiator for the polymerization of olefins.

In order to ensure the noncoordination requirement for the coinitiators, the following criteria must be used in designing an efficient coinitiator:

- The negative charge on the anionic species formed from the activation step (refer to Scheme 5) should be distributed over a great number of ligand atoms.
- The peripheral atoms should be fluorine or hydrogen atoms, fluorine is preferable. They should not be oxygen or chlorine atoms, which coordinate more strongly.

- Kinetic stability toward the ligand abstraction is needed. BF_4^- and PF_6^- are unstable toward electrophilic attack and will lose F^-.
- The anions should be stable toward oxidative attack. An element that is easily oxidized should not appear in the anions.

1.1.2.3 Commonly Used Coinitiators

The most commonly used coinitiators in the polymerization of olefins are: methylaluminoxane (MAO), $B(C_6F_5)_3$ and ammonium or trityl derivatives of $B(C_6F_5)_4^-$. A brief introduction to each of them is as follows.

1.1.2.3.1 MAO

MAO, a mixture of linear (**i**) and cyclic (**ii**) oligomeric compounds consisting of -Al(Me)-O- subunits, is perhaps the only practically used coinitiator in industry for the polymerization of olefins via metallocene initiation systems. Although MAO can be readily made from the controlled hydrolysis of $AlMe_3$, its detailed structure is not clearly known yet. A simple representative is a mixture of the one-dimensional linear chain (**i**) and cyclic rings (**ii**) as shown in Scheme 7.

Scheme 7

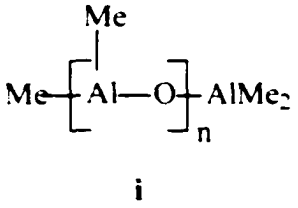

i

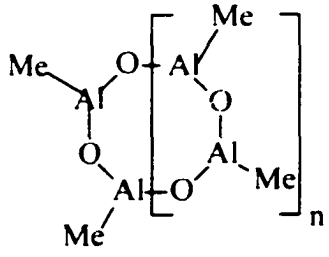

ii

$$Cp_2ZrCl_2 \xrightarrow{MAO} CpZrMe_2 \xrightarrow{MAO} CpZr^+Me\ (Me^-MAO)$$

Normally, MAO is used with a metallocene dihalide in a molar ratio of MAO/metallocene dichloride of several hundreds or thousands. MAO first methylates the metallocene dichloride and then activates it by abstracting one methyl group from the center (Scheme 7). The counter-ion containing the MAO moiety thus formed is sufficiently non-coordinative, therefore, polymerization of olefins can occur. A large excess of MAO is necessary.

1.1.2.3.2 $B(C_6F_5)_3$

$B(C_6F_5)_3$ was first synthesized by Massey et al in 1964.[10] However, it did not attract much attention until its application as a coinitiator for the polymerization of olefins had been found in the early 1990s. $B(C_6F_5)_3$ satisfies all of the aforementioned requirements for a coinitiator: 1) it is a strong Lewis acid, with an acidity higher than $AlCl_3$, and in between those of $SbCl_3$ and BCl_3;[9] 2) it forms a moderately non-coordinative species with methide (CH_3^-);[11] 3) the solubility of $B(C_6F_5)_3$ in common nonpolar solvents, e.g. toluene, is high, which makes homogeneous polymerization possible and study on the polymerization systems easier (compared with heterogeneous systems), and 4) it is quite stable; it won't decompose under the polymerization conditions. When reacted with equimolar amount of dimethyl zirconocene, it abstracts one methyl group from the metallocene and forms cationic zirconocene species. For example:

$$Cp_2ZrMe_2 + B(C_6F_5)_3 \rightarrow Cp_2Zr^+(Me)\ Me^-B(C_6F_5)_3$$

In addition, $B(C_6F_5)_3$ has several advantages over MAO, which makes it a better candidate for the coinitiator. First, $B(C_6F_5)_3$ is easily synthesized and has a clear single structure, which makes the characterization of the active species formed from it easy and free from interference. MAO, on the contrary, has a complicated structure and is not

clearly characterized. Therefore, an unambiguous characterization of the initiation system contain MAO is much harder, if not completely impossible. Second, when $B(C_6F_5)_3$ is used as the coinitiator, equimolar amounts of it and the metallocenes are sufficient for the formation of the active species. However, when MAO is used, a large excess of MAO is needed, which raises the cost of the polymerization and a more complicated work up procedure is necessary to deal with the high ash content (Al_2O_3) in the product polymer.

1.1.2.3.4 Derivatives of $B(C_6F_5)_4^-$

$B(C_6F_5)_4^-$ is a more non-coordinative species than $[CH_3B(C_6F_5)_3]^-$ formed from $B(C_6F_5)_3$. When it is combined with a powerful alkide-abstracting reagent, such as Ph_3C^+ or ammonium cations $HNRR'_2^+$, an efficient coinitiator is formed. This kind of coinitiator activates dimethyl metallocenes readily and yields highly an active initiation center for the polymerization for olefins. For example:

$$Cp_2ZrMe_2 + [Ph_3C]^+[B(C_6F_5)_4]^- \rightarrow Cp_2Zr^+(Me)\ B(C_6F_5)_4^- + MeCPh_3$$

However, the active complex of cationic metallocene species formed with $B(C_6F_5)_4^-$ exhibits poor thermal stability, which decreases the time in which it is capable of initiating polymerization. Moreover, this active complex is generally crystallizes poorly, and instead an oil form is often obtained. In addition, due to its ionic character, this complex has a low solubility in nonpolar solvents, and only a low concentration of the active center can be obtained in the polymerization system. Consequently, it would be easily destroyed by residual water or oxygen in the system when the system is not rigorously dried and deoxygenated. System containing derivatives of $B(C_6F_5)_4^-$ as coinitiators are generally less efficient as the polymerization initiation system than those containing $B(C_6F_5)_3$.

1.2 Metallocene Initiation Systems for Olefin Polymerizations

The metallocene catalysis era began in 1980s when Kaminsky et al [12] first discovered the highly efficient coinitiator MAO for the polymerization of ethylene with metallocenes. Since then a substantial amount of research has been directed to both the industrial application and the theoretical understanding of the metallocene initiation systems. Today, metallocene initiation systems have been used around the world to make 2 billion lb of polyethylene a year[13] and a rather clear picture for these systems has been obtained. In addition, the research interests in this area have been partially shifted to the polymerization of polar monomers and the copolymerizations of nonpolar olefins with polar monomers.

Although this thesis focuses on the polymerization of a polar monomer methyl methacrylate (MMA), a brief introduction to the metallocene initiation systems for olefin polymerizations will certainly help clarifying the basic concepts of these initiation systems, provide guidance for the research on polar monomers and help understand the polar monomer polymerizations better by comparison with the results of olefin polymerizations.

1.2.1 Advantages of Metallocene Initiation Systems for Olefin Polymerization

Metallocene initiation systems are superior to other initiation systems because of their high activity and unprecedented control of the polymerizations (and copolymerizations). By using metallocene initiation systems, polymer molecular weight and molecular weight distribution (MWD), comonomer distribution and content, and tacticity can be independently controlled. These advantages provide the possibility of

tailoring the polymer products for specific applications, which is a long-term goal in the field of polymer material science.

1.2.2 General Mechanism for the Polymerization

1.2.2.1 Formation of the Active Center and the Initialization of the Polymerization.

It is believed that the active center for the olefin polymerization via metallocene initiation systems is a single-site, "14-electron" species with 0 electrons in the outer d shell (d^0) of its central metal, as shown in Scheme 8.

This active center can be formed directly from Group 3 metallocenes, which are neutral species, or from Group 4 metallocenes. In the latter case, the active center is a cationic species, which is formed via the activation step (Scheme 5) with a Lewis acid

Scheme 8

Metallocene initiation center:

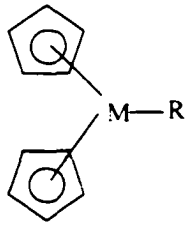

M = Sc, Y, Sm, Yb, Lu, etc

Group 3 and lanthanides

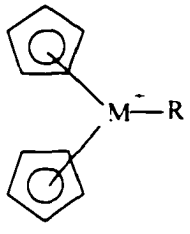

M = Ti, Zr, Hf

Group 4

present as coinitiator. The cationic active center of a Group 4 metallocene is an isolobal analogy to the neutral active center of a Group 3 metallocene. Once the active center is formed, the polymerization can then occur by insertion of the monomer unit into the M—Me bond.

In the following part of this section, the introduction will be focused mainly on

Group 4 metallocene initiation systems, because these are the systems that have been most studied from the literature and widely used in industry. However, to a large extend, the content presented there also applies to Group 3 systems.

1.2.2.2 Propagation Step.

Several possible mechanisms have been proposed for the insertion process in the propagation steps of the Ziegler polymerizations. However, to be more specific to the polymerization of the metallocene initiation system, only two mechanisms are considered relevant,[14] as shown in Scheme 9.

The three-center, two-electron covalent bond shown in the bottom mechanism in Scheme 9 is termed the "α-agostic interaction", which occurs when the hydrogen atom

Scheme 9.

Cossee-Arlman Mechanism (Direct insertion)

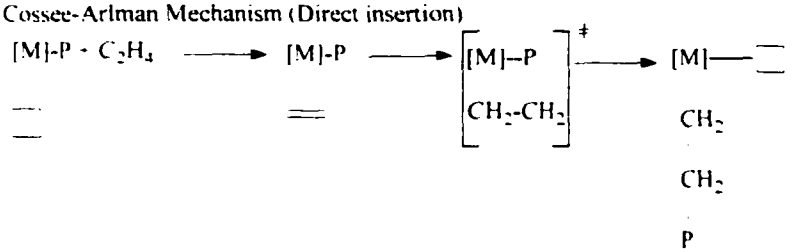

Transition State α-Agostic Mechanism

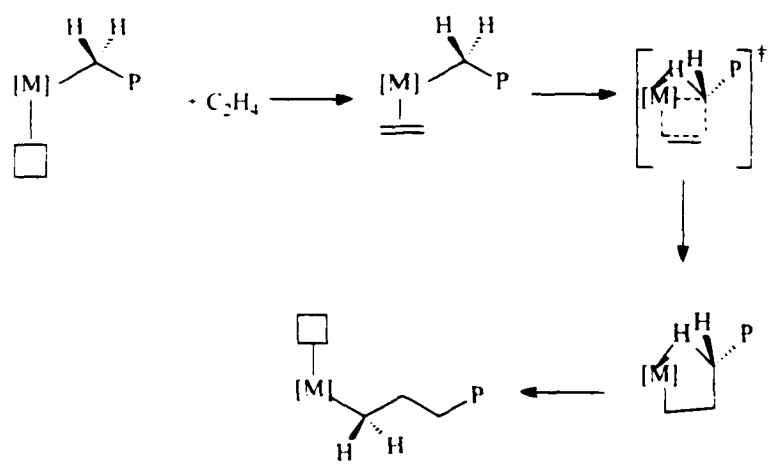

is simultaneously bonded to both a carbon and a metal atom. The common things for the two mechanisms are that both include two fundamental steps, 1)the coordination of the olefin molecule to the metal center involving one of its empty coordinating sites; 2) the insertion of the coordinated olefin molecule into the M—P bond, after which a new empty coordinating center is formed. The following coordination of the monomer will occur on this new site, followed by the insertion step which migrates the chain to this new site with release of the original empty coordination site. Therefore, the polymer chain increases by shifting alternately between these two sites. The different part of these two mechanisms is the transition state of the insertion. In the Cossee-Arlman Mechanism, the insertion occurs directly, while in the Transition State α-Agostic Mechanism, the insertion is aided by an α-agostic interaction, which acts like a hyperconjugation interaction that reduces the electron-deficiency of the metal and facilitates the concerted cyclic transition state of the insertion step. The α-agostic interaction is of particular interest since it might dramatically lower the activation barrier to olefin insertion and influence the stereochemical outcome of the olefin insertion step. In some metallocene initiation polymerization systems, the α-agostic interaction was discovered due to the existence of a secondary isotope effects in these systems. However, due to the lack of secondary isotope effects in some other metallocene initiation polymerization systems, the Cossee-Arlman Mechanism can not be totally ruled out, and therefore the two mechanisms are both taken as possible explanations for the propagation process in the polymerization of olefins via metallocene systems.

1.2.2.3 Termination (and Transfer) Step

The major chain breaking pathways for the growing chain in metallocene initiated polymerization are β-H elimination and β-CH_3 elimination (only for propylene polymerization, not for higher α-olefin polymerizations) shown in Scheme 10. β-H transfer to the coordinated olefin is another possible way of chain breaking, also shown in Scheme 10.

After the termination step, the polymer chains stop growing. However, the regenerated metal species may start growth of a new chain.

1.2.3 Control of the Polymerization

One big advantage of the metallocene initiation system for the polymerization of olefins is that a variety of controls on the polymerization can be carried out to tailor thefinal polymers. A brief introduction of these controls are given below.

Scheme 10

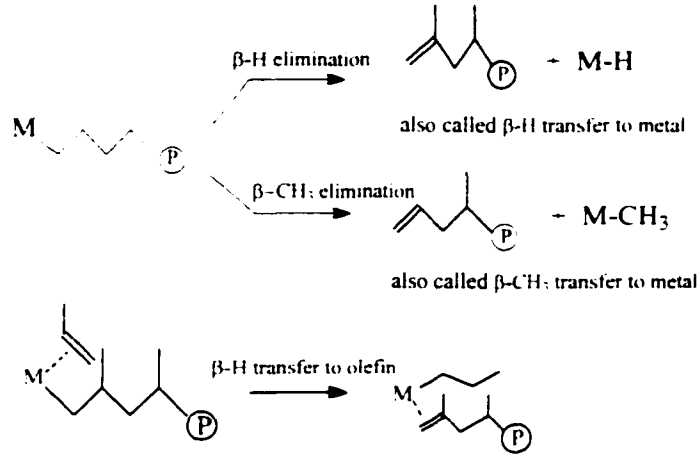

1.2.3.1 Control of the Initiation

The process of initiation is the step of forming the active center. It is a reaction between the initiator and the coinitiator. The parameters that affect the initiation include:

- The electron-deficiency on the metal atom in the metallocene.

  The more electron-deficient the metal atom, the more difficult it is for the coinitiator to abstract a methyl group away from it and therefore a coinitiator with a stronger Lewis acidity is necessary for the initiation. As mentioned before (section 1.1.1.2), the electron density on the metal atom can be adjusted by the substituents on the π-ligands in the metallocene. Both alkyl groups and fused aromatic groups on the Cp ring will enrich the electron density of the Cp and consequently increase the electron density on the metal atom through the coordination between the Cp and the metal and facilitate methyl abstraction.

- The steric accessibility of the alkyl group (R, generally the methyl group) on the metal.

  In the metallocene molecule, the metal atom is sandwiched between two relatively large π-ligands, which block out some of the space from which R can be accessed. For some π-ligands with large substituents, such as substituted Ind or Flu, the M—R moiety of the metallocene is almost completed enfolded by the π-ligands, which makes access to R from the coinitiator difficult. In this situation, only smaller sized coinitiators have the possibility of reaching the R group. Consequently, the relative sizes of the metallocene and the coinitiator is another parameter that can be adjusted to control the activation process of the metallocene.

- The distance between the cation-anion pair of the active center.

  After the activation process has occurred, the (partically) cationic metallocene species, which is the real active center for polymerization, is formed. However,

its capability of initiating the polymerization depends on the competitive coordination abilities of the monomer, the solvent, the counterion and other nucleophilic species in the system. For example, sometimes the excess neutral metallocene may participate in this competition. However, in most cases of olefin polymerization, the main competition comes from the counterion and the olefin monomer. If the counterion has too a high coordination capability, it will combine tightly with the (partially) cationic metallocene species and prevent the coordination of olefin to the active center. No polymerization will occur. The coordination ability of the counterion can be adjusted by both the electronic effect and the steric effect of the coinitiatior. For the polymerization of olefins, the counterion should be more weakly coordinating to the cationic active center than the π electrons from the double bonds of the olefins. Since the coordination capability of the counterion comes directly from the coinitiator, several aforementioned requirements for the coinitiators (Section 1.1.2.2) must be satisfied. Moreover, a large size of the coinitiator can induce steric hindrance between the cation-anion interaction, especially when the π-ligands of the metallocenes are also large. In such cases, the tight cation-anion interaction is sterically prevented, which facilitates the coordination of the olefin molecules to the cationic active center and favors the polymerization.

1.2.3.2 Control of the Propagation.

Both stereospecific control and regiospecific control are achieved in the propagation process due to the steric configuration of the metallocene active center. A simple model for these controls is shown in Scheme 11, in which a chiral metallocene with C_2

symmetry, i.e., *rac*-$Me_2Si(IndH_4)ZrMe_2$, is used to display how and why stereospecific and regiospecific controls are realized. The scheme shows the active center and eight boundary orientations that the propylene molecules may possibly take for the coordination to the metal center. I_1 and I_2 describe the two possible orientations that the polymer chain may take due to the steric effect. In I_1, because of the top 4HInd group, the polymer chain can only orient downward to the right, while in I_2, polymer chain orients upward to the left. The eight boundary orientations for propylene are:

- Parallel orientations p_1, p_2, p_3 and p_4

  In these situations, the planes (plane β, γ, η and ϕ) on which three carbon atoms of the propylene molecule sit are parallel to the central plane (plane α) of the cationic metallocene with the methyl group sitting at four different positions relative to the double bond.

- Normal orientations n_1, n_2, n_3 and n_4

  In these situations, the planes (plane δ, ω, λ and φ) on which three carbon atoms of the propylene molecule sit are perpendicular to the central plane (plane α) with the methyl group sitting at four different positions relative to the double bond.

Certainly, many other orientations exist in addition to these boundary ones.

From the steric hindrance point of view, while the metallocene active center is in the I_1 state, orientation n_2 is the most energetically favorable. When the propylene molecule approaches the Zr—P bond in this orientation, the methyl group on it will meet the least steric hindrance from both the metallocene template and the polymer chain (P). Therefore, this will be the most easily achievable orientation for olefin coordination to

Scheme 11

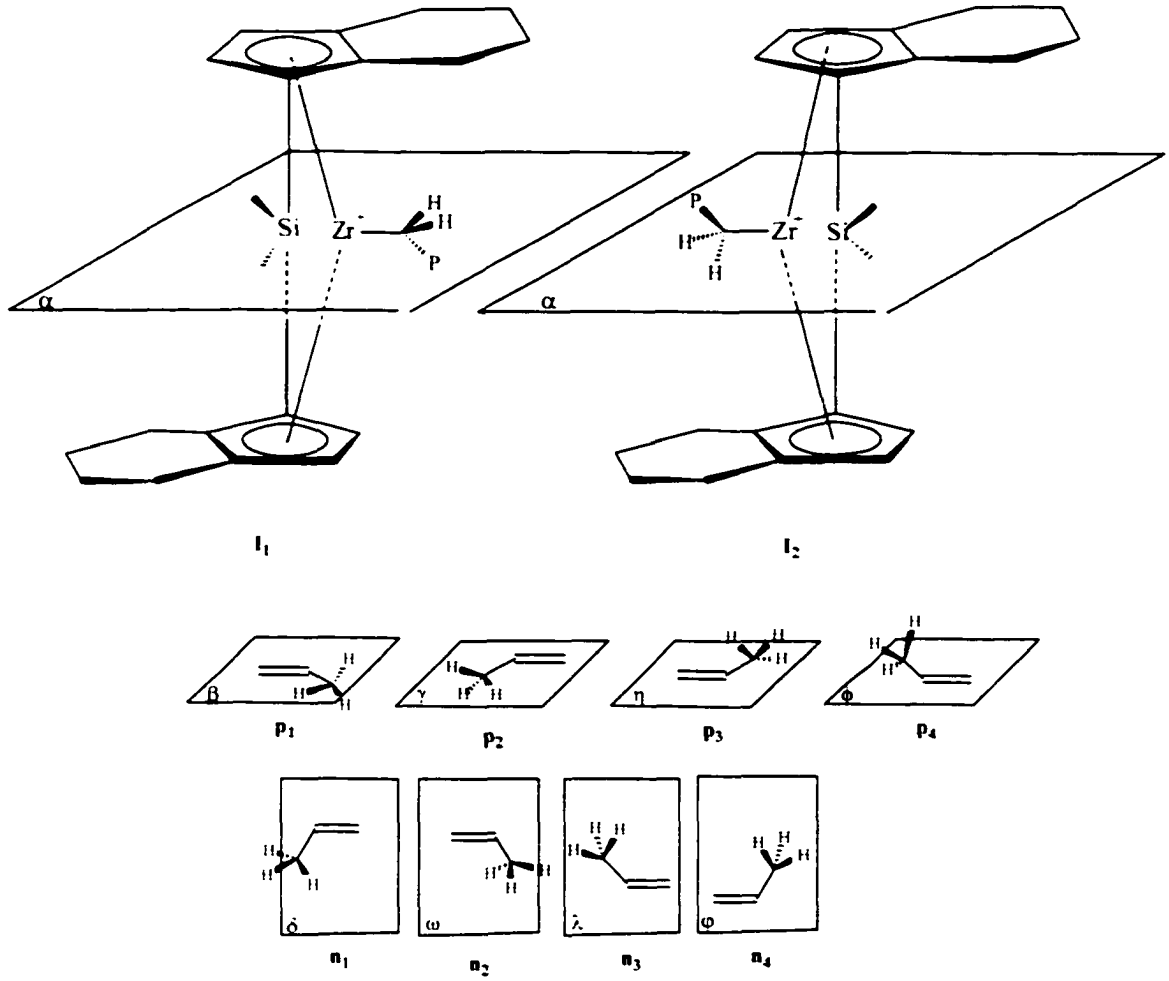

a metallocene center in the I_1 state, and the olefin will insert into the polymer chain in a regiospecific (1,2-insertion) and isotactic manner. After the insertion occurs, the polymer chain migrates to the original empty coordination site, leaving the original occupied site empty. This state is referred to as the I_2 state in Scheme 11. In the I_2 state, the n_3 orientation is now the least sterically hindered and will be most easily taken for the coordination of monomer to metallocene center. As far as the polymer chain is concerned, the relative orientation of n_3 is equivalent to the orientation n_2 bound to I_1, so

the monomer is inserted into the polymer chain in the same way as the previous unit was inserted, and the metallocene center converts back to the I_1 state. In this manner, an isotactic polymer chain is generated. However, some interference to ideality exists. Compared to the n_2 and n_3 orientations, p_1 and p_2 have some steric hindrance from the polymer chain that has already grown, but they also have a small steric hindrance from the active template of the active center. Therefore, they are less likely to be taken for the coordination than n_2 and n_3, but are much more favorable to be taken than other orientations. For other orientations, stronger steric repulsion will be met. When p_1 is taken, a 1,2-insertion will occur and the propylene molecule will coordinate to Zr-Me bond from both the front and the back with equal ease, and the tacticity of the monomer unit inserted this way will be either *meso* or *racemic* to the previous unit, with 50% of probability for each. When p_2 is taken, a 2,1-insertion will occur. Therefore the insertions with the p_1 and p_2 orientations will introduce both stereospecific and regiospecific errors into the ideal case. Depending on the transition state energy differences for reaction via the n_2 and n_3 orientations and via the p_1 and p_2 orientations, different degrees of stereospecific and regiospecific error will be induced in the ideal polymer chain. If both of the stereospecific and regiospecific errors are minor, a highly isotactic polymer chain will be obtained.

By the same token, other stereospecific polymers can be made by using metallocenes with different symmetries. In the polymerization of olefins, the general rules correlating the tacticity of the polymers and the symmetry of the metallocene initiators may be stated as follows: (Scheme 12)

- Atactic poly(α-olefin)s: normally result from the use of achiral C_{2v}-symmetric metallocenes.
- Hemi-isotatic poly(α-olefin)s: normally result from the use of C_1-symmetric metallocenes.
- Isotactic poly(α-olefin)s: normally result from the use of *racemic* C_2-symmetric metallocenes.

These are only the general rules, exceptions to these rules do exist.

Scheme 12

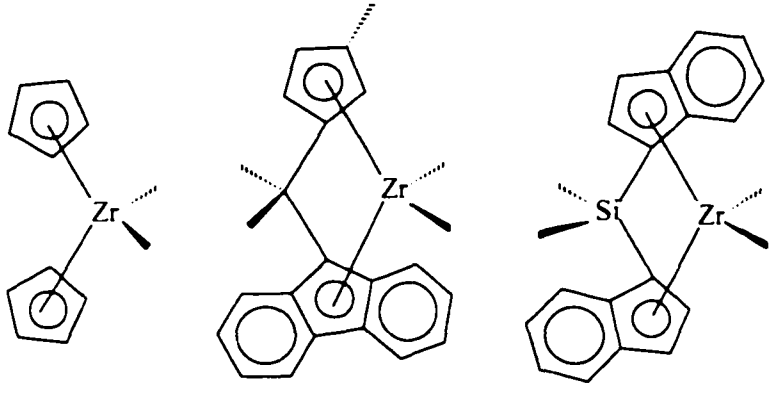

C_{2v} C_1 C_2

1.2.3.3 Control of the Chain Breaking (Chain Termination and/or Chain Transfer)

In the polymerization of olefins via the metallocene initiation systems, chain breaking reactions (chain termination or chain transfer) occur. The polydispersity is usually close to 2 ($\bar{M}_w/\bar{M}_n = 2$). Development of truly living α-olefin polymerization systems (with $\bar{M}_w/\bar{M}_n$ close to 1) remains a challenge in this area. Several parameters have been found to control the chain breaking process. For example, increasing the size

of the π-ligands in the metallocene initiators will increase the polymer chain length due to two effects:

- An increase in the rate of chain propagation.

  When large π-ligands are used, the steric limitation will prevent the tight interaction between the cation active center and its counterion, thus increasing the propagation rate.

- A decrease in the rate of termination

  When large π-ligands are used, the approach to the metal center of the tertiary β-CH_3 on the growing chain to the metal center is sterically hindered, hence decreasing the termination rate because chain transfer has a higher activation energy than chain propagation.

- A decrease in the rate of transfer

  β-H transfer from the growing polymer chain directly to a coordinated olefin (see Scheme 10) is a dominant chain transfer process. Using an *ansa*-metallocene initiator with α-methyl substituents, β-H transfer directly to a coordinated olefin is largely blocked, as indicated by the strong increase of the molecular weight almost in proportion to the olefin concentration by such α-methyl substituted *ansa*-metallocenes, while using an *ansa*-metallocene without α-methyl substituents, a near-constancy of molecular weights with increasing olefin concentration is obtained from the.[11]

The polymerization temperature may also affect the termination process. It is generally found that at a higher temperature, a lower molecular weight polymer is obtained.

1.3 Metallocene Initiation Systems for the Polymerization of Polar Monomers

Initiation systems containing metallocenes of early transition metals, such as Group 3 or Group 4 metals, have been extensively studied for the polymerization of olefinic hydrocarbons. However, the study of the polymerization of polar monomers, e.g. methyl methacrylate (MMA), with such systems is much less studied. This section will review the work that has been done in this area.

1.3.1 Significance of this Polymerization

It has been a long-standing goal for polymer scientists and the plastics industry to copolymerize the hydrocarbon olefins with polar monomers. Polyolefins, especially polyethylene (PE) and polypropylene (PP), have been used in an extensively wide range of applications. They have an excellent combination of mechanical, chemical and electronic properties due to their simple chemical compositions. However, a lack of functional groups in their structure somewhat limits their applications in certain areas, e.g. those in which adhesiveness, compatibility to other functional polymers, or dyeability of the polymers are strongly required. Therefore, the incorporation of some polar monomers or functional groups into the polyolefin chain is highly desirable. There are two routes that can be taken to accomplish this goal:

- Direct copolymerization of the olefins with the polar monomers or functionalized olefins.
- Modification of the polyolefins, either through controlled end functional groups or by inducing reaction sites on the polymer chains.

It is obvious that the former method is easier, faster and more straightforward, if copolymerization is readily possible. A wide range of new materials with novel physical and chemical properties would be made by this way. However, traditional Ziegler-Natta catalysts used in the preparation of polyolefins are normally intolerant of the Lewis basicity of the oxygen, nitrogen or halogen on the functional groups in polar monomers due to catalyst poisoning through acid-base interactions between the catalysts and the lone pair electrons on the functional groups. Since the 1990s, more and more polyolefins have been polymerized using metallocene initiation systems and a "metallocene era" started since then. A new possibility was imagined: can the copolymerization of olefins with polar monomers be achieved using the metallocene initiation systems? To answer this question, the following question needs to be answered first: can the polar monomers be homopolymerized by the metallocene initiation systems?

1.3.2 Difficulties of this Polymerization

Unfortunately, the answer to the above question is mostly (but not all) negative. Because the metallocene initiation systems are in essence Lewis acidic, which is especially true for the Group 4 metallocene initiation systems, the Lewis acidic components (i.e., the active metal centers and Al or B atoms in coinitiators) of these systems tend to complex with electron lone pairs on N, O and X of functional monomers, which impedes the coordination between the double bonds in polar monomers and the metal centers. No polymerization will consequently occur. Several research groups[15-17] reported specifically that the ordinary Group 4 metallocene initiation systems for nonpolar olefin polymerization do not polymerize polar monomers, such as methyl methacrylate (MMA). Also in some recent reviews[1, 3, 4] on the metallocene initiation

systems, no such successful polymerizations are mentioned when these reviews are talking about the polymerization of polar monomers. Group 4 metallocenes are only reported to copolymerize olefins with functionalized α-olefins, in which the functional groups are separated from the double bonds by a chain of several methylene units,[18-23] e.g. 5-(*N*,*N*-diisopropylamino)-1-pentene.[19]

In contrast to Group 4 metallocene initiation systems, Group 3 metallocene systems are successful in both homopolymerization of polar monomers and copolymerization of polar monomers with nonpolar olefins. This may be ascribed to the less electrophilic metal centers in Group 3 metallocenes. As mentioned in Section 1.2.2.1, the active center of Group 3 metallocene initiation systems is neutral, rather than the cationic centers of Group 4 systems. Therefore, the complexation between the lone pair electrons on the polar monomers and the active centers is not so strong that the double bond, either from polar monomers or from the nonpolar olefins, can also coordinate to the metal centers, and, (co)polymerization does occur.

Besides the above successful Group 3 metallocene initiation systems, several *special* Group 4 metallocene initiation systems are also found to be active toward the polymerization of polar monomers, such as MMA. These systems will be discussed in the following sections. However, most of these initiation systems are not active for olefin polymerizations and no copolymerization of polar monomers and nonpolar monomers is reported for these special systems. The copolymerization of polar monomers with the olefins is still a challenge for Group 4 metallocene initiation systems.

1.3.3 Historical and Recent Activities in Searching Metallocene Initiation Systems for Polymerization of Polar Monomers

In 1992, two metallocene initiation systems for the polymerization of MMA were discovered by Yasuda *et al*[24] and Collins *et al*,[25] respectively. Later on, Soga *et al*[15] and Marks et al,[17] respectively, reported other successful Group 4 metallocene initiation systems for the polymerization of MMA. Recently, some new studies in this area appeared, however, they are follow-up work of one the above four pioneer works.

1.3.3.1 Yasuda's Study[7,24, 26,27]

Yasuda *et al* reported the polymerization of MMA by metallocenes of Group 3 or rare earth metals, e.g. $[(C_5Me_5)_2SmH]_2$ or $(C_5Me_5)_2MMe(THF)$ (M = Sm, Y, Lu). Syndiotactic-rich poly(methyl methacrylate)s (PMMAs, [rr]=82%) with a very narrow molecular weight distribution (MWD, $\bar{M}_w/\bar{M}_n$ < 1.05) were quantitatively produced in less than 1 hour in toluene at 0 °C. These polymerizations are living with both a linear relationship of $\bar{M}_n$ versus monomer conversion and a continuous chain growth on the sequential addition of MMA.

These Group 3 metallocene initiation systems can also be used to polymerize other polar monomers, such as methyl acrylate, ethyl acrylate, lactones, lactide and oxirane. Also Yasuda *et al*[7] successfully achieved block copolymerizations of ethylene and MMA or lactones via these metallocene initiation systems. The polyethylene derivatives produced in this way have high chemical reactivity in dyeing. Table 1 summarizes their work.

Based on the X-ray analysis of the 1:2 adduct (molar ratio) of $[(C_5Me_5)_2SmH]_2$ with MMA the mechanism in Scheme 13, which includes an 8-membered ring for the polymerization, was proposed.

The MMA monomer coordinats to the metal center through the lone pair on its carbonyl oxygen and then an enolate complex is formed. Another monomer coordinats with the metal from another coordination site and forms a new enolate structure through the interaction with the enolate moiety that is already on the metal. In the mean time, the original enolate structure is converted back to its carbonyl form and the metal- oxygen bond is broken, leaving an empty site for the coordination of a new monomer. Through this alternate coordination at two sites and carbonyl-enolate exchange, the monomer molecules insert into the polymer chain to form a syndiotactic structure.

Scheme 13

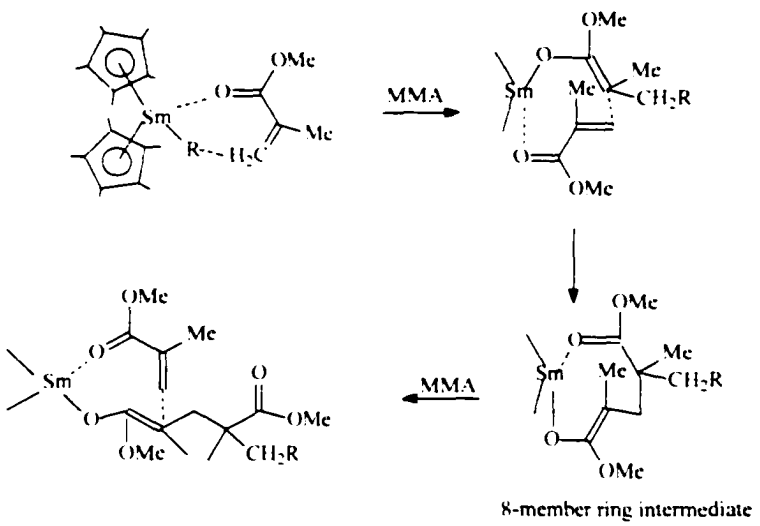

Table 1. Yasuda's work on Group 3 metallocene initiation systems

Monomer	Initiator	Characters of Polymers
MMA	$[(C_5Me_5)_2SmH]_2$ or $(C_5Me_5)_2MMe$ (THF) M=Sm, Y, Lu	quantitative yield (< 1 h) Syndiotactic PMMA.([rr] >95%, -95°C) $\bar{M}_n$ > 50 k, $\bar{M}_w/\bar{M}_n$ < 1.05 good living polymerization
Alkyl acrylate	$(C_5Me_5)_2MMe$ (THF) M=Sm, Y	PMA PEA PBA $\bar{M}_n$ 48 k 55k 70k $\bar{M}_w/\bar{M}_n$ 1.04 1.04 1.0
MMA with butyl crylate	$(C_5Me_5)_2SmMe$ (THF)	ABA triblock copolymer Rubber-like elastic polymer
Ethylene with MMA or lactones	$[(C_5Me_5)_2SmH]_2$	Block polymers of ethylene and MMA or ethylene and lactones.

1.3.3.2 Collins' Study[25, 28, 29]

A mixture consisting of a neutral dimethyl zirconocene, Cp_2ZrMe_2, and a cationic zirconocene species from $[Cp_2ZrMe(THF)]^+[BPh_4]^-$ was discovered by Collins *et al*[24] to polymerize MMA. This initiation system quantitatively produced syndiotactic-rich PMMAs ([r]~80%) with a narrow MWD ($\bar{M}_w/\bar{M}_n$ = 1.2-1.4) in about 1 h in methylene chloride at 0 °C. They also found that a chiral dimethylzirconocene with C_2-symmetry, i.e. *rac*-$C_2H_4(IndH_4)ZrMe_2$, with coinitiator $[n\text{-}Bu_3NH]^+[BPh_4]^-$, produced isotactic PMMAs.[28]

A mechanistic study was also performed by Collins *et al.*[29] The proposed mechanism is shown in Scheme 14. A MMA molecule first coordinates to the cationic species in the initiation system and forms a complex **2·MMA**. **2·MMA** then reacts with the neutral metallocene in the system forming an enolate intermediate **3** with the release of a cationic metallocene species **2**. The reaction between **3** and **2·MMA** connects the enolate MMA species in **3** with the MMA unit in **2·MMA**, and forms the intermediate **4**. **4** adds one molecule of MMA and regenerate **2·MMA** and **3**, in which one more unit of MMA has been added to the growing chain. These processes repeat and the chain grows with the addition of one more monomer unit at each repetition.

Collins' initiation system was the first Group 4 metallocene initiation system that polymerized MMA. It enlarged the range of the monomers that can be polymerized by this kind of system and raised a possibility that the copolymerization of olefins and polar monomers could be accomplished by certain Group 4 metallocene initiation systems. However, the counterion (BPh_4^-) in their systems is not sufficiently noncoordinative to the metal center, and the cationic metallocene center will tend to coordinate with BPh_4^-.

Scheme 14

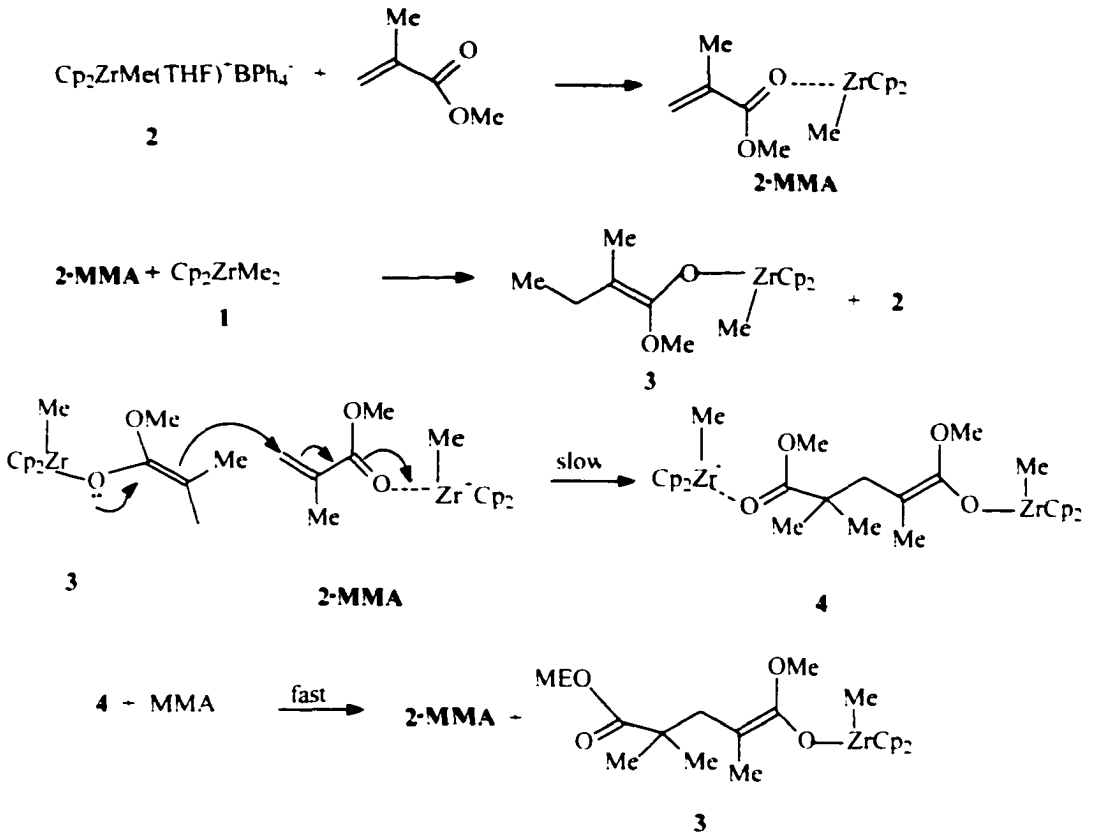

favorably than with the olefin double bonds. Hence, Collins' systems are inactive to the polymerization of olefins (refer to 1.1.2.2).

1.3.3.3 Soga's Study[15,16,30,31]

Soga *et al* developed a Group 4 metallocene initiation system for the polymerization of MMA by adding a third component, e.g. alkyl zinc or alkyl aluminum, to the two-component initiation systems, i.e. an equimolar amount of dimethyl zirconocene and $B(C_6F_5)_3$ or derivatives of $B(C_6F_5)_4^-$. The use of an achiral dimethylzirconocene (e.g., Cp_2ZrMe_2) gives syndiotactic-rich PMMAs, while the use of a chiral dimethylzirconocene, e.g. *rac*-$Et(Ind)_2ZrMe_2$ with C_2-symmetry, gives highly isotactic

PMMAs. However, the necessary amount of the third component is typically several hundred times the dimethylzirconocene and the typical polymerization time is 24 h.

1.3.3.4 Marks' Study[117]

Another successful Group 4 metallocene initiation system for the polymerization of MMA was found by Marks *et al*, who synthesized a coinitiator, tris(2,2',2''-nonafluorobiphenyl)borane, and used it with dimethyl zirconocenes L_2ZrMe_2 (L = Cp, η^5-1,2-$Me_2C_5H_3$, L_2 = $Me_2Si(Ind)_2$) to accomplish the polymerization of MMA. Stereochemical control of PMMAs similar to Collins' and Soga's results was accomplished by changing the symmetry of the dimethyl zirconocenes.

1.3.3.5 Other Studies

Besides the above pioneering work in the field of metallocene-initialized polymerization of polar monomers, some further recent reports in this area appear, most of which are, however, follow-up work of the above systems. A brief introduction of these works is given below.

- Work that follows Yasuda's.

Using bimetallic complexes of the type $(C_5Me_5)_2Sm$-R-$Sm(C_5Me_5)_2$ (Scheme 15), Novak *et al*[132] polymerized MMA and ε-caprolactone in a living way. The polymerization occurred at both Sm centers of the initiator and polymers with discrete functionalities at the center of the backbone (so called "link-functionalized" polymers) were produced.

Using bivalent organolanthanides with unbridged substituted Ind or Flu ligands (1-$SiMe_3Ind)_2Yb{\cdot}THF$ or (9-$SiMe_3Flu)_2Yb{\cdot}THF$, Knjazhanski *et al*[133] obtained polymerization of MMA with stereoregularity (isotatic rich) due to the fluctuation of the initiator (with Flu ligands) around its C_2 symmetric twisted-conformation.

Scheme 15

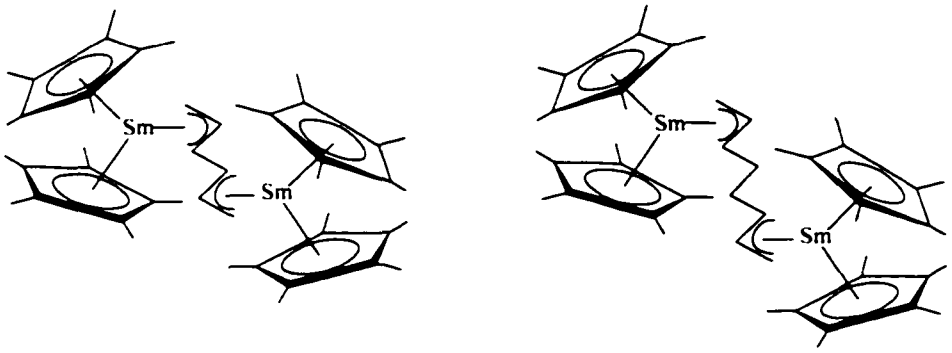

Using (diisopropylamido)bis(methylcyclopentadienyl)lanthanides $(MeC_5H_4)_2LnN(i\text{-}Pr)_2(THF)$ (Ln = Yb, Er, Y), Shen *et al*[34] obtained syndiotactic rich PMMA over a broad range of temperature (-78 to 40 °C).

Using both Group 3 and Group 4 metallocene dichlorides ($Cp_2YCl(THF)$, Cp_2ZrCl_2 and Cp_2HfCl_2) together with MAO and a third component, $Zn(C_2H_5)_2$, Jiang et al[35] obtained polymerization of MMA in a living manner. This work is more like Soga's work, which typically showed a polymerization time of 24 h.

- Work that follows Soga's

Using the same initiation systems as Soga's, Hadjichristids *et al*[36] performed the polymerization of MMA and other alkyl methacrylates, such as n-butyl and n-hexyl, under highly purified conditions. Copolymerization of MMA with n-hexyl methacrylate was also successfully carried out and multiblock copolymers were obtained.

- Work that follows Collins'

In contrast to other cationic complexes, $Me_2CCpIndZrMe(THF)^+BPh_4^-$ and $Me_2CCp_2ZrMe(THF)^+BPh_4^-$ were found to be highly active for MMA polymerization by Hocker *et al.*[37] In these initiation systems, no neutral zirconocene dimethyl was used

unlike Collins' work. The cationic species alone acted as the initiator. Isotactic PMMA was produced by $Me_2CCpIndZrMe(THF)^+BPh_4^-$ and syndiotactic PMMA was produced by $Me_2CCp_2ZrMe(THF)^+BPh_4^-$. Since there was only one component in the initiation system, a mechanism similar to Yasuda's mechanism was proposed. However, other cationic zirconocene species, such as $Cp_2ZrMe(THF)^+BPh_4^-$, $Me_2SiCp_2ZrMe(THF)^+BPh_4^-$, $C_2H_4Ind_2ZrMe(THF)^+BPh_4^-$, $Me_2CCpFluZrMe(THF)^+BPh_4^-$ were found inactive for MMA polymerization without the addition of the corresponding neutral zirconocenes.

It is worth mentioning finally that Gibson et al[38] reported an active initiation system for the polymerization of MMA that consisted of equimolar amounts of dimethyl zirconocene and $B(C_6F_5)_3$, a system that previous studies[15-17] showed to be inactive. Gibson et al ascribed this difference to the feeding sequence, i.e., the order in which the reaction components are charged to the reaction vessel.

1.3.4 Goal and Idea of this Study

The long range goal of this project is to search for a successful Group 4 initiation system for the copolymerization of olefins with polar monomers. The first effort is to find a Group 4 metallocene initiation system that can efficiently homopolymerize a polar monomer, e.g. MMA, but it should also have similar components to the initiation system in olefin polymerization.

Group 4 metallocene initiation systems show good control of olefin polymerizations and have been used to produce olefins in industry. However, hydrophobic polyolefins lack chemical functionality, which results in poor adhesive properties, poor affinity for dyes and paints, and poor compatibility with more polar polymers, metal, and glass. Therefore,

a copolymerization of nonpolar olefins with some polar monomers via metallocene initiation systems is highly desirable. Since in industry, Group 4 metallocene systems are the only systems used to produce polyolefins, the present study will focus on Group 4 metallocene systems, though some Group 3 metallocene systems have been reported to copolymerize ethylene with alkyl methylates or lactones successfully.[7]

As stated above, some Group 4 metallocene initiation systems have been found to homopolymerize MMA. However, no copolymerization of olefins with MMA is reported via these initiation systems. Besides, all these systems are quite different from those used in olefin polymerizations, which either induce components that are intolerant for olefin polymerizations, e.g., alkyl zinc and BPh_4^- in Soga's[15] and Collin's[25] systems, respectively, prevent the polymerization of olefin from occurring, therefore, no such polymerization can be obtained via these systems, or they include very complicated processes to synthesize the initiation component.[17] In searching for an active initiation system for the polymerization of MMA, two basic criteria are kept in mind: 1) the new initiation system should be very similar to those of olefin polymerizations. Hopefully, the similarity between these two systems will result in copolymerization. 2) the new initiation system should be simple. A complicated system generally is more difficult to apply.

The impedance to the polymerization of polar monomers from the ordinary initiation systems for olefin polymerizations is the strong coordination between active centers and the lone pair electrons from the polar monomers, which prevents the coordination of double bonds onto the active centers to start insertion. Several parameters can be adjusted to control the above coordination between active centers and polar monomer: 1) inducing

steric hindrance to the initiation system, which will prevent the coordination. 2) reducing the electrophilicity of the active centers, which decreases the attraction to the polar monomers. Method 1 will certainly cause more synthetic work, i.e., to introduce steric groups onto the metallocene or coinitiator (Marks' method[17]). The initiation system will become more complicated. Moreover, the knowledge that how big the steric groups must be to give sufficient steric hindrance is not disclosed, so a lot of syntheses and work needs to be done before an efficient initiation system is found. Therefore, this is not the preferred choice. Method 2 also seems complicated at first glance, since reducing electrophilicity of the active centers may involve placing electron-donating groups onto the π-ligands in the metallocenes. However, considering that the electrophilicity of the active centers appears due to the coinitiator's activation of the metallocene, as shown in Scheme 5, therefore, the electrophilicity of the active centers is essentially determined by the electrophilicity (or acidicity) of the coinitiator. If the acidicity of the coinitiator is reduced, the electrophilicity of the active centers should be lowered, therefore coordination between the active centers and the lone pairs on polar monomers will be weakened. Chances for C=C double bonds to coordinate to the active centers and to induce the consequent insertion will increase, polymerization will occur. However, to keep the new initiation system as similar to those of olefin polymerizations as possible, the identity of the coinitiator is not supposed to be radically changed in order to reduce its acidicity, which reduces much synthesis work. The protocol chosen to reduce the acidicity is simple, just reduce the amount of the coinitiator used in the system. Will this protocol work? The results show that it works surprisingly well. Therefore, an efficient active initiation system for the polymerization of MMA is found.

2. Experimental Part:

2.1 General Operations for Air-sensitive Compounds

2.1.1 Dry and Inert Reaction Environment

All materials involving air- and moisture-sensitive compounds were manipulated under an atmosphere of high purity argon (Welco) using bench-top inert-atmosphere techniques or in a nitrogen-filled glove-box[39] (Labconco Protector 50800) with a high-capacity recirculator (AtmosPure Regenerative Drying Train, H_2O < 5 ppm and O_2 < 1 ppm). A double vacuum/gas manifold as shown in Figure 1 was used for the manipulation of all the reactions in liquid state, i.e., for liquid monomer and solvents and solutions of initiators and coinitiator. The glove-box was used to handle the solid air- and moisture-sensitive compounds. To generate a local dry and inert environment in the reaction vessels, all glassware was baked in oven at 120 °C overnight or was flamed under vacuum (for quick use). The dried hot glassware was capped with septa and cooled under vacuum. The glassware was then filled with argon through needle connected on the manifold. Glassware was purged with argon at least three times before use. To reduce the moisture in the high purity argon, the gas passed though a column filled with newly regenerated 4Å molecular sieves. Some blue Drierite was incorporated in the column to visually indicate the moisture content. All experiments were performed while the Drierite was bright blue. To guarantee the dry and inert environment in the glove-box, the nitrogen was purified by passage through a Supelco High Capacity Gas Purifier and an activated 4Å molecular sieves column. A tray of P_2O_5 powder to absorb the trace moisture was exposed to the inner environment of the glove-box. To monitor the oxygen and moisture content in the glove-box, some green MnO and blue Drierite were exposed in the glove-box.

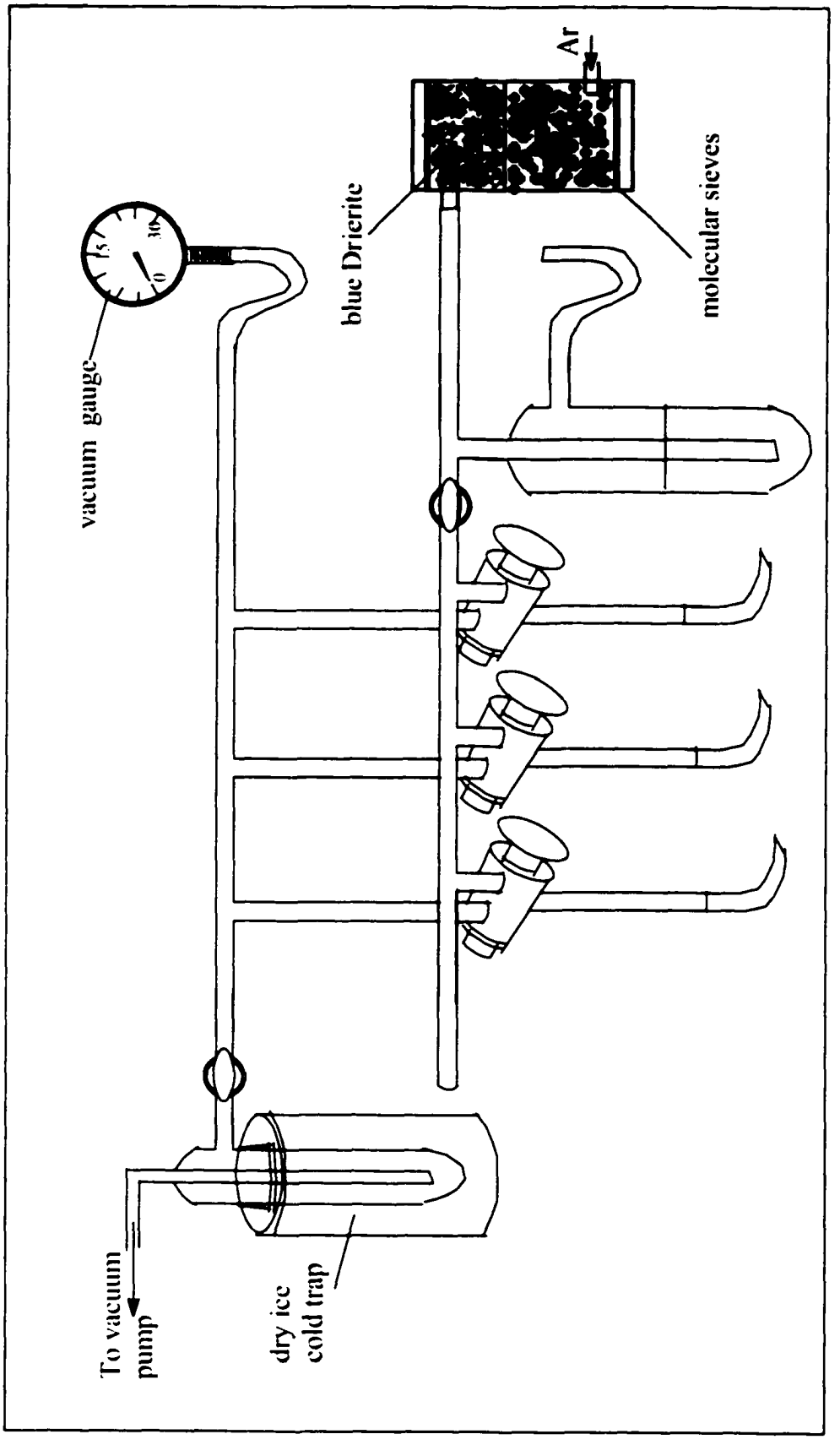

Figure 1. Vacuum/gas manifold used for the bench-top experiments.

41

respectively. These colors did not change through all the experiments performed in the glove-box.

2.1.2 Transferring of Reagents

All reagents either in liquid state or in solution were transferred by standard syringe and cannula techniques.[39] The syringes and cannulae were dried as described above before use. To exclude the air in the needle and cannula, a septum-covered test tube as shown in Figure 2 was used. The needle and cannula were purged with argon three times before transferring. Solid compounds were measured in a glove-box into septum-covered vials, which were then transferred out of the glove-box. Solvent was charged into these vials by cannula and these solutions were later transferred to the reaction vessals.

2.2 Purification of Solvents and Reagents

Hydrocarbon solvents (toluene and pentane) were distilled under nitrogen from Na/K alloy/benzophenone ketyl and stored over activated molecular sieves before their use. Anhydrous diethyl ether was purified by distillation from Na/K alloy/benzophenone ketyl just before its use. Deuterated chloroform was obtained from Aldrich, distilled from P_2O_5 and sealed in an argon-filled Wheaton serum bottle. Methyl methacrylate was dried over CaH_2 and distilled into a sealed Wheaton serum bottle containing activated 4Å molecular sieves.

2.3 Synthesis of Initiators and Coinitiator

2.3.1 Cp_2ZrMe_2 (1)

Cp_2ZrMe_2 (**1**) was synthesized from Cp_2ZrCl_2 (Aldrich).[40] The procedure is as follows:

A suspension of 2.92g (10 mmol) of zirconocene dichloride in 40 mL of ethyl ether was cooled to -78 °C in the reaction flask. Under magnetic stirring, 13.8 mL of 1.6 M

43

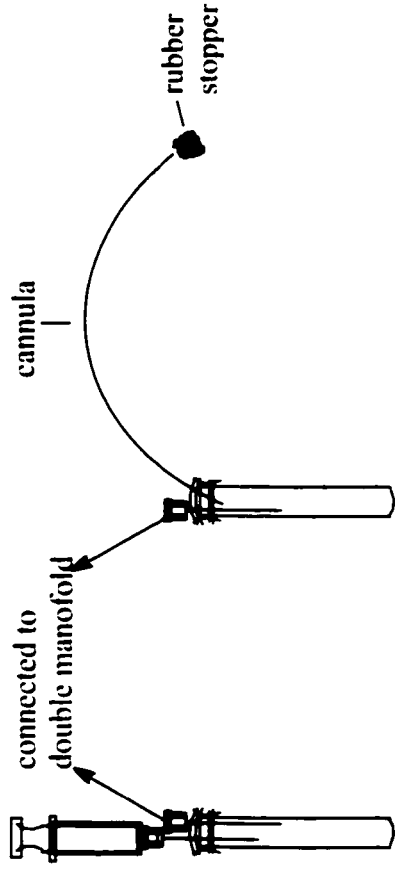

Figure 2. Syringe and cannula transferring technique.

methyllithium in ethyl ether was added dropwise via a septum-covered addition funnel over a period of 45 min. The temperature was then allowed to rise to 0 °C and was maintained at this temperature for an additional 30 min, during which time the reaction suspension turned from white to off-white. The solvent was then evaporated (Figure 3) and the solid residue was transferred to a sublimation apparatus in the glove-box. Sublimation at 85 °C under the vacuum overnight produced 1.86g (74%) of Cp_2ZrMe_2 as a white crystalline solid. Its purity was checked by ^1H NMR ($CDCl_3$): δ = -0.37 (s, 6H, Zr-CH_3), 6.10 (s, 10H, C_5H_5) (Figure 4).

2.3.2 *rac*-$Me_2Si(IndH_4)_2ZrMe_2$ (2)

rac-$Me_2Si(IndH_4)_2ZrMe_2$ (**2**) was synthesized from *rac*-$Me_2Si(IndH_4)_2ZrCl_2$ according to a literature procedure,[41] which methylates a similar zirconocene dichloride, *rac*-$Me_2Si(Ind)_2ZrCl_2$. The procedure is as follows:

To a suspension of 5.94 g of *rac*-$Me_2Si(IndH_4)_2ZrCl_2$ (13 mmol) in 200 mL of diethyl ether at -78 °C was added dropwise with stirring 20 mL of 1.4 M solution of MeLi in diethyl ether (28 mmol). The suspension was stirred for 45 min before being allowed to slowly warm to room temp. Stirring was continued for another 4 h, during which the color of the reaction mixture changed from greenish yellow to pale yellow. The diethyl ether was removed under reduced pressure and the residue was extracted by 140 mL dry toluene. The resultant toluene solution was concentrated to 8 mL (Figure 3) and cooled at -20 °C overnight. 2.2g (65%) light yellow crystals of *rac*-$Me_2Si(IndH_4)_2ZrMe_2$ was obtained. An alternative work up method was sublimation. After evaporation of diethyl ether (Figure 3), the residue was transferred to a sublimation apparatus in the glove-box. Sublimation was performed at 160 °C under the vacuum overnight. Elemental analysis:

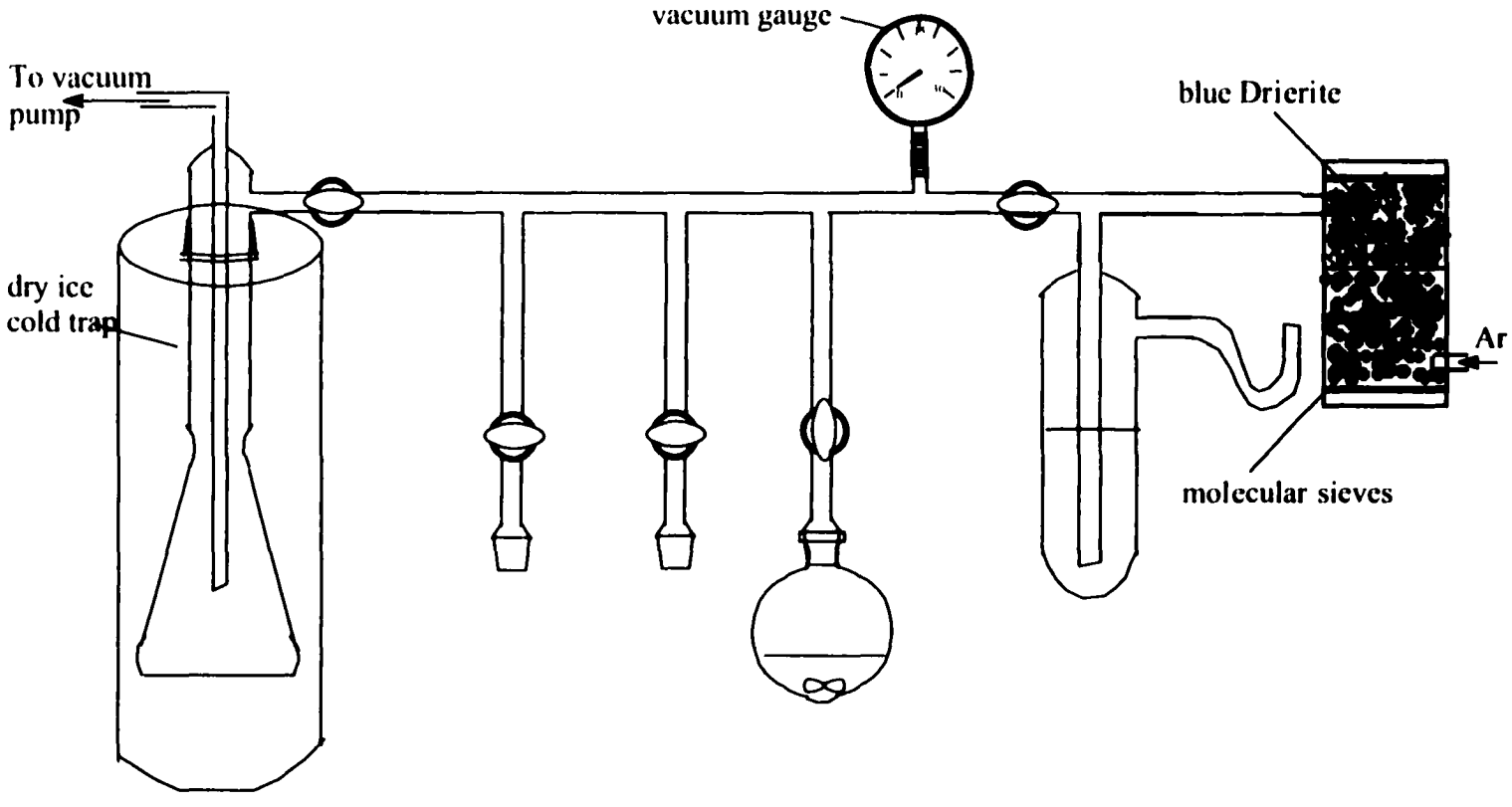

Figure 3. Apparatus for solvent evaporation under the vacuum

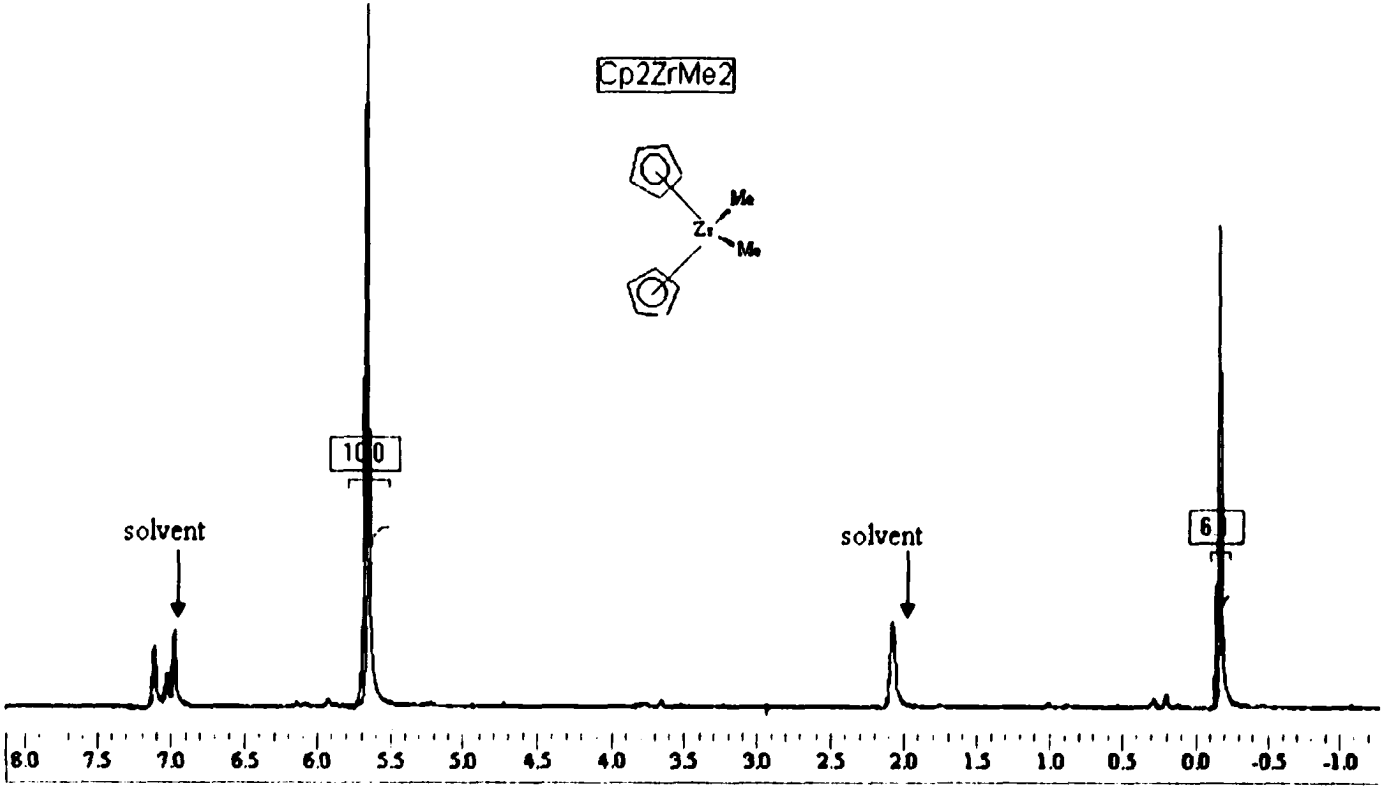

Figure 4. ^{1}H NMR of Cp_2ZrMe_2 (in toluene-d_8)

($C_{22}H_{32}SiZr$: Calcd. C 63.55, H 7.76; Found C 63.27, H 7.75.). ^1H NMR ($CDCl_3$): δ = -0.45 (s, 6H, Zr-CH_3), 0.51 (s, 6H, Si-CH_3), 1.47 – 2.89 (m, 16H, methylene protons on $IndH_4$), 5.24 (d, 2H, J_{H-H} = 3.00 Hz, aromatic protons on $IndH_4$), 6.49 (d, 2H, J_{H-H} = 3.00 Hz, aromatic protons on $IndH_4$). The ^1H NMR spectrum is shown in Figure 5.

2.3.3 $B(C_6F_5)_3$

$B(C_6F_5)_3$ was synthesized following a modified procedure of Waymouth's.[18] The detailed procedure is as follows (reaction apparatus is shown in Figure 6):

Bromopentafluorobenzene (9.9g, 40 mmol) was added to a 250 mL round-bottomed flask equipped with an addition funnel and a stir bar. The starting material was diluted with 50 mL of dry pentane, and the resultant solution was cooled to -78 °C. Over 20 min n-BuLi was added as a 2.5 M solution in hexane (16 mL, 40 mmol). The additional funnel was rinsed with 20 mL of dry pentane and the resulting solution was then added to the reaction flask. A white solid formed quickly, and the reaction was allowed to stir for an additional 10 min before the BCl_3 was added as a 1.0 M solution in hexane (13.4 mL 13.4 mmol). The resulting white slurry was allowed to stir for several minutes at -78 °C before it was gradually warmed to room temperature and permitted to stir for an additional 80 min. The resultant off-white slurry was poured quickly to a specially made Hirsch funnel (Figure 6) and filtered to remove the lithium salts. The residue was washed several times with dry pentane. The solvent of the filtrate was evaporated and the solid was transferred to the sublimation apparatus in glove-box. Sublimation was performed under the vacuum at 110 °C for 45 min and white needle crystals of $B(C_6F_5)_3$ was obtained in 4.8 g (72%). ^1H and ^{19}F NMR spectra are shown in Figure 7 and Figure 8, respectively. The ^1H spectrum in Figure 7 shows that no proton existing in the final

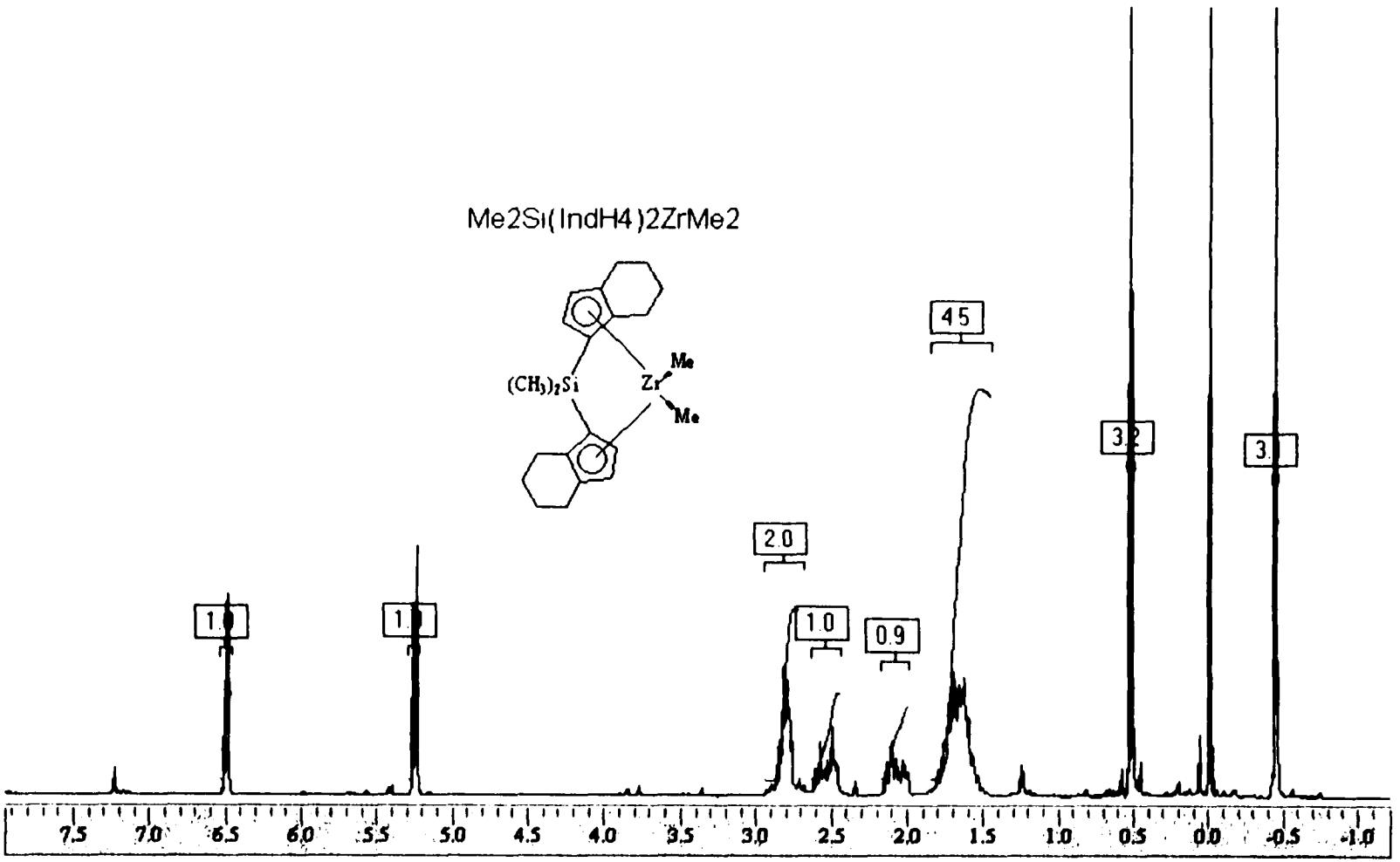

Figure 5. ^{1}H NMR of *rac*-$Me_2Si(IndH_4)_2ZrMe_2$ (in $CDCl_3$)

49

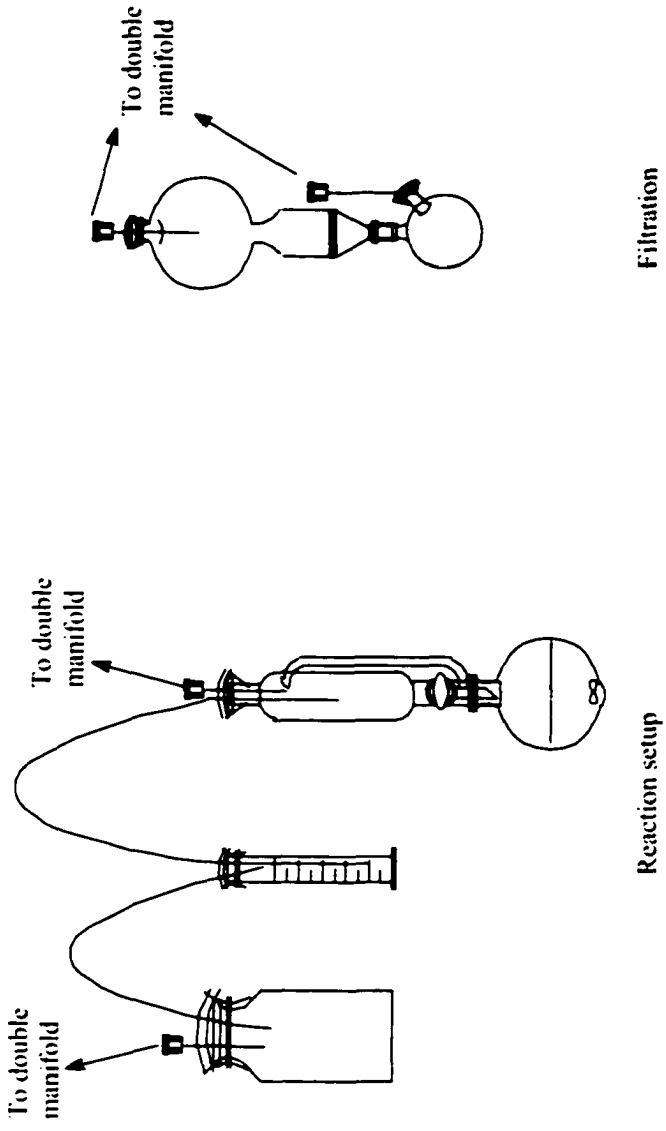

Figure 6. Reaction apparatus for the synthesis of $B(C_6F_5)_3$.

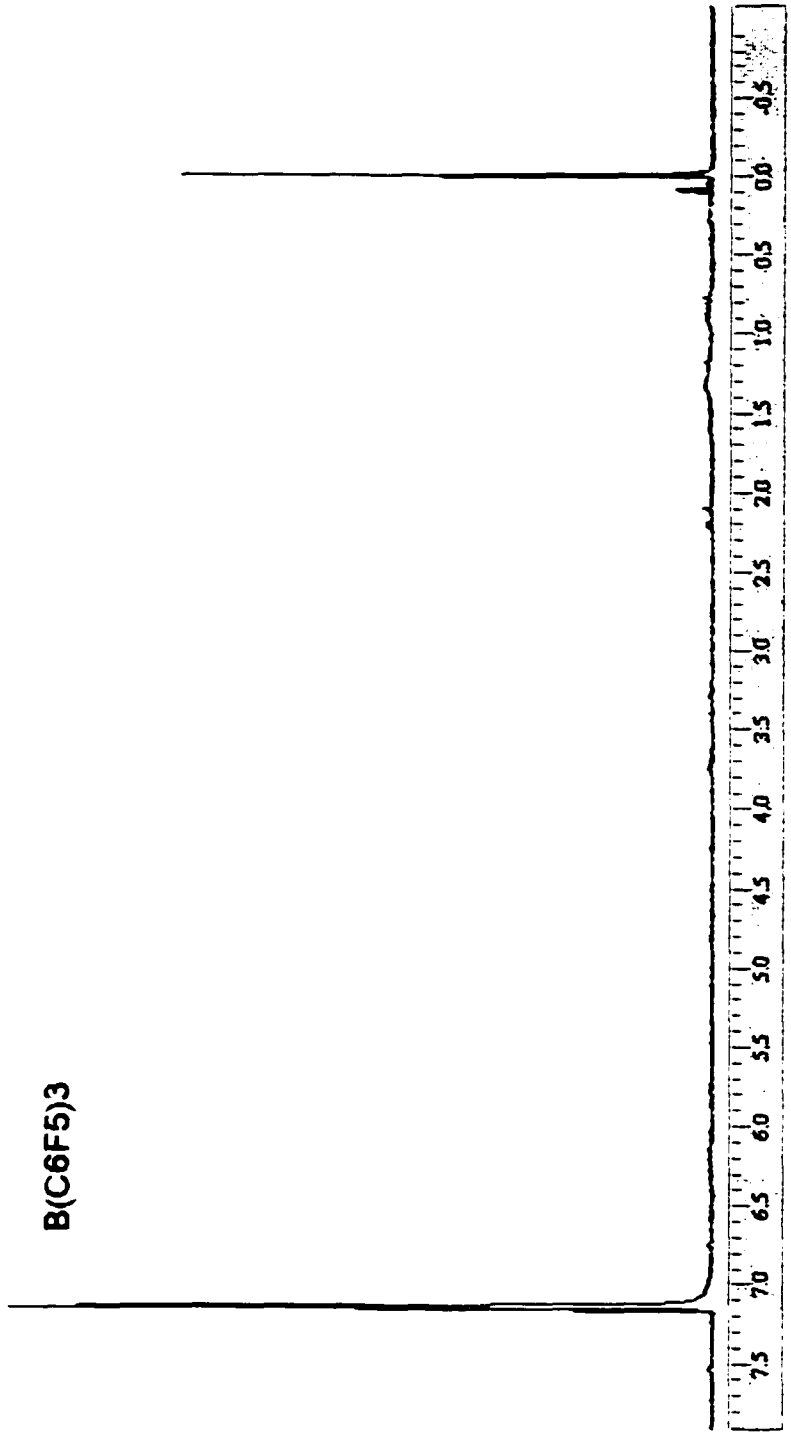

Figure 7. ^{1}H NMR spectrum of $B(C_6F_5)_3$ (in $CDCl_3$)

50

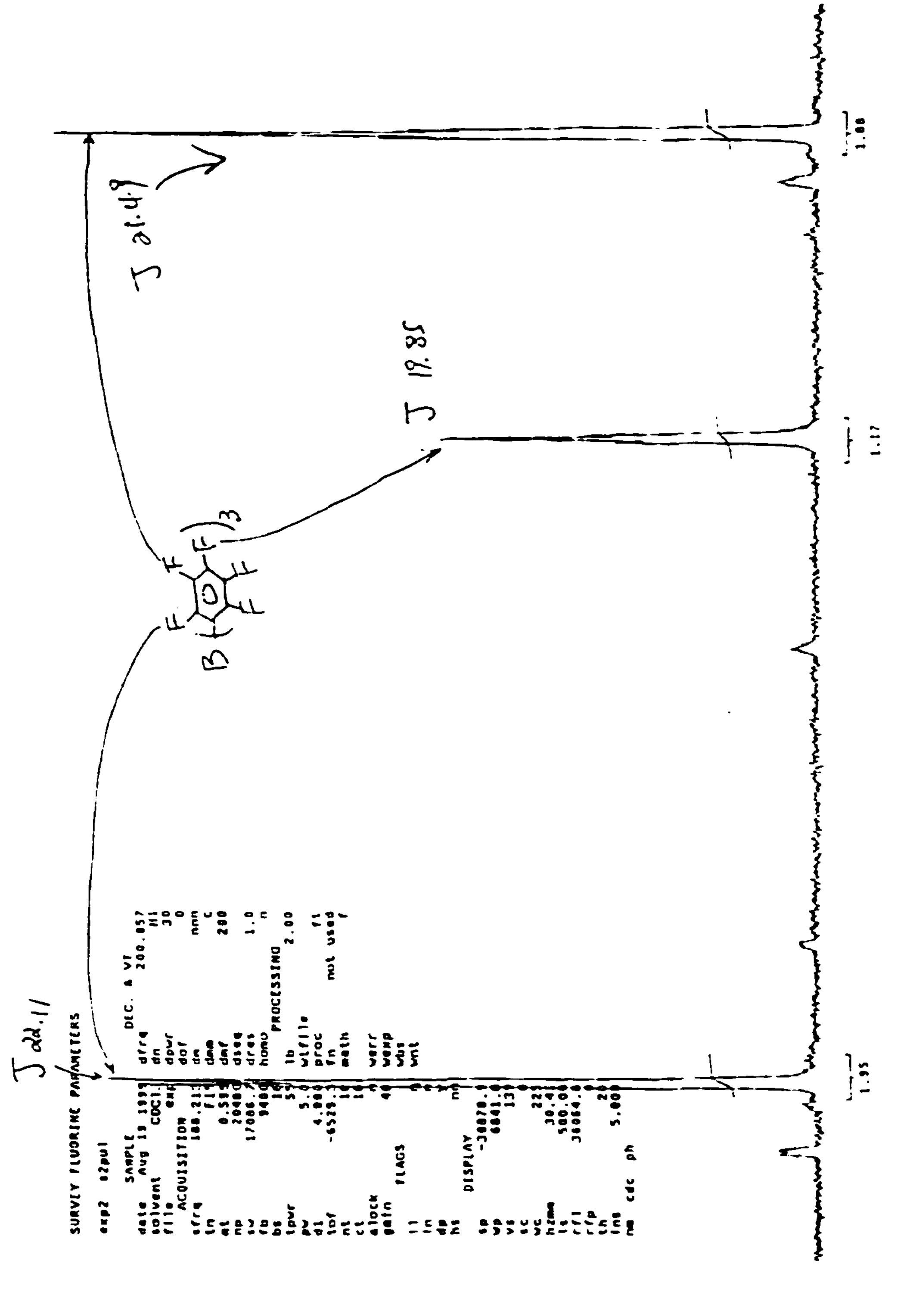

Figure 8. ^{19}F NMR spectrum of $B(C_6F_5)_3$ (in $CDCl_3$)

product and ^{19}F spectrum in Figure 8 shows that three different types of F existing in the final product with an integral ratio of close to 2:1:2, corresponding to F at *ortho*, *para* and *meta* position of $B(C_6F_5)_3$.

2.4 Polymerization Methods:

Polymerization of MMA was performed by two methods: gravimetry and NMR. The general procedures are as follows:

2.4.1 Gravimetry

The polymerization was performed in a 50 mL volumetric flask equipped with a magnetic stirrer and covered with a septum. Because the magnetic stirrer was in the volumetric flask, the volume mark was recalibrated as following: measuring 50 mL distilled water from a 50 mL pipet and charging it into the flask, marking the water level on the neck of the volumetric flask. The flask was then totally dried as described before, capped with a septum, purged with argon three times and weighed (assuming *a* grams). MMA was charged into the flask by syringe. The flask was again weighed (assuming *b* grams). The amount of initiator and coinitiator was weighed individually in glove-box and they were transferred out of the glove-box in septum-covered vials. The solutions of the initiator and coinitiator were then made by transferring solvent into these vials. The initiator solution was first added to the reaction flask. After dilution, the coinitiator solution was charged and the timer was started. The flask was immediately filled to the calibrated mark with solvent and stirring was started. The mass of the flask with contents was then measured (assuming *c* grams). At various times, an aliquot of the reaction mixture was taken out via cannula to a test tube containing acidic methanol as quenching agent. The amount of this sample was determined by gravimetry (assuming the test tube

with quenching agent was *d* grams and after the aliquot reaction mixture was charged to it, the total weight changed to *e* grams, therefore *e-d* is the weight of the aliquot sample). The amount of monomer in the aliquot sample was calculated (assuming *f* grams, which was obtained from the formula: $f = (e-d)/(c-a)\times(b-a)$). The polymer products were precipitated from hexane and collected by filtration followed by drying in vacuum at 45 °C overnight (assuming *g* grams polymer was obtained). The conversion was calculated on the basis of the amount of the collected PMMA and the calculated amount of monomer (yield = $g/f \times 100\%$).

2.4.2 NMR

A 10 mm NMR tube was used as the reaction vessel. The total reaction solution was 6 mL and a mark for it was made on the NMR tube. The feeding sequence and method were the same as for the gravimetry method except that instead of using a magnetic stirrer, a touch mixer was used for mixing after each addition of chemicals. The NMR tube was then put into the NMR probe of a 300 MHz Varian spectrometer, which was programmed to acquire ^{1}H spectra at desired time intervals. Each time, a spectrum with one scan was taken. The conversion was calculated based on the integrals of the vinyl signals (at 5.2 and 6.1 ppm) and the total ester -OCH_3 signal (2.7 – 4.4 ppm).

2.5 Analysis:

2.5.1 GPC

Molecular weights and molecular weight distributions were measured by GPC (Waters model 510 pump, Waters model 717+ autosampler, Waters model 410 differential refractometer, and three hydrogel columns HR4, HR3, HR1) at room temperature using chloroform as solvent with a flow rate of 1 mL/min and calibrated with

10 PMMA standards with molecular weights ranging from 620 to 780,000. The GPC samples were made at a concentration of about 2 mg/ml. TriSEC GPC software version 3.0 was used to treat the data.

2.5.2 NMR

2.5.2.1 Routine NMR Method

The ^{1}H NMR spectra for small molecular weight compounds were measured in chloroform-*d* or toluene-d_8 with a Varian 200 MHz spectrometer. TMS was added as reference. 30° pulse, 1s acquisition time, 2s delay between pulses was used.

The ^{19}F NMR spectra for $B(C_6F_5)_3$ was measured in chloroform-d with the Varian 200 MHz spectrometer. Since only the splitting pattern of the signals was concerned, no reference agent was added.

2.5.2.2 Quantitative Analysis of Tacticity of PMMA by ^{13}C-NMR

Quantitative ^{13}C NMR spectra for polymers were performed on a 600 MHz Varian spectrometer with inverse gated decoupling and a 20 s delay. The central peak of chloroform (77.0 ppm) was used as reference. For a flat baseline, the following parameters were set: `rof2=8.2 alfa=2 dsp='r'`. The carbonyl signals were used to investigate the pentad distribution of PMMA, whose assignments are shown in Figure 9.[116]

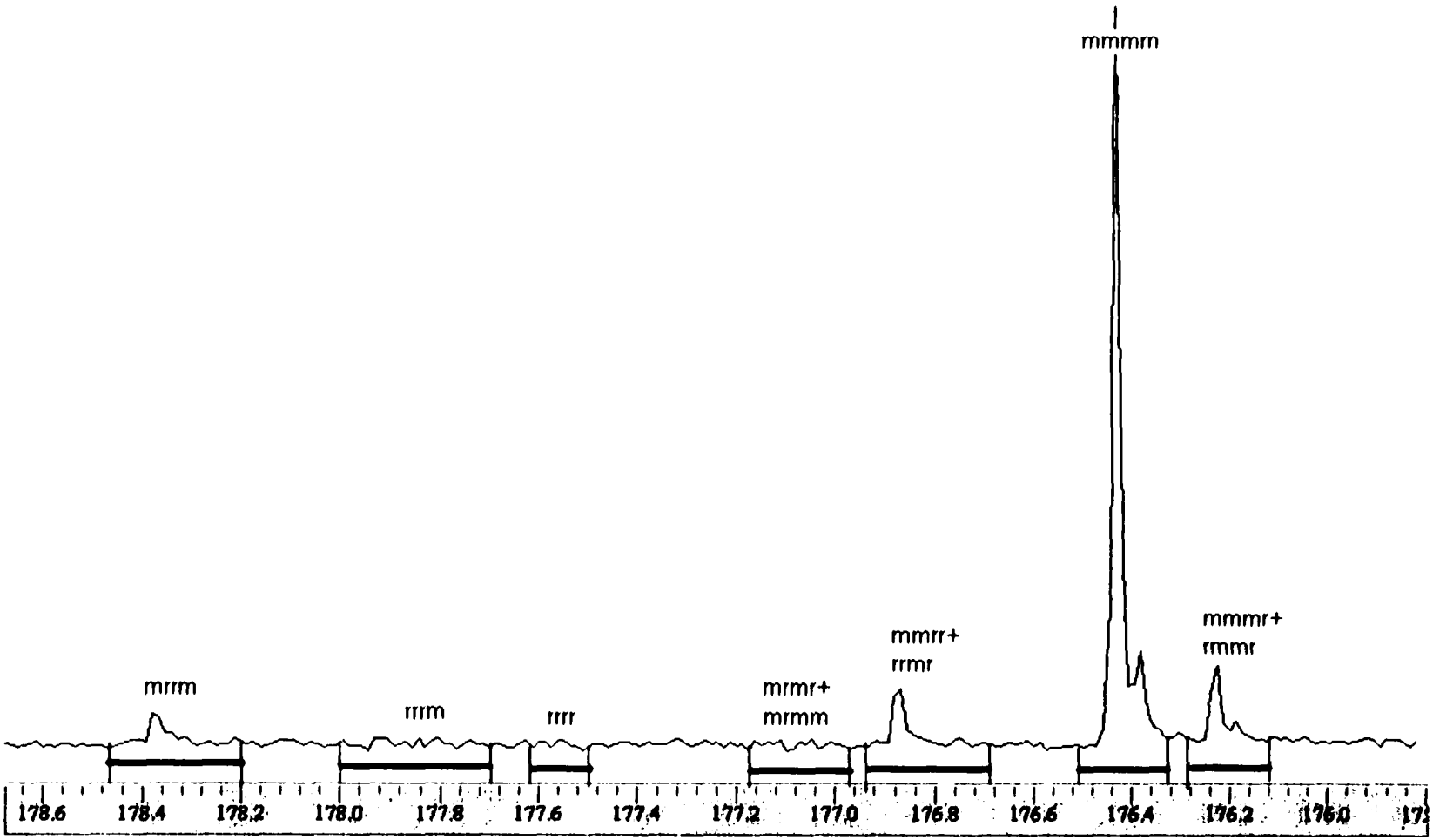

Figure 9. Pentad distribution of carbonyl carbon in PMMA.

3. Results and Discussion

3.1 Experimental Considerations

Both initiators (**1** and **2**) and the coinitiator $B(C_6F_5)_3$ used in this study are organometallic compounds. They are active to the oxygen and moisture in the environment. Inert atmosphere techniques are needed in both synthesis and storage of these compounds. .

3.1.1 Air-sensitivity of the Initiators and Inert-atmosphere Techniques

Initiator **2** was used as a representative to study the air sensitivity of the dimethyl zirconocenes. To obtain **2** with high purity, various inert atmosphere techniques must be tightly followed. Impurities were readily formed with less careful manipulation and with improper storage. Figure 10a shows a ^1H NMR spectrum of **2** that is not highly pure. Small signals between 5.0 and 6.4 ppm are the indication of impurities, which were introduced during the synthesis process. After deliberately exposing this compound to air for 3.5 h, the impurity increased and the signals (the doublets at 5.3 and 6.5 ppm) of **2** decreased (Figure 10b). The impurity can be collected by washing **2** with toluene and its spectrum is shown in Figure 10c. This spectrum fits well with the dinuclear structure with M-O-M bond (M stands for metal center). Figure 11 shows the dinuclear structure and the assignment of the ^1H NMR. Most of the impurity in **2** came from this dinuclear compound (Figure 10). Other impurities also existed, which corresponded to the small broad signal between 5.4 and 6.6 ppm in Figure 10b, which are minor.

Since the above major impurity can be collected by washing **2** with toluene, this provides a method of purifying **2**. The purest **2** obtained in this lab was obtained by

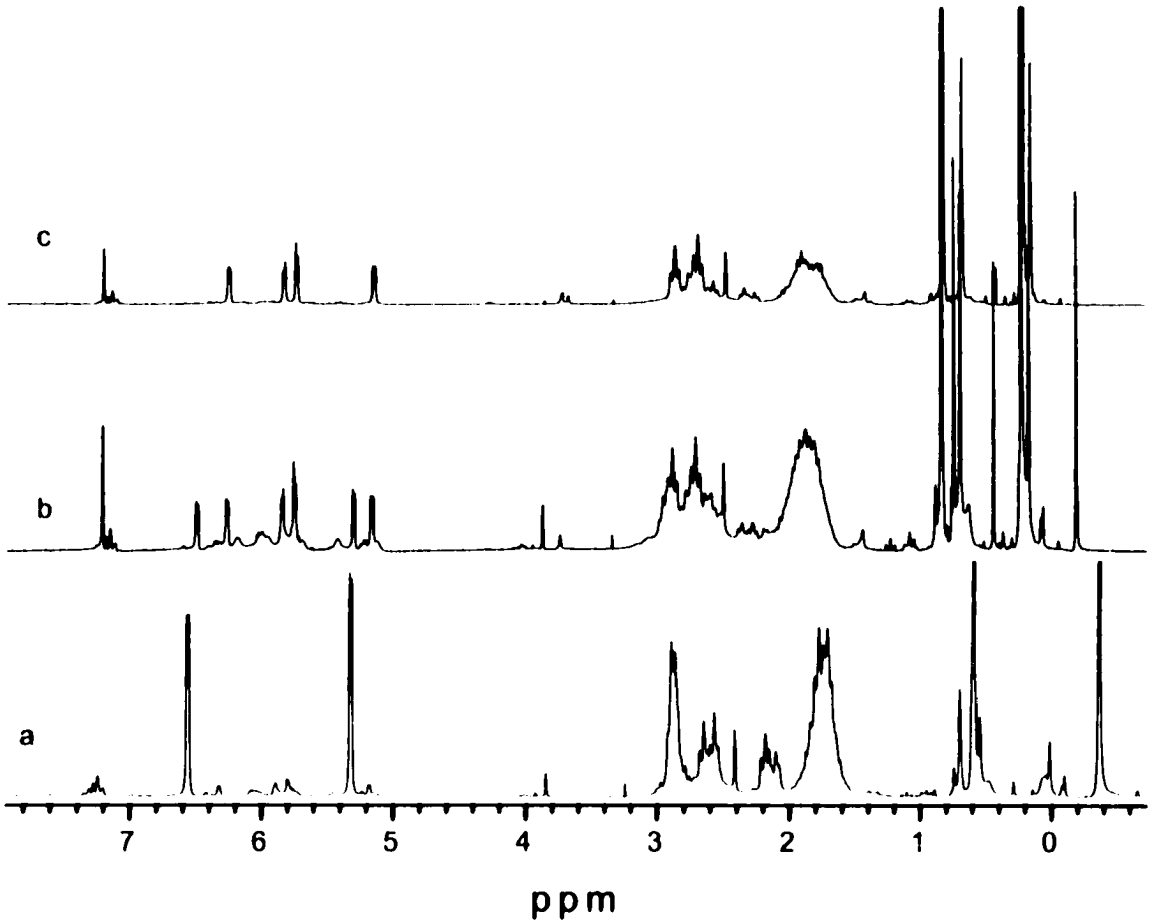

Figure 10. ^{1}H NMR spectra of **2** with impurity (in $CDCl_3$). a) **2** with impurity; b) **2** exposed to air; c) the impurity

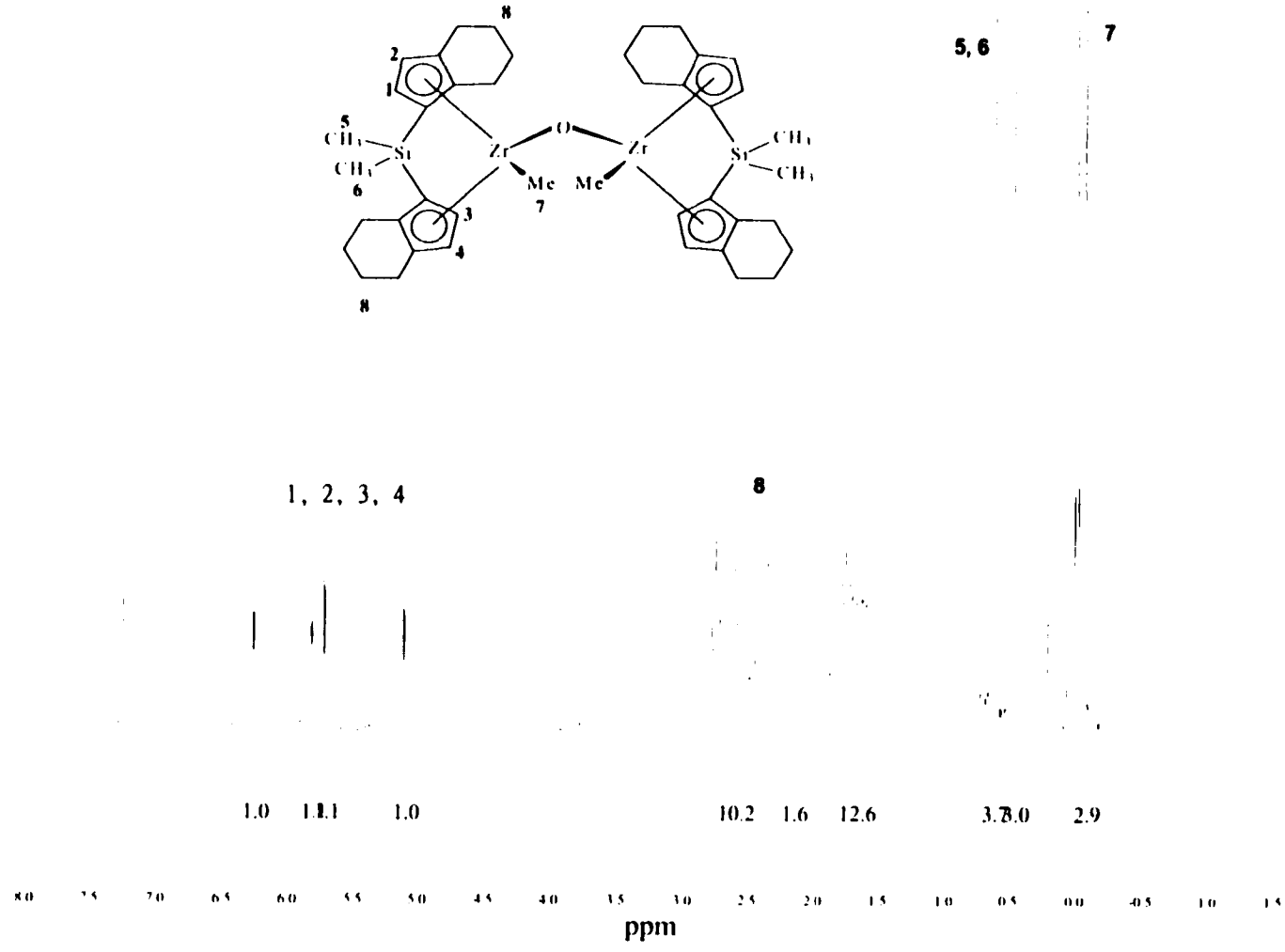

Figure 11. The impurity in **2** (Solvent: $CDCl_3$)

recrystallization as mentioned in the experimental part, which extracted **2** from the reaction mixture residue after evaporation of the solvent. However, because **2** does not have a high solubility in the toluene, (a concentration of about 40 mM in toluene is the highest obtained) this method needed a lot of toluene, most of which needed to be evaporated for crystallization in the following step. Therefore, this method is not so useful. Sublimation is an alternative method for the purification of **2**. However, sublimation can not guarantee the purity of the product, though long needle-shaped crystal was obtained from the sublimation. Small impurity signals were still seen between 5.0 and 6.4 ppm in ^{1}H NMR spectrum. (Figure 12). It seemed some impurities were also sublimed. Because the sublimation method is easy to perform, easy to maintain inert local environment and easy to produce **2** in large amount (several grams), it is an economical procedure for producing **2** and quite pure **2** (with impurities less than 5%) can be obtained.

Proper storage of the purified initiators was important. Trace moisture or oxygen in the environment would react with the initiators and deteriorate their quality. Figure 13 shows how a $CDCl_3$ solution of **2** changed with time in a sealed NMR tube. The trace moisture or oxygen in the solvent induced some changes in **2**. In a time period of less than 5 h, the changes were not significant. However, when the solution stayed longer than one day (30 h), some obvious changes were seen: the original impurity signals increased and some new impurity signals (signals at 6.37 ppm, 5.17 ppm, and 3.85 ppm, respectively) appeared. All impurity signals increased with time. This observation shows that it is not a good idea to store the initiators in solution since the initiators in solution deteriorate gradually with the time. Also, the solvent used should be totally dried and

60

Figure 12. **2** obtaind from sublimation (in $CDCl_3$)

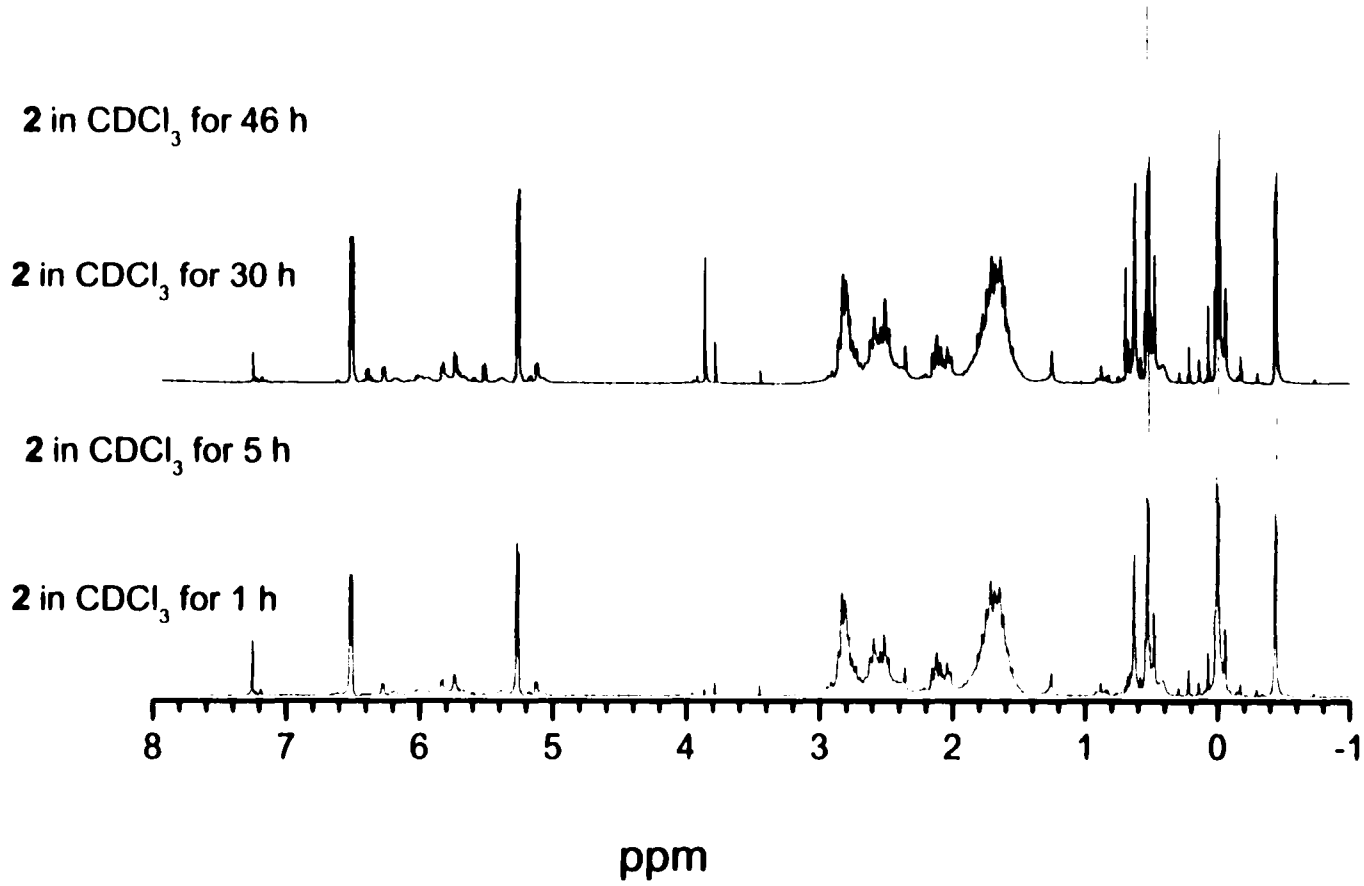

Figure 13. Chloroform-d solution of **2** changed with time.

purged with nitrogen to exclude oxygen.

Figure 14 shows two ^{1}H NMR spectra of **2** before and after 10-day's storage respectively, in the glove-box in the solid state. Virtually no changes were observed, which shows a good storage method for the initiators. Therefore, all organometallic compounds in this study were stored in the glove-box in the solid state and their solutions were made just before use.

3.1.2 Sensitivity of the Two Polymerization Methods

Two methods: NMR and gravimetry were used to study the kinetics of the polymerizations. The results of the polymerization in System 1, in which initiator **1** was used as the initiator, revealed that the NMR method is a much more sensitive method for the polymerization of MMA than the gravimetry method.

It was reported[15-17] that initiation systems with equimolar amounts of dimethyl zirconocenes and $B(C_6F_5)_3$ show no polymerization of MMA. The polymerization of MMA with 1:1 of **1**/ $B(C_6F_5)_3$ were also tested using the gravimetry method. After 100 min, no polymer was observed by dropping the reaction mixture into the nonsolvent hexane. This result is consistent with the literature reports. However, when the NMR method was used, a very slow polymerization was observed from the ^{1}H NMR spectra, (Figure 15) i.e. the appearance and growth of the CH_2 signal (from PMMA) in the region between 0.8 and 1.6 ppm. The polymerization proceeded gradually to high conversion (> 80%) in 20 h at 0 °C (Figure 16). From these results, it is shown that the gravimetry method was a less sensitive way of observing the polymerization of MMA. In the gravimetry method, the sensitivity to the polymerization was limited by the amount of the polymer that could be recovered. In the above slow polymerization, only a low

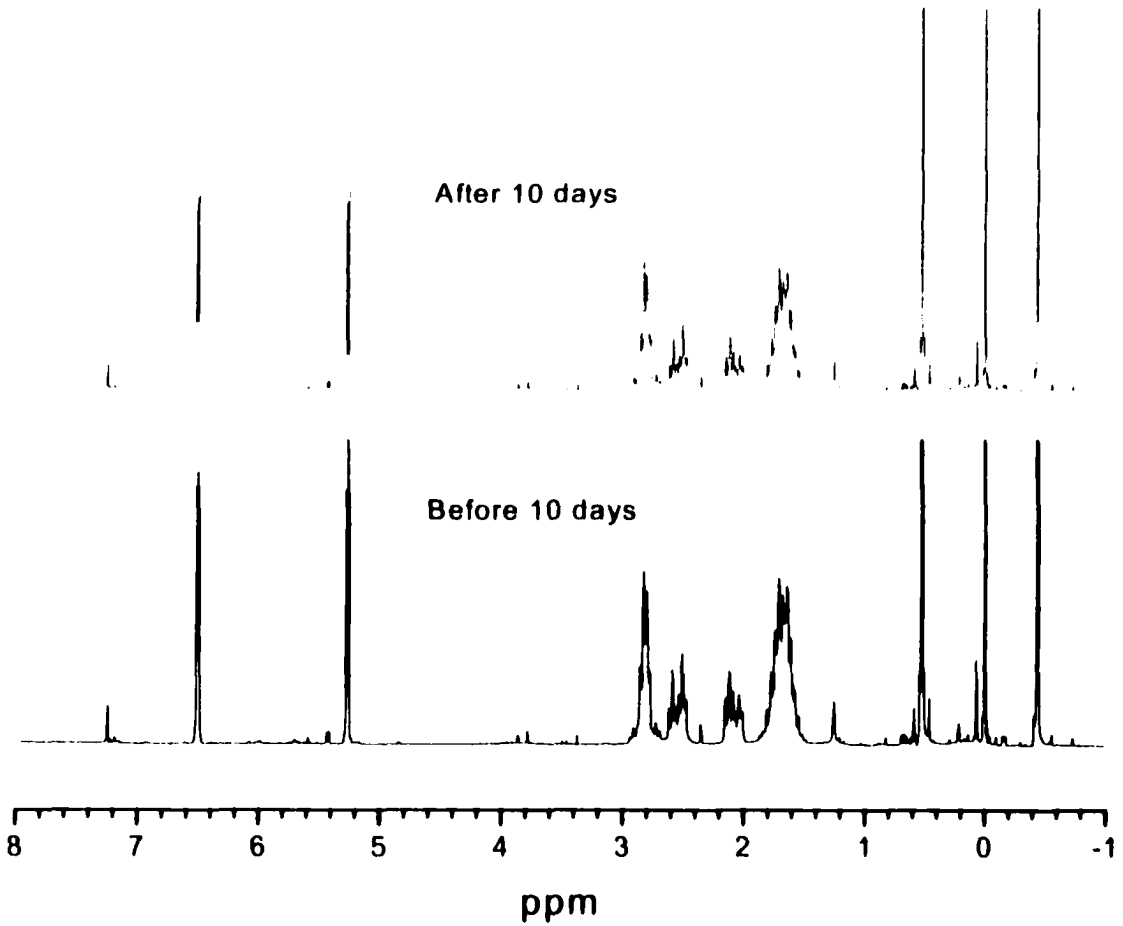

Figure 14. ^{1}H NMR of **2** before and after 10-day's storage in glove-box in solid state.

64

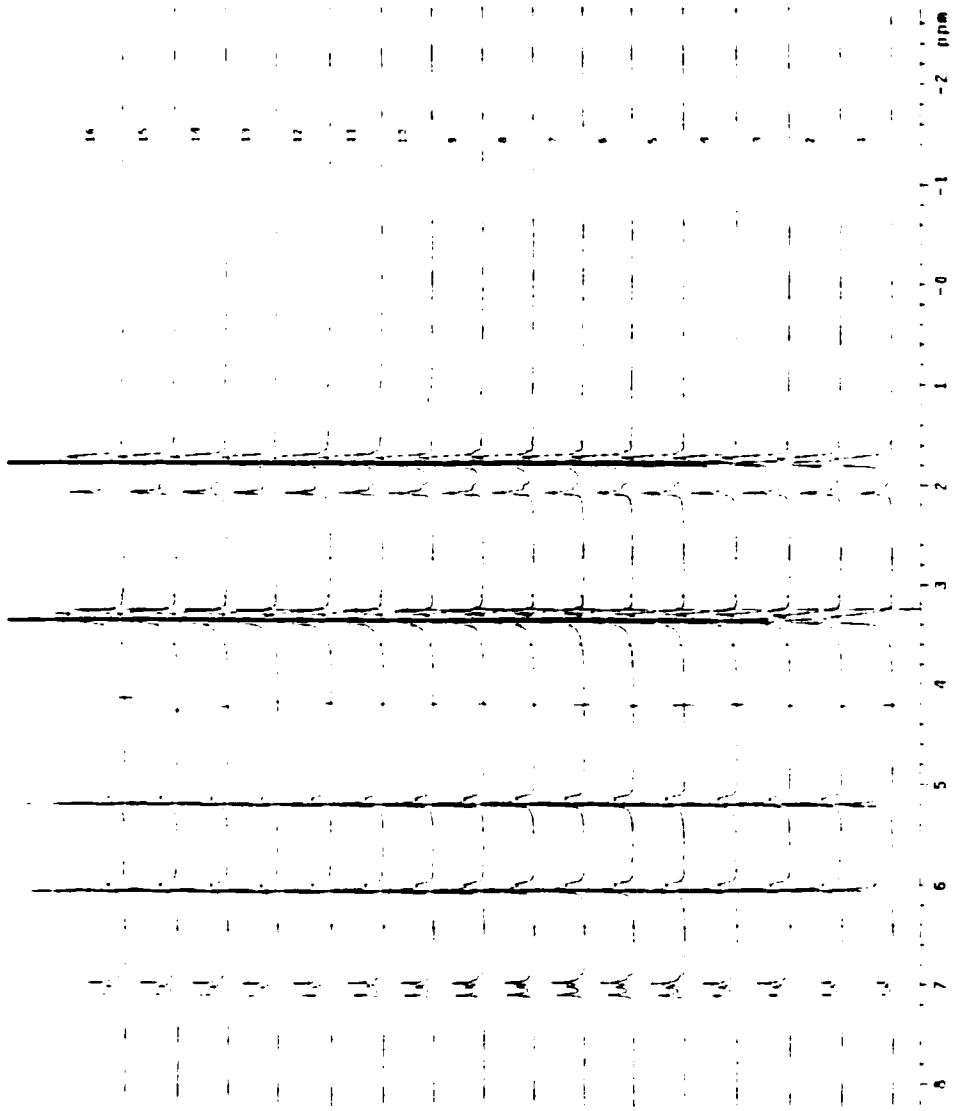

65

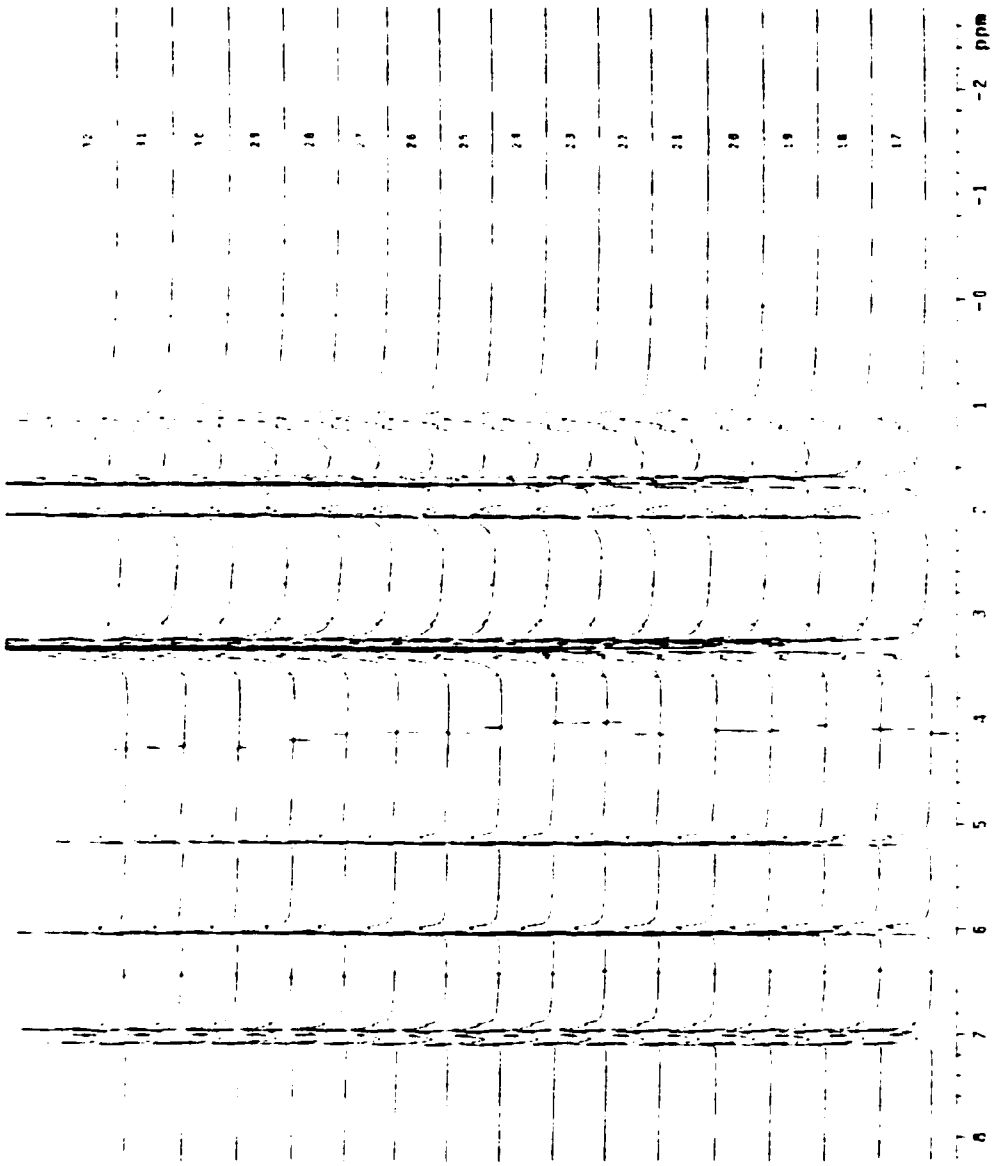

66

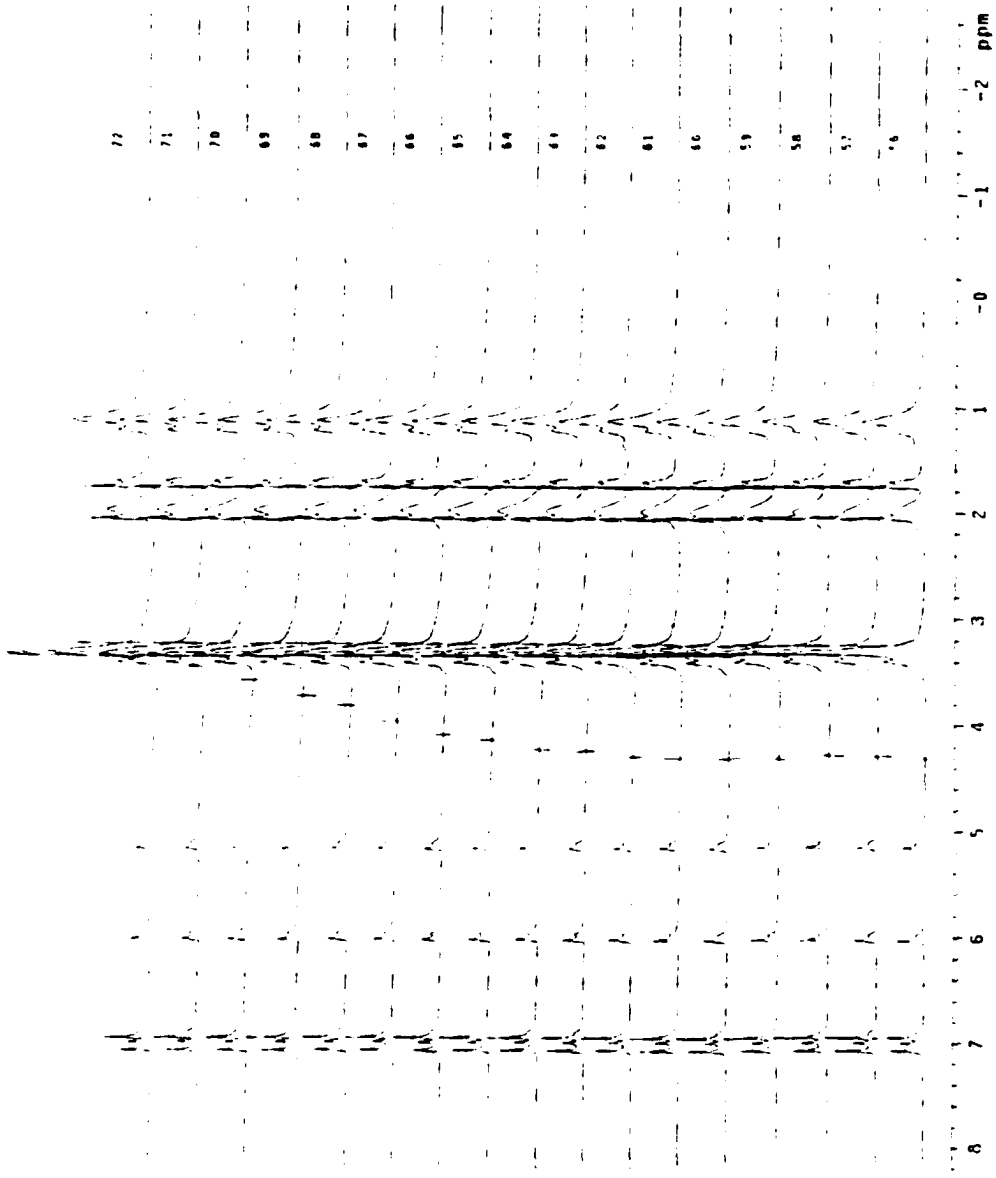

Figure 15. NMR method of monitoring the polymerization of MMA

67

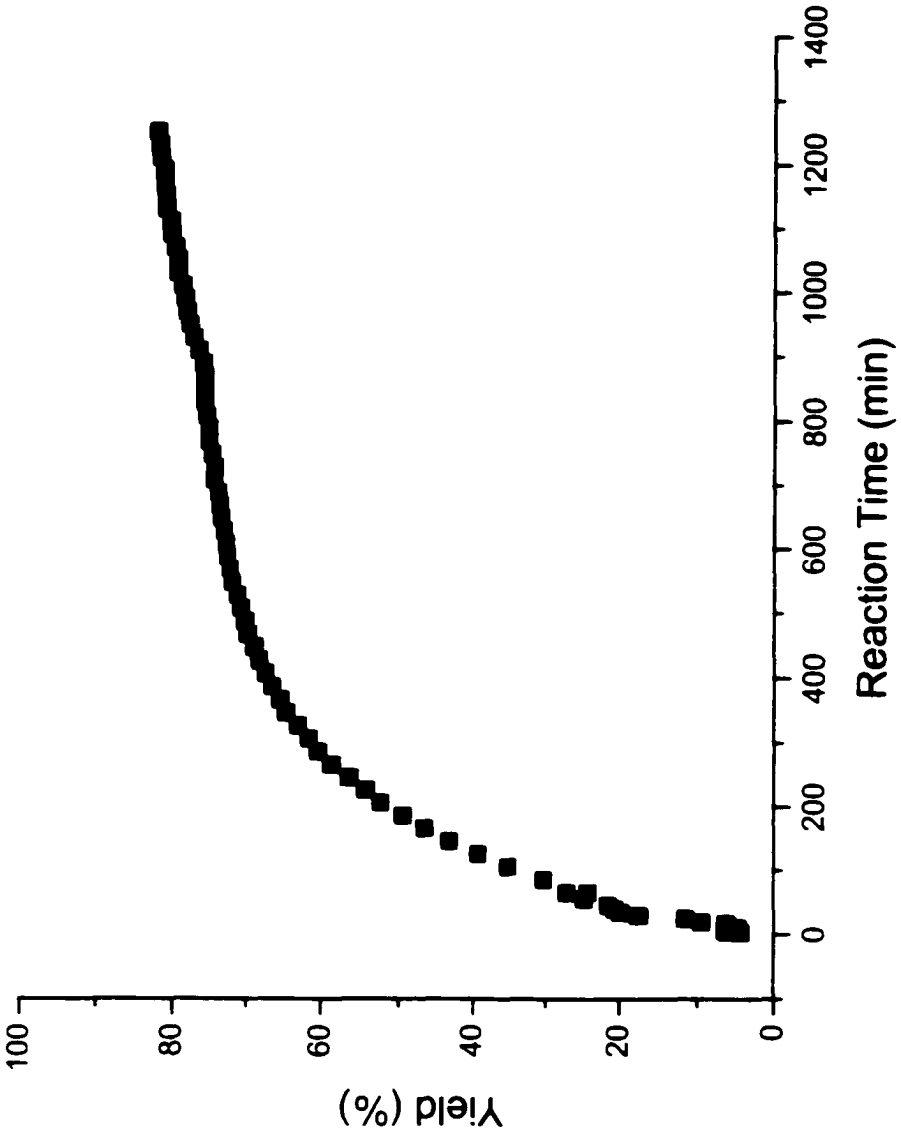

Figure 16. Polymerization of MMA via 1:1 molar ratio of 1/B(C_6F_5)$_3$, observed by NMR method.

conversion of MMA was accomplished in a short period of time (100 min), which may result in a low molecular weight of the polymer (the following study shows that molecular weights of the polymer increase with the conversion) and prevent a full precipitation of such polymer in the nonsolvent. The NMR method, however, can readily detect this low conversion. To search for an efficient initiation system and study the kinetics of the polymerization, the NMR method was used because of its high sensitivity and simple manipulation. However, to further investigate the polymerization systems that have been found via NMR method, the gravimetry method was used to obtain polymer samples at different reaction times. For an efficient polymerization system, since high conversion of the monomer to the polymer is achieved in relatively short time, from the gravimetry method, both polymer samples and kinetics data (yield vs. reaction time) can be obtained and the kinetics data obtained from gravimetry is consistent well with that NMR method. (Figure 17) In Figure 17, the polymerization rate, which is proportional to the slope of %yield vs. reaction time, repeats well from the two methods. However, the curve of %yield vs. reaction time in the NMR method shifted to the right of that in gravimetry method. An induction time was observed in the NMR method. Considering that in the NMR method, no constant mixing of the reaction solution was performed during the polymerization process as was done in the gravimetry method, the induction time may be thus explained. In other words, the real starting time for the polymerization in two methods were different. In the gravimetry method, due to the good mixing, after the addition of the $B(C_6F_5)_3$ solution, the polymerization started and the recorded starting time matched the real one. However, in the NMR method, after the addition of $B(C_6F_5)_3$ solution, due to the lack of constant mixing, the polymerization did not start immediately.

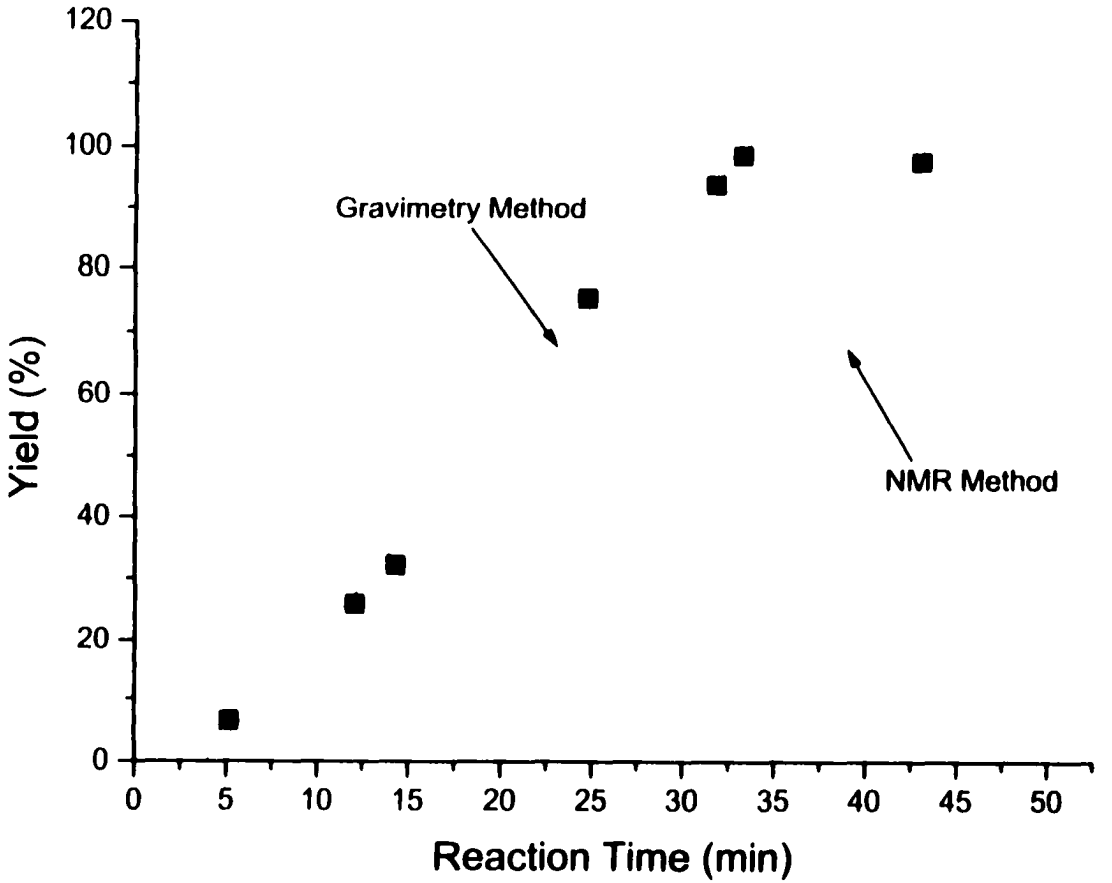

Figure 17. Kinetics plot obtained from gravimetry and NMR method, respectively. $[I]_0$ = 5.0 mM, $[B(C_6F_5)_3]_0$ = 2.5 mM, $[MMA]_0$ =1.0 M, toluene as solvent, temp = 0 °C

Some time was spent on the dispersing of $B(C_6F_5)_3$ to the reaction mixture, the real starting time for the polymerization was later than the recorded one. An apparent induction time was therefore observed.

3.1.3 Reproductivity of the Polymerization

Due to the air-sensitivity of the initiators and coinitiator used in this study, attention should be paid to maintain the activity of the initiation system. When the procedure mentioned in the Experiment Part was followed and the inert atmosphere techniques in 3.1.1 were considered, the repeatability of the polymerization of MMA in this study was good. Figure 18 shows some representative repeatability tests on both systems.

3.2 Polymerization of MMA via Metallocene Initiation Systems

3.2.1 Parameters that Affect the Polymerization

3.2.1.1 Effect of Initiator/Coinitiator Ratio

Initial polymerizations were performed to determine the optimum reaction conditions. More specifically, the effect of initiator/coinitiator ratio and the feeding sequence (i.e. the order of addition of initiator, coinitiator and monomer) on the polymerizations were studied because there are literature reports that indicate these parameters may affect polymerization rate, polymer molecular weight and yield.[15-17,38] The attention was focused on the initiation systems consisting of a dimethyl zirconocene (initiator) and $B(C_6F_5)_3$ (coinitiator). Two dimethyl zirconocenes were used: Cp_2ZrMe_2 (**1**), a general representative of Group 4 metallocene initiators and *rac*-$Me_2Si(IndH_4)_2ZrMe_2$ (**2**), a frequently used isospecific Group 4 metallocene initiator for α-olefin polymerization. Methyl methacrylate was used as the monomer. Two polymerization systems were studied: System 1, in which **1** was used as the initiator, and System 2, in which **2** was the initiator.

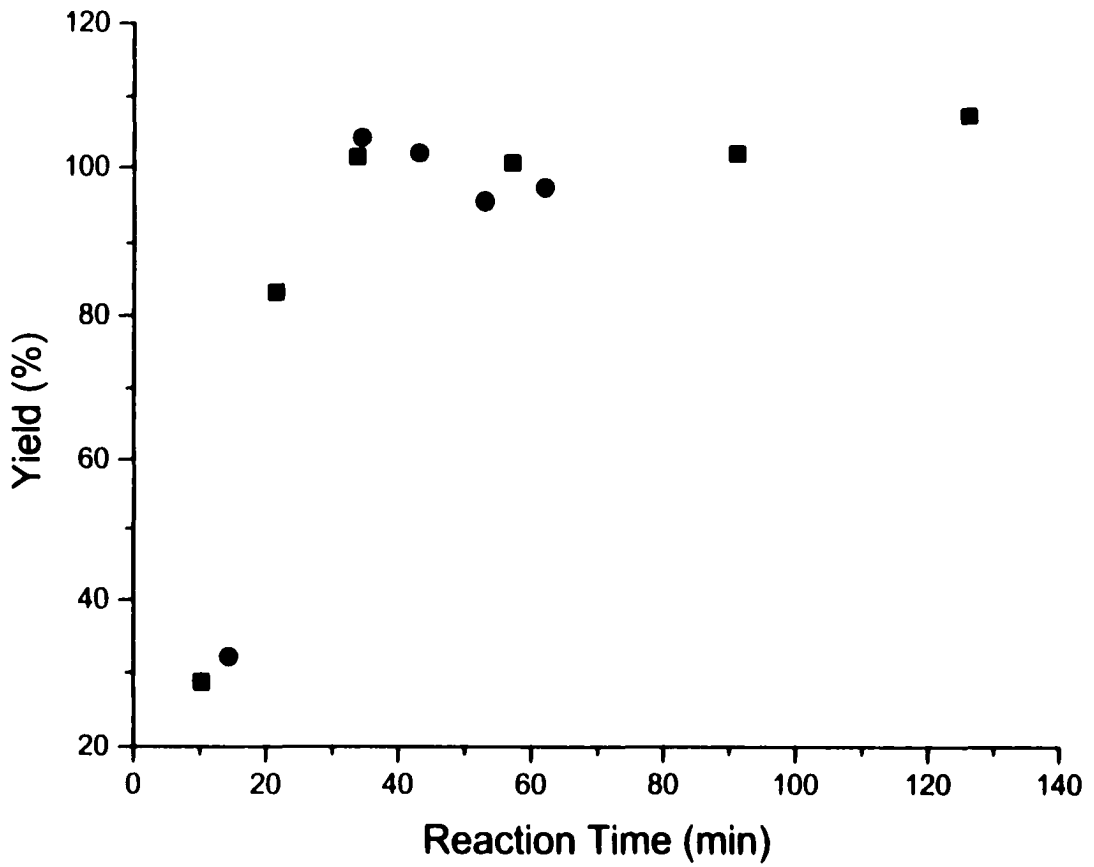

Figure 18. a) Repeatability test of System 1 using gravimetry mthod.
$[1]_0$ = 5.0 mM, $[B(C_6F_5)_3]_0$ = 2.5 mM, $[MMA]_0$ = 1.0 M, toluene as solvent, temp = 0 °C

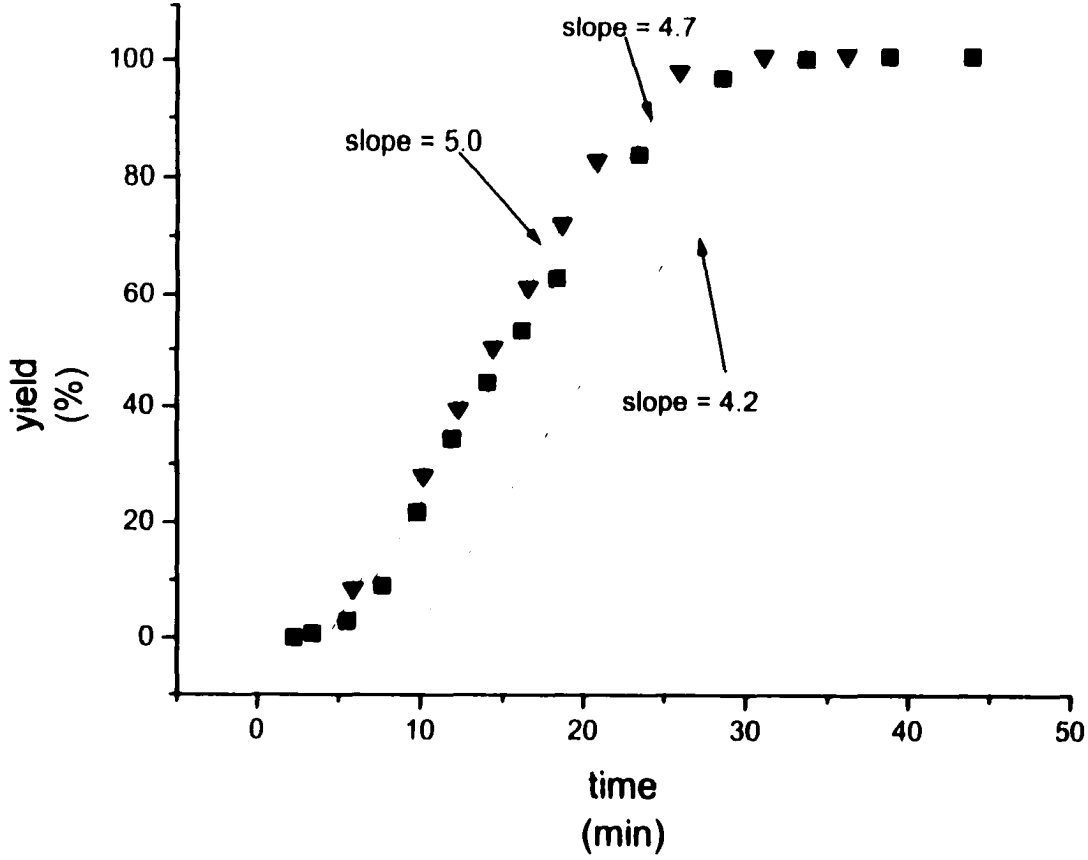

Figure 18. b) Repeatability test of System 1 using NMR mthod.
$[1]_0$ = 5.0 mM, $[B(C_6F_5)_3]_0$ = 2.5 mM, $[MMA]_0$ =1.0 M, toluene as solvent, temp = 0 °C

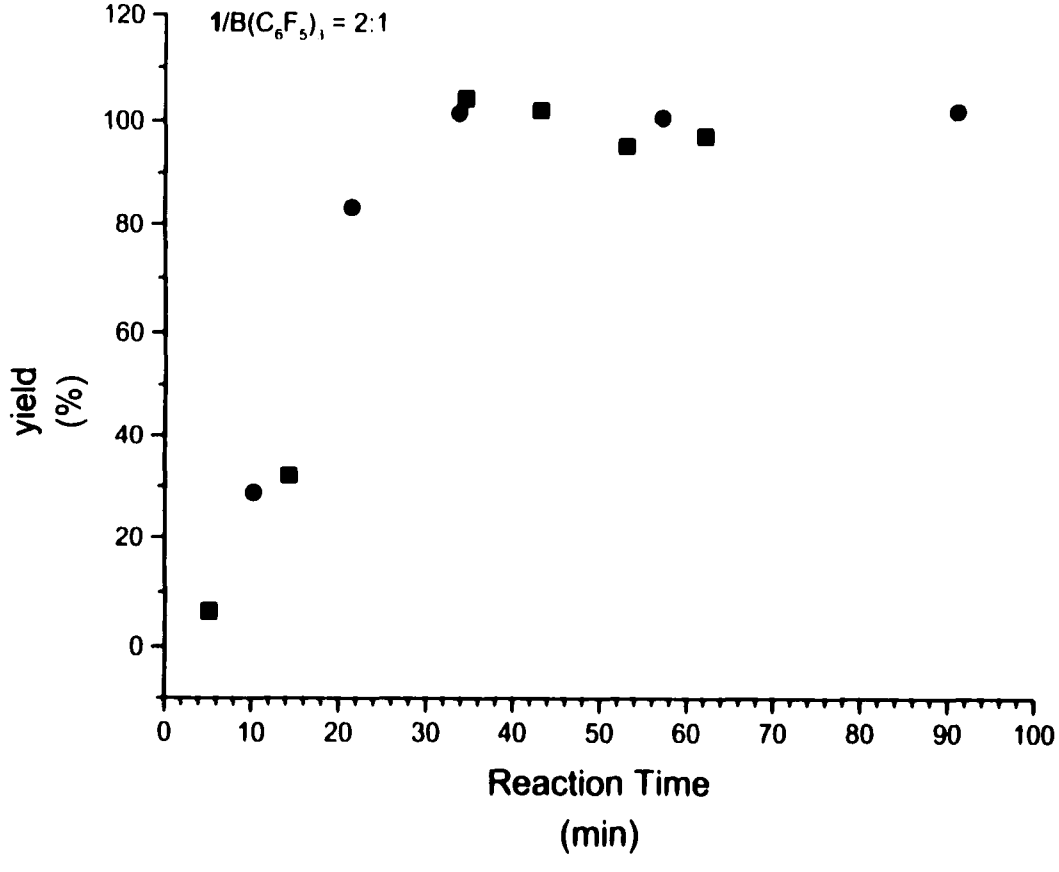

Figure 18. c) Repeatability test of System 1 using gravimetry mthod.
$[2]_0$ = 5.0mM, $[B(C_6F_5)_3]_0$ = 2.5 mM, $[MMA]_0$ =1.0 M, toluene as solvent, temp = 0°C

73

74

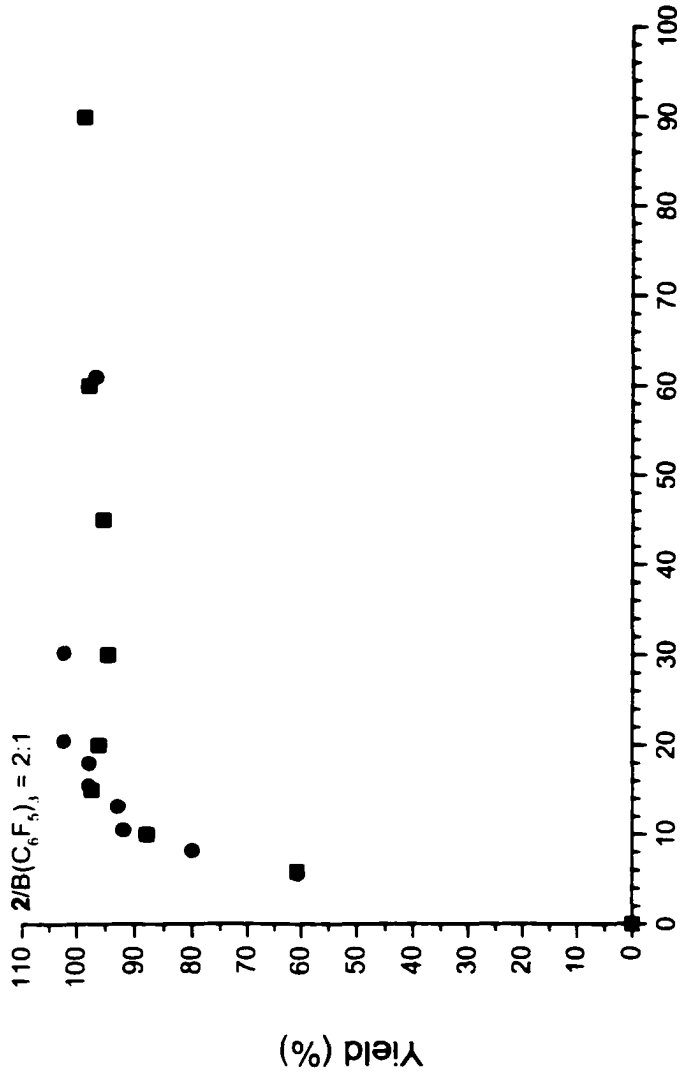

Figure 18. d) Repeatability test of System 2 using gravimetry mthod. $[2]_0$ = 10 mM, $[B(C_6F_5)_3]_0$ = 5.0 mM, $[MMA]_0$ = 1.0 M, toluene as solvent, temp = 22 °C

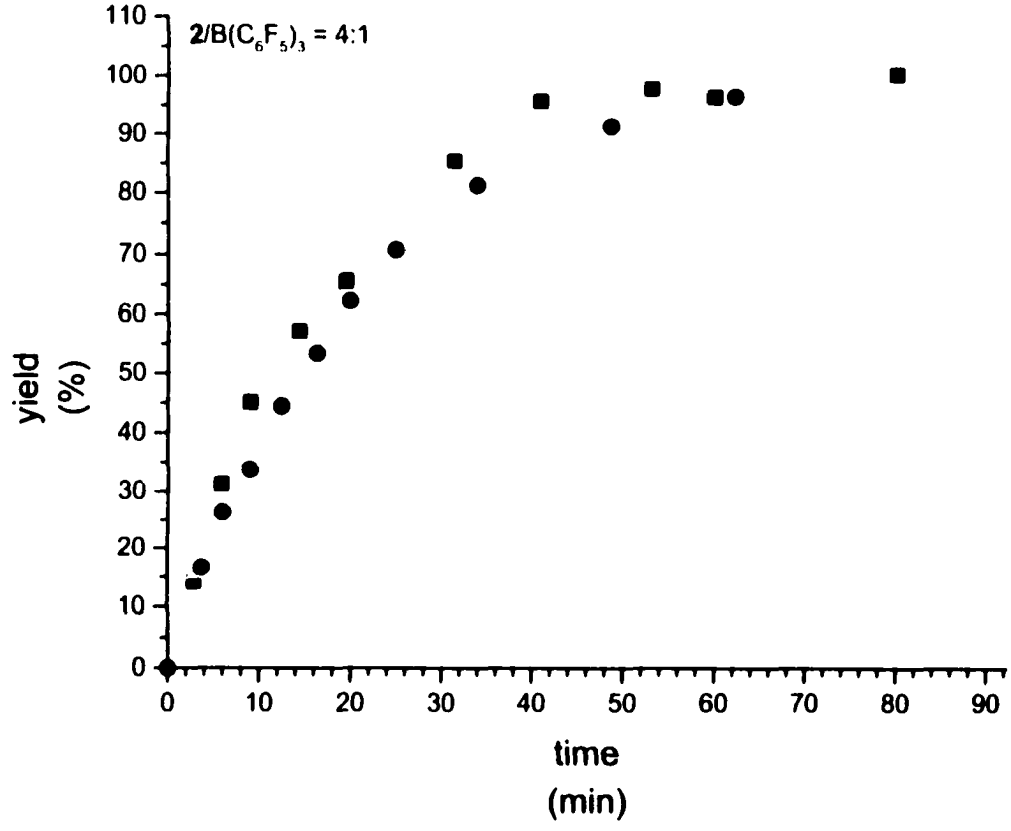

Figure 18. e) Repeatability test of System 2 using gravimetry mthod.
$[\mathbf{2}]_0$ = 10 mM, $[B(C_6F_5)_3]_0$ = 2.5 mM, $[MMA]_0$ =1.0 M, toluene as solvent, temp = 22 °C

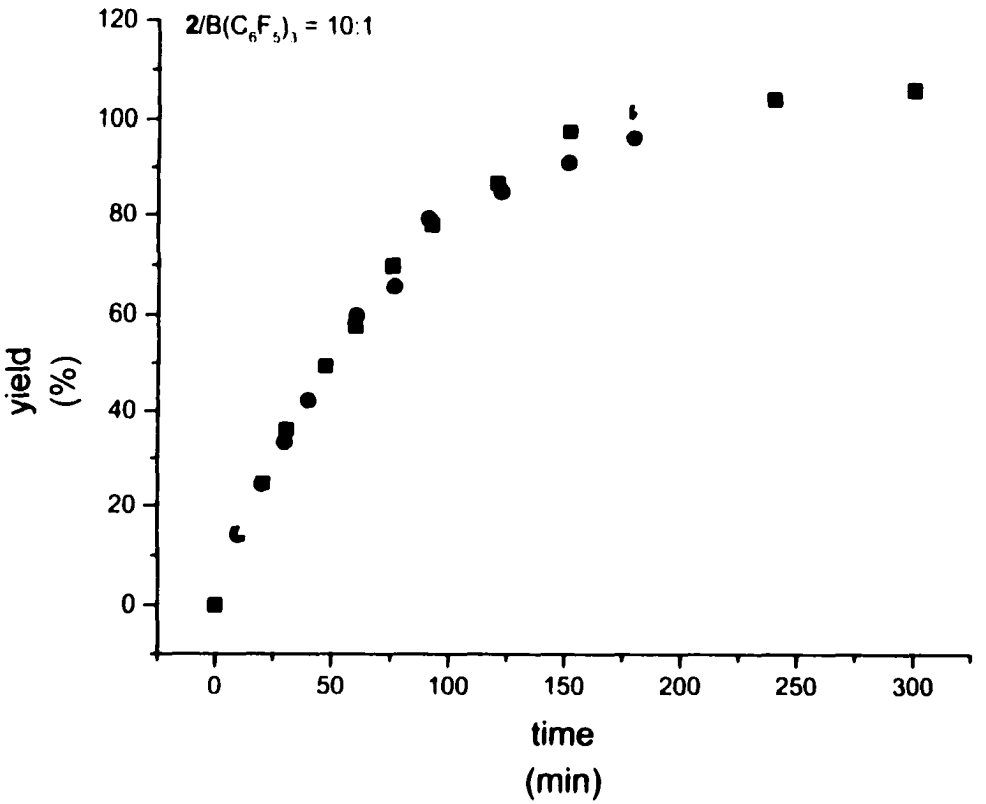

Figure 18. f) Repeatability test of System 2 using gravimetry mthod.

$[2]_0$ = 10 mM, $[B(C_6F_5)_3]_0$ = 1.0 mM, $[MMA]_0$ =1.0 M, toluene as solvent, temp = 22 °C

76

The initiation systems with equimolar amounts of dimethyl zirconocenes and $B(C_6F_5)_3$ show no or very slow polymerization of MMA, which can be detected by the NMR method. By using this method, a series of polymerizations using different ratios of **1**/$B(C_6F_5)_3$ were carried out for System 1. For System 2, however, on the basis of the results from System 1 similar polymerizations were performed using the gravimetry method since only the effective polymerization systems were primarily concerned, and they can be detected nicely by the gravimetry method. The polymerization processes with different ratios of initiator/coinitiator are shown in Figure 19 and the rate constants obtained from these polymerization conversion curves are listed in Table 2.

Table 2 shows that the molar ratio of initiator/coinitiator had a significant effect on the polymerization of MMA. By changing the ratio of dimethyl zirconocene/$B(C_6F_5)_3$ from 1:1 to higher ratios, in System 1, a 20-fold increase in polymerization rate was accomplished. A similar trend also existed in System 2, in which by changing the molar ratio of the two initiation components, the polymerization rate changed from no polymerization in several hours with a 1:1 ratio to a 100% conversion in 1 h with a ratio of 2:1 or higher. There seemed to be a threshold value between 1 and 2 for the ratio of initiator/coinitiator for both initiation systems. Below this value, the polymerization rate increased slowly with increasing value of the initiator/coinitiator ratio; above this value, the polymerization rate increased by an order-of-magnitude. A further increase of the ratio did not result in additional acceleration. In System 1, to be more accurate, the threshold ratio was about 1.4. Therefore, it is safe to say that an initiation system with initiator coinitiator ration of 2:1 was an efficient initiation system. In System 1, moreover, this value can go down to 1.5. When this requirement for the ratio value is

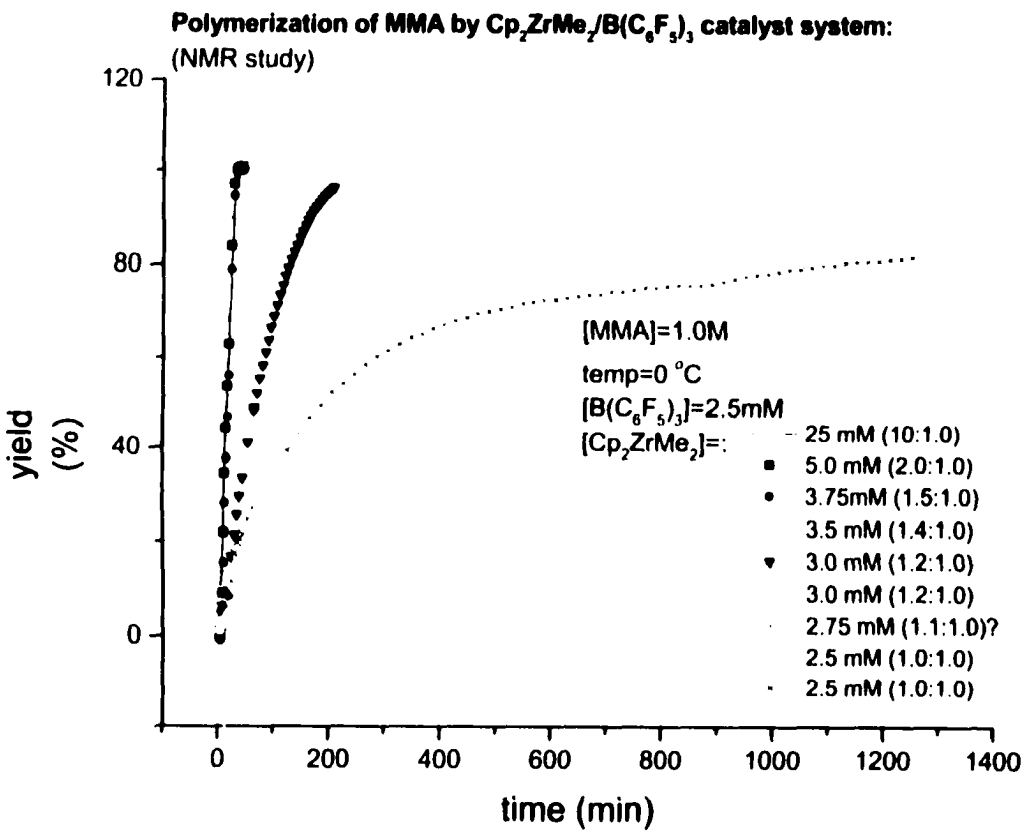

a

Figure 19a. Polymerization of MMA via 1/ $B(C_6F_5)_3$ in different ratios. $[B(C_6F_5)_3]_0$ = 2.5 mM, $[MMA]_0$ =1.0 M, toluene as solvent, 0 °C.

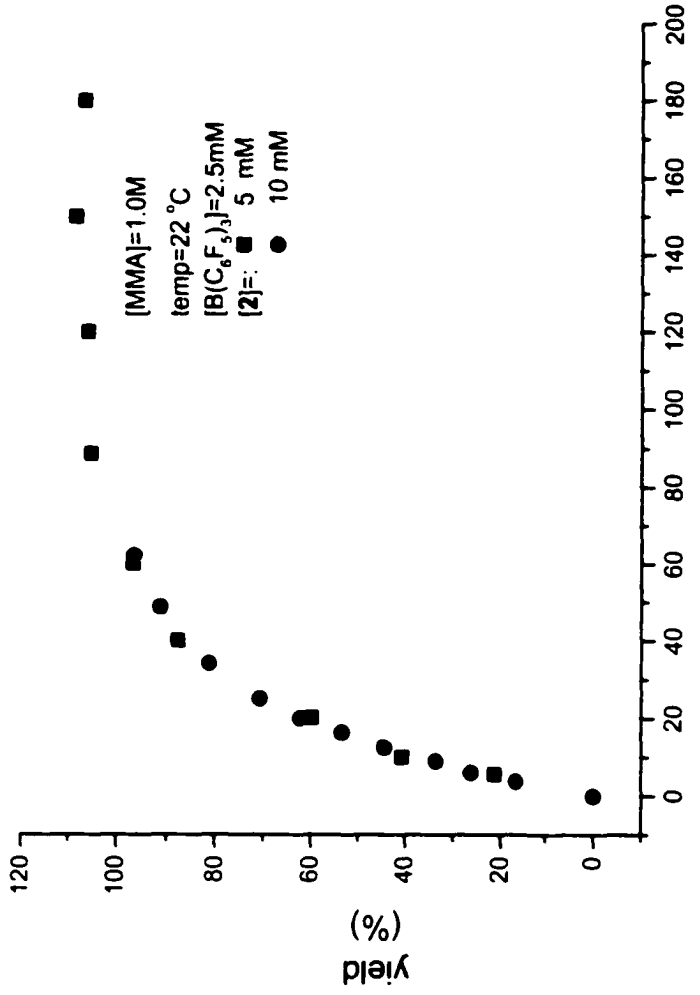

b

Figure 19b. Polymerization of MMA via **2**/ $B(C_6F_5)_3$ in different ratios. $[B(C_6F_5)_3]_0$ = 2.5 mM, $[MMA]_0$ =1.0 M, toluene as solvent, 22 °C.

79

Table 2. Initiator/Coinitiator($B(C_6F_5)_3$) ratio (I/C) effect on the polymerization of MMA[a]

Entry	Initiator	I/C	k_{app}[b] x10^{-2}	%Yield	$\bar{M}_n$ x10^{-5}	M_w/M_n[c]
1[d]	**1**	10:1	3.8	10	1.96	1.2
2[d]	**1**	2:1	4.2	10	2.19	1.2
3[d]	**1**	1.5:1	4.3	10	2.15	1.2
4[d]	**1**	1.4:1	4.1	10	[f]	[f]
5[d]	**1**	1.2:1	0.37	82	[f]	[f]
6[d]	**1**	1:1	0.19	82	3.63	1.4
7[e]	**2**	4:1	5.7	10	0.324	1.4
8[e]	**2**	2:1	5.3	10	0.532	1.2
9[e]	**2**	1:1	No obvious	-	-	-

[a] In all polymerizations, $[MMA]_0$ = 1.0 M, $[B(C_6F_5)_3]_0$ = 2.5 mM. System 1 was performed at 0 °C, System 2 at 22 °C.

[b] Apparent rate constant, for polymerizations in System 1, the units is mol L^{-1} min^{-1} (zero order in [MMA]); for polymerizations in System 2, the unit is min^{-1} (first order in [MMA]).

[c] Measured by GPC on the samples at the final conversion of each polymerization, calibrated by PMMA standards.

[d] By NMR method.

[e] By gravimetry method.

[f] Not measured.

satisfied, an efficient polymerization system for MMA polymerization can be accomplished with these Group 4 metallocenes.

Figure 19a shows that when the ratio of **1**/ $B(C_6F_5)_3$ was between 1.0 and 1.4, there was poor repeatability of the polymerization rate. In System 1, in general, a ratio of 1.2:1 gave a faster polymerization than a ratio of 1:1. However, two runs of the polymerization in the same conditions for ratios of 1:1 and 1.2:1, respectively, showed large deviations, while at high ratio (above the threshold value), the repeatability of the polymerization was quite good (Figure 18b). It seemed that at this critical ratio range (between 1.0 and 1.4), the concentration of the active species in the polymerization system was difficult to control closely. It was very sensitive to small changes in the experimental conditions. Although careful manipulation of the experiments was carried out and all the conditions were kept the same for each run as much as possible, some small uncontrolled or unnoticed variation of the experimental conditions may exist. For example, the extent of the mixing for the reaction mixture at each run, the trace content of moisture in the solvent, the moisture in the air on the day that the experiment was done, etc. It is believed that the extent of the mixing may play a major role in causing the variation since it was the least quantitatively controlled experimental parameter. In the experiment, a Fisher touch mixer was used for the mixing of the content in NMR tubes. However, because 6 ml of total solution was used for the polymerization (in order to keep high precision on the measurement of the amount of the initiator and the coinitiatior), it filled over half the height of the NMR tube, which caused a problem of efficient mixing using Fisher touch mixer. Unfortunately, this situation just happened at the time when the coinitiator $B(C_6F_5)_3$ was charged since a feeding sequence (will be discussed in detail in the later

part of this section) of MMA first followed by solvent, **1** solution, solvent, $B(C_6F_5)_3$ solution and solvent was used . Therefore different extents of mixing between $B(C_6F_5)_3$ and **1** may result. Since no further mixing except turning over the NMR tube once before it was put into NMR probe was performed in the NMR method, the variation of the mixing at this early stage may cause a large difference in the later polymerizations. It was observed that a polymerization with the 1.1: 1 ratio occurred as fast as those with ratios above 1.4:1, (Figure 19a) for which an explanation can not be fully provided. However, when the ratio of **1**/ $B(C_6F_5)_3$ went beyond this critical region, the mixing effect on the generation of the active species in the polymerization system disappeared. Good reproducibility of the polymerization process was then obtained. A rational explanation for the above observation is as follows: the formation of the active species for the polymerization goes through two general steps, in step one, 1 equivalent of initiator and 1 equivalent of coinitiator react and form a complex, **X**, e.g., $Cp_2ZrMe\cdots MeB(C_6F_5)_3$ in System 1; in step two, **X** reacts further with the excess initiator forming the active species. The reaction of step one was reported by Marks and coworkers[111], and was also observed in this lab (Figure 20). This reaction is a fast reaction. When $B(C_6F_5)_3$ was mixed with **1**, the reaction was completed in minutes and all **1** was converted to **X**, indicated (in Figure 20) by the shifting of Cp signal from 5.67 ppm to 5.41 ppm and the total disappearance of the signals of **1** at -0.14 ppm with the appearance of signals at 0.29 and 0.09 ppm, which belong to Zr-CH_3 and $CH_3B(C_6F_5)_3$ in **X**, respectively. **X** was reported by Marks and coworkers as the inactive species in the polymerization of MMA,[117] and the present results also showed that the 1:1 ratio of **1**/$B(C_6F_5)_3$ gave a very slow polymerization of MMA, if not close to no polymerization. Step 2 is the key step in

83

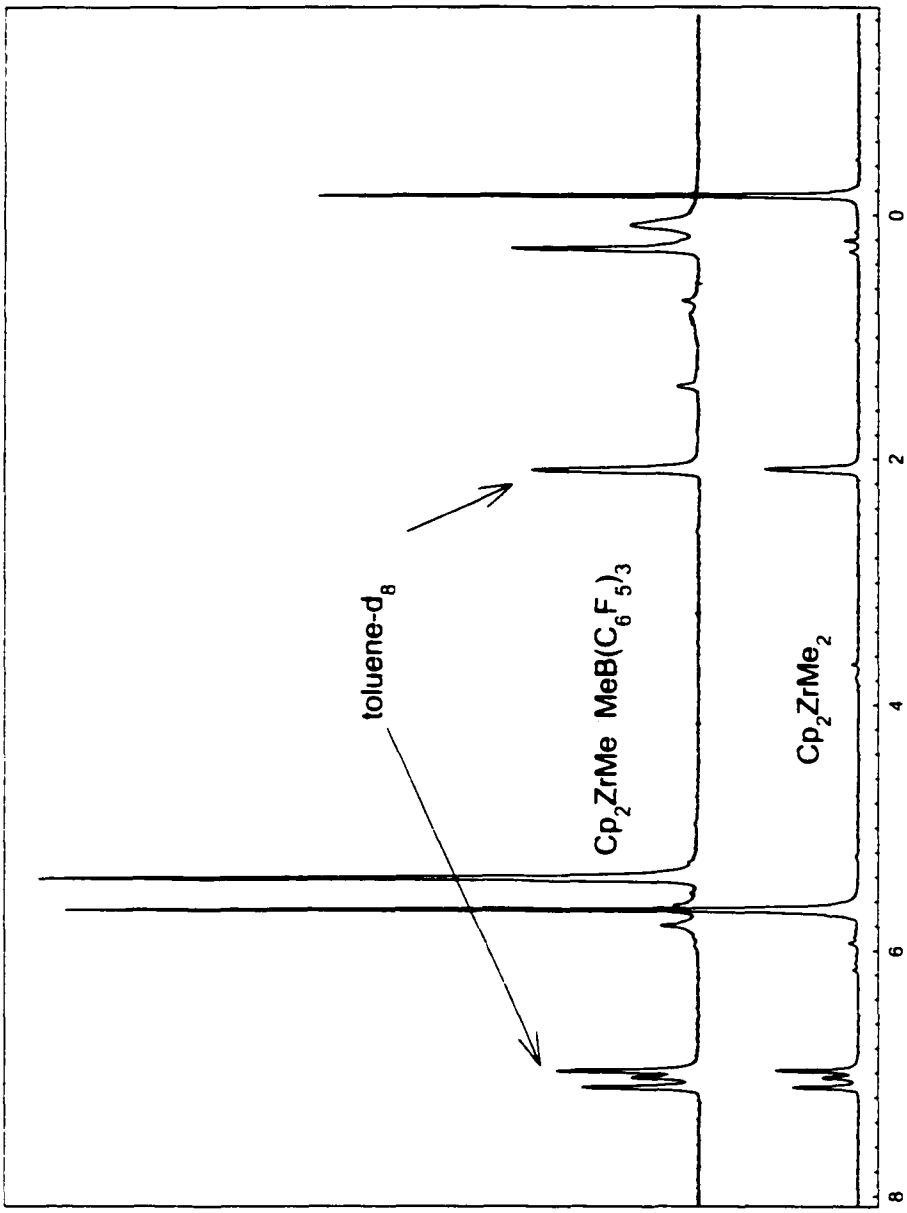

Figure 20. NMR of I and 1:1 of I/B(C_6F_5)$_3$

which the actual active species is generated, although the details of this process are not clear, but is based on the above ratio study. When the ratio of **1**/$B(C_6F_5)_3$ is close to 1, the mixing effect plays a role in affecting the polymerization rate. Inefficient mixing results in high ratio (greater than 1.4) of **1**/$B(C_6F_5)_3$ in some local region, which leads to the formation of the active species and the consequent polymerization. However, efficient mixing leads to the formation of 1 equivalence of **X**, which is inactive to the polymerization. The small amount of the excess of the initiator then reacts with **X** forming a small amout of the active species, therefore, slow polymerization results. When the ratio of **1**/$B(C_6F_5)_3$ is higher, the mixing effect will play a less significant role in the polymerization because some large amount of active species will be formed by the larger access amount of the initiator, no matter where it forms, either from some local region or from the total conversion to **X** followed by the reaction between **X** and the excess initiator. The above scenario also explains why any further excess of the initiator, i.e., increasing ratio of **1**/$B(C_6F_5)_3$ past the threshold value, has no effect on the polymerization rate. Because the further excess of the initiator has no **X** to react with in the system, no more active species will be obtained.

Figure 19b shows the polymerization process of MMA in System 2 with different **2**/$B(C_6F_5)_3$ ratios. Since it was concerned to find a similar active initiation system in System 2, only polymerization tests with ratios of 2:1 and higher were performed to be compared with those of the ratio of 1:1, with which no polymerization was observed after 1 h by the gravimetry method. It shows clearly again the significant effect of the ratio of initiator/coinitiator on the polymerization. With higher ratios (greater than or equal to 2), the polymerization was completed in 1h as observed by gravimetry method.

The above results are an important discovery of this study, which points out that a new simple initiation system of zirconocene can be used to efficiently polymerize MMA, a polar monomer. As mentioned in the introduction, the copolymerization of nonpolar olefins with polar monomers to functionalize the final polymer is a useful goal. Although Group 4 metallocene initiation systems have shown great capability for the polymerization of nonpolar olefins, their application to the polymerization of polar monomer is limited due to the possible poison reactions of polar monomer toward the active propagation center in the polymerization system.

Initiation systems containing Group 4 metallocenes are discovered by Collins,[25,28,29] Soga[15,16,30,31] and Marks[17] and their co-workers. However, all of these systems have some drawbacks. Collins' system needs the separate synthesis of the borate derivative of the zirconocene (e.g. $[Cp_2ZrMe(THF)]^+[BPh_4]^-$) to provide the corresponding cationic zirconocene species (e.g. Cp_2ZrMe^+) in the system. Although they also reported the initiation systems formed directly from dimethyl zirconocene and coinitiator[28], another major disadvantage of their systems is that the coinitiator ($[n\text{-}Bu_3NH]^+[BPh_4]^-$) in their systems is not the appropriate coinitiator for the polymerization of nonpolar monomers (refer to 1.1.2.2). Therefore, the copolymerization of olefins and polar monomers via these initiation systems is difficult to achieve.

Three major drawbacks exist with Soga's system. 1) in their initiation system, a large amount of third component is used, which is not cost efficient; 2) the polymerization of MMA via their initiation systems is not efficient, a typical polymerization time is 24 h, which is too long for a commercial process; 3) The introduction of the third component may damage the original two components' capability

of polymerizing olefins. No polymerization of olefins is reported by Soga's three-component initiation systems.

Marks's initiation system is simple in composition, only a normal dimethyl zirconocene and a special coinitiator (tris(2,2',2"-nonafluorobiphenyl)borane). Both polymerization of MMA and olefins via this initiation system respectively was reported, which shows the potential capability of the copolymerization of polar and nonpolar monomers by this initialization system. However, the synthesis of the above highly hindered coinitiator is not an easy job.

Compared with the above systems, the initiator and coinitiator in the present system are both commonly used for olefin polymerization and have been extensively studied. They are easily synthesized and some of them are commercially available. In addition, because both of the initiation components are used in olefin polymerization, it may be possible to copolymerize olefins with MMA via this initiation system. The tests of the polymerization of olefin (1-hexene) and copolymerization of MMA with 1-pentene via the present system are reported in Section 4.

Recently, Gibson and co-workers[38] reported an active initiation system for the polymerization of MMA with equimolar amounts of dimethyl zirconocenes and $B(C_6F_5)_3$. The feeding sequence was reported crucial for the polymerization, i.e., polymerization only occurred when the initiator and coinitiator were mixed separately prior to monomer addition. However, this work is contradictory to the previous literature reports[15-17] and observation in this lab. A detailed discussion about this difference will be given in the following section after the feeding sequence effect on the present systems is discussed.

3.2.1.2 Effect of Feeding Sequence on Polymerization

The effect of the feeding sequence on the polymerization of MMA was studied for System 1 (Table 3). Compared with the initiator/coinitiator ratio effect, the feeding sequence played a less significant role in the polymerization rate in the present system. Table 3 shows that as long as the optimum initiator/coinitiator ratio was kept, i.e. above 1.4, fast polymerizations were obtained for all feeding sequences. A polymerization rate constant that was at least 10 times as great as that of the system with the ratio of 1 was obtained. However, some variation of the polymerization rate did exist with different feeding sequences. The fastest rate was obtained with a rapid mixing of MMA with both initiation components (Entries A and A'). A mixing of MMA with either initiation component followed by the addition of the other one after a delay time lowered the rate slightly (Entries B and D). The slowest polymerization rate came from an initial mixing of the two initiation components followed by a monomer addition (method C), in which, a precipitate formed in 30 min after the mixing of the two initiation components and disappeared after MMA was added. The corresponding polymerization processes are shown in Figure 21. Neither initiation component was observed to polymerize MMA alone. Table 3 also shows that the molecular weight and MWD of the final polymer were the same regardless of the feeding sequence.

The above results suggested that in this polymerization system the propagating center was formed from all of the three reaction components (initiator, coinitiator, MMA). The complex formed from the two initiation components was not by itself the propagating center. The participation of MMA was necessary, which reacted with the precipitate formed from the two initiation components and converted it to the initial

Table 3. Effect of feeding sequence on the polymerization[a]

Entry	Feeding Sequence[b] 1	2	3[c]	4	k_{app}[d] x 10^{-2} ($mol \cdot L^{-1} \cdot min^{-1}$)	$\bar{M}_n$[e] x 10^{-5}	$\bar{M}_w/\bar{M}_n$[e]
A	MMA	**1**	0 min	$B(C_6F_5)_3$	4.2	2.10	1.2
B	MMA	**1**	22 min	$B(C_6F_5)_3$	3.3	2.19	1.2
C[f]	**1**	$B(C_6F_5)_3$	30 min	MMA	1.6	2.14	1.2
A'	MMA	**1**	0 min	$B(C_6F_5)_3$	4.3	2.10	1.2
D	MMA	$B(C_6F_5)_3$	66 min	**1**	3.1	2.15	1.2

[a] For all entries, $[MMA]_0$ = 1.0 M, $[B(C_6F_5)_3]_0$ = 2.5 mM, temp = 0 °C, toluene as solvent. For entries A, B and C, $[\mathbf{1}]_0$ = 5.0 mM, for entries A' and D, $[\mathbf{1}]_0$ = 3.75 mM.

[b] Performed according to the order of 1 -> 2 -> 3 -> 4 as listed. After each addition of the components, thorough mixing was carried out. The total solution was diluted to the calibrated marker immediately after 4 was charged.

[c] Delay time: time elapsed between the addition of 2 and 4.

[d] Apparent rate constant. All polymerizations here were zero order in [MMA].

[e] Determined by GPC, calibrated by PMMA standards.

[f] After mixing 1 and 2, a brown precipitate appeared in 30 min, which disappeared after the addition of 4.

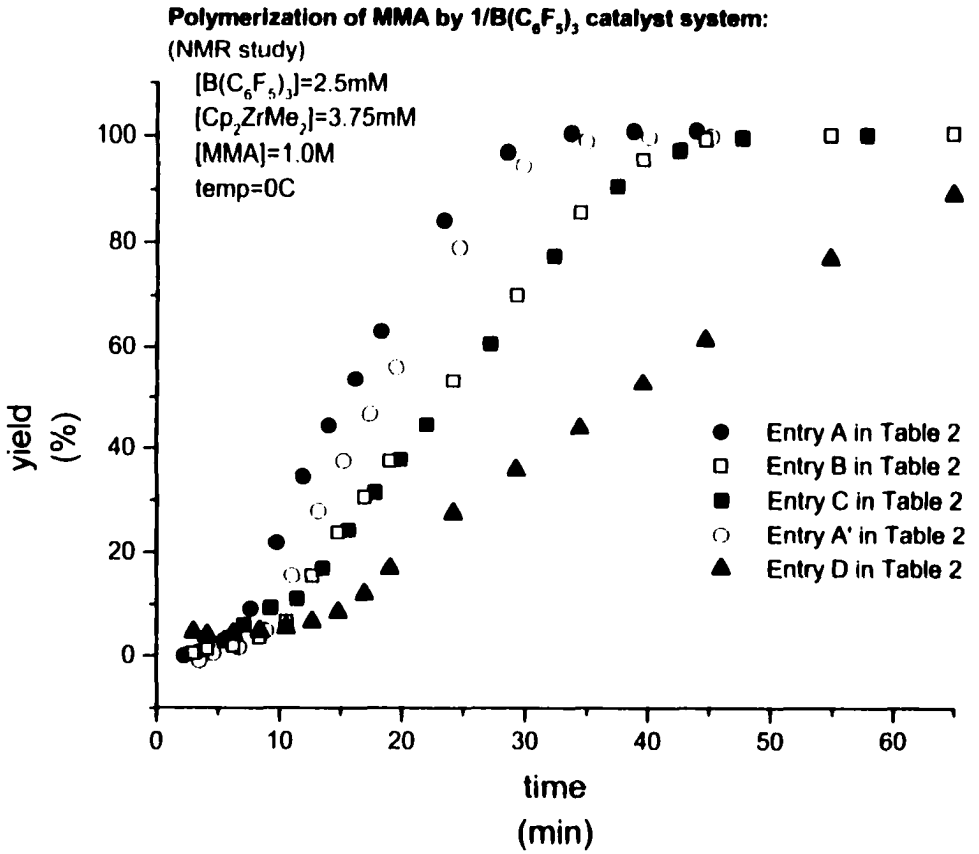

Figure 21. Feeding sequence effect on the polymerization of MMA by **1**/$B(C_6F_5)_3$ (2:1) initiation systems.

$[\mathbf{1}]_0$ = 5.0 mM, $[B(C_6F_5)_3]_0$ = 2.5 mM, $[MMA]_0$ =1.0 M, toluene as solvent, temp = 0 °C.

propagating center. This conversion may take some time, resulting in a low polymerization rate. Some complexes may also form if MMA was first mixed with either initiation component, and there may be a slow conversion from them to the initial propagating center when the other initiation components were added. A complex formed between MMA and $B(C_6F_5)_3$ is reported by Gibson *et al.*[38] After the formation of the initial propagating center, polymerization started, which led to the final polymer with the same molecular weight and MWD no matter which feeding sequence was used.

In contrast to Gibson's work, the feeding sequence of the present system is not the predominant factor for the efficient polymerization of MMA. There are some more differences between the present systems and those of Gibson's.

To explain the lack of polymerization of MMA via equimolar amount of dimethyl zirconocene and $B(C_6F_5)_3$ in the literature,[15-17] Gibson *et al* wrote "In the procedure reported by Soga and co-workers, the zirconocene is added to the monomer in toluene *followed* by addition of the $B(C_6F_5)_3$ activator. Under these conditions, it seemed likely that the borane would form a strong interaction with the Lewis basic carbonyl oxygen of the monomer and that this may prevent the borane activating the zirconium center" and they used NMR study to confirm the existence of the adduct formed between MMA and $B(C_6F_5)_3$. The present results agreed with the fact that the adduct from MMA and $B(C_6F_5)_3$ exists, but showed that their proposed explanation was not correct. In the present initiation system with a higher ratio of dimethyl zirconocene/ $B(C_6F_5)_3$, when the exact same feeding procedure as Soga's was taken, i.e., "the zirconocene is added to the monomer in toluene *followed* by addition of the $B(C_6F_5)_3$ activator", polymerization of MMA did occur, which is shown by A, A' and B in Table 3. Mixing MMA with $B(C_6F_5)_3$

followed by the addition of dimethyl zirconocene **1** (Entry D, Table 2) also gave a polymerization of MMA, although at a slower rate. The reduction of the rate can be explained by the adduct formed between MMA and $B(C_6F_5)_3$. However, according to Gibson's proposal, no polymerization should occur in this feeding sequence.

In their paper, Gibson *et al* also stated that "the two-component system of a dimethyl zirconocene and Lewis acid activator (usually $B(C_6F_5)_3$) can initiate controlled and rapid formation of poly(MMA) as long as the active species is formed before monomer addition. If this is not the case, then the Lewis basic monomer binds to the alkyl abstractor, rendering it ineffective". However, an experiment according to their method was carried out for both **1** and **2** with equimolar amount of $B(C_6F_5)_3$, respectively, in this laboratory. No fast polymerization was obtained. The results of the present 2:1 initiation system showed that the active species was not formed from the two initiation components exclusively and the first combination of the dimethyl zirconocene and $B(C_6F_5)_3$ formed some precipitate, which led to a slower polymerization rate than those of other feeding sequences. The present results showed that the predominate factor for fast polymerization of MMA was the molar ratio of two initiation components rather than the feeding sequence.

Gibson's polymerizations were run at $[B(C_6F_5)_3]_0$ = 50 mM, which is 10 times the concentration used in the present work. This may be the reason why their polymerization of MMA by **1**/ $B(C_6F_5)_3$ finished in 2 min, roughly 10 times faster than the present polymerization rate. However, all their polymerizations were performed in a glove-box, thus no kinetic data were given in their paper. The detailed kinetics of the present polymerization system was studied and the results are given in later sections.

To try to accommodate the similarities and differences between the present systems and Gibson's, special attention was paid to the polymerization procedure used by Gibson *et al.* All their polymerizations were performed in the glove-box and the 1 mL of $B(C_6F_5)_3$ solution in 50 mM was added to 1 mL of **1** solution in 50 mM followed by the addition of MMA. As discussed in section 3.2.1.1, the molar ratio of **1**/$B(C_6F_5)_3$ between 1 and 1.4 is a critical region that is hard to control well. Some unnoticed and uncontrolled experimental conditions may cause large differences in the polymerization rate. Based on the glove-box manipulation experience in this lab, some quantitative operations, as simple as transferring solutions, are not easy to handle in the glove box. Total transfer of $B(C_6F_5)_3$ solution to **1** solution requires careful operation and rinsing the $B(C_6F_5)_3$ vessel and any transferring tools, e.g., syringe, several times. An incomplete transfer of $B(C_6F_5)_3$ will automatically bring the **1**/$B(C_6F_5)_3$ ratio from 1:1 to higher values, which become an active system for MMA polymerizations.

3.2.1.3 Effect of the Excess Initiator on the Polymerization

As long as the initiator/coinitiator ratio is above the threshold value, efficient polymerization is obtained. Further excess of the initiator did not bring any further improvement in the polymerization rate or any effect on the molecular weight of the final polymer. An excess amount of the initiator plays no role in the polymerization. However, when the concentration of the coinitiator, $B(C_6F_5)_3$, is low, a side effect of the initiator on the polymerization occurs. Figure 22 shows this effect in System 2. At low concentration of $B(C_6F_5)_3$, i.e., 1 mM, polymerization leveled off at low conversion (about 20%) for a 2:1 initiation, which was always true for every trial done in this lab. However, when a high ratio was used, e.g. 10:1, and all other conditions were the same, the polymerization

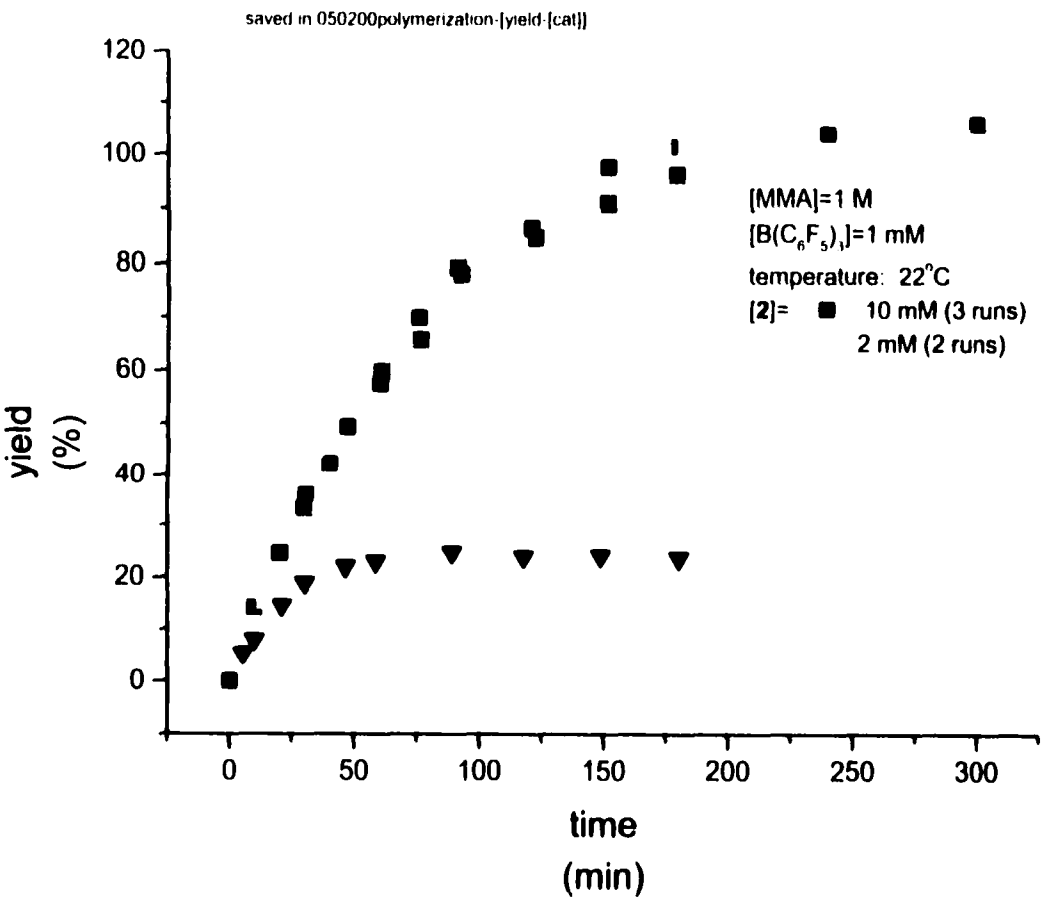

Figure 22. Effect of the excess initiator on the polymerization (in System 2).

went to quantitative conversion readily. This observation suggests that the excess initiator **2** acted as a scavenger in the polymerization system that prevented the deterioration of the active species from the residual impurities in the systems.

Other effects of the excess initiator are shown in 3.2.2.2.2, 3.2.2.3.1 and 3.2.2.3.2.

3.2.1.4 Solvent Effect on the Polymerization

Figure 23 shows a solvent effect on the polymerization in System 1. Polymerization of MMA can be achieved via this 2:1 initiation system in a solvent with higher dielectric constant, e.g., chloroform ($\varepsilon = 4.3$), than those of the less polar hydrocarbon solvents ($\varepsilon <$ 2.2, hexane, pentane, benzene and toluene, etc.). This may be ascribed to the strong nucleophilicity of the polar monomers, which makes the polar monomer the winner in the competition for coordination to the electro-deficient active propagation center between the solvent and the monomer molecules. However, with increasing polarity of the solvent, the competition from the solvent grows, therefore, the polymerization rate decreases.

3.2.1.5 Ratio Effect Explanation:

To better understand the above ratio effect, a rational explanation is gives as following (Schem 16):

Scheme 16

Initiation:

$$I + C \underset{}{\overset{K_1}{\rightleftharpoons}} X \qquad (1)$$

$$X + MMA + I \overset{K_2}{\rightleftharpoons} A \qquad (2)$$

Propagation: $A + MMA \rightarrow Polymer$ (3)

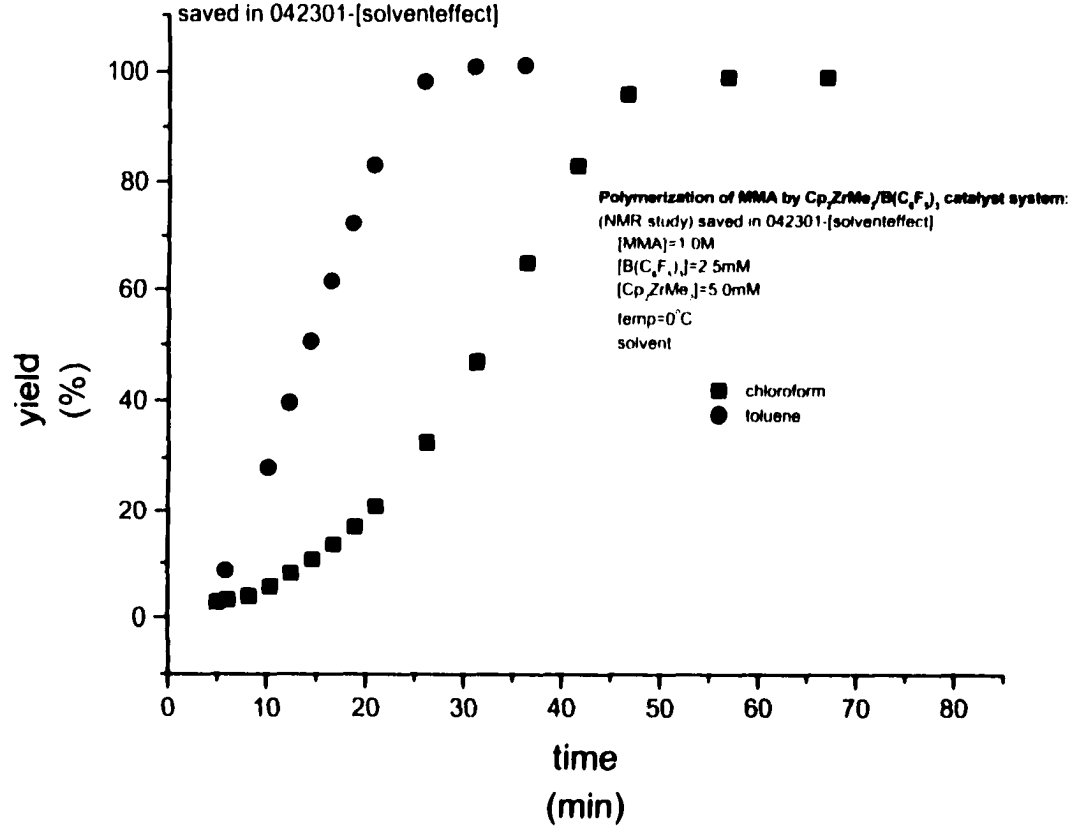

Figure 23. Effect of the solvent on the polymerization of MMA (in System 1).

95

Where, I stands for initiator, C for Coinitiator, X for the complex formed from equimolar amount of I and C and A for chain initiation species.

The polymerization was performed by first mixing monomer MMA with the initiator in solvent, then the coinitiator was added. Very quickly, equimolar amounts of I and C reacted and complex X was formed. The newly formed X has an ion-pair structure and reacted with monomer MMA and excess I to produce the chain initiation species. The whole process is considered to involve an equilibrium. Consequently, monomers grew onto the chain initiation species by a polymer transfer mechanism between two metal centers in A,[17,25,28,29] and the concentration of the active species was not changed during the polymerization process.

Suppose the initial concentration of C is c, the initial concentration of I is nc, and the initial concentration of MMA is 400c, as used in present experiments. After all the reactants were added to the system, two equilibria in Scheme 16 were established, and the relationship between concentrations of various species in the system were as follows:

	$I + C \underset{}{\overset{K_1}{\rightleftharpoons}} X$			$X + MMA + I \overset{K_2}{\rightleftharpoons} A$			
initial conc.	nc	c	0	0	400c	nc	0
conc. at equilibrium:	nc-y-x	c-y	y	y-x	400c-x	nc-x-y	x

Therefore,

$$K_1 = \frac{y}{(nc - y - x)(c - y)} \qquad (4\text{-}1)$$

$$K_2 = \frac{x}{(y - x)(400c - x)(nc - x - y)} \qquad (4\text{-}2)$$

Considering that x is much less that 400c, 400c-x can be replaced by 400c. In the present experiment, 400c = 1 M was used. Therefore, rearranging Equation 4-2, Equation 5-1 was obtained:

$$x = K_2(nc - x - y)(y - x) \qquad (5\text{-}1)$$

From Equation 4-1, the relationship between y and x can be solved as:

$$y = \frac{-b \pm \sqrt{b^2 - 4aC}}{2a} \qquad (5\text{-}2)$$

where $a=K_1$,

$b=K_1x-K_1c-K_1nc-1$ and

$C=K_1nc^2-K_1cx$.

Replacing y in Equation 5-1 by Equation 5-2, an equation for x was obtained, which shows the relationship between the concentration of active species A and the concentration of initiator (or coinitiator). If K_1,K_2 are given and c is known, the relationship between the concentration of active species (x) and the amount of initiator (nc) can be obtained from Equation (5-1). In the present experiment, c = 2.5 mM. Picking different values of K_1 and K_2, the Equation 5-1 was solved numerically (Appendix A). The relationship between the concentration of A and that of the initiator was therefore shown in Figure 24. Assuming that the concentration of the active species in the system is constant throughout the polymerization, the polymerization rate is directly proportional to the concentration of [A], so Figure 24 also depicts the relationship between the polymerization rate and the concentration of the initiator. It is shown in Figure 24 that when K_1 and K_2 are both greater than 10^5, the calculated relationship between [A] and [initiator] fits well with the experimental results. Some combination of K_1 and K_2 shows

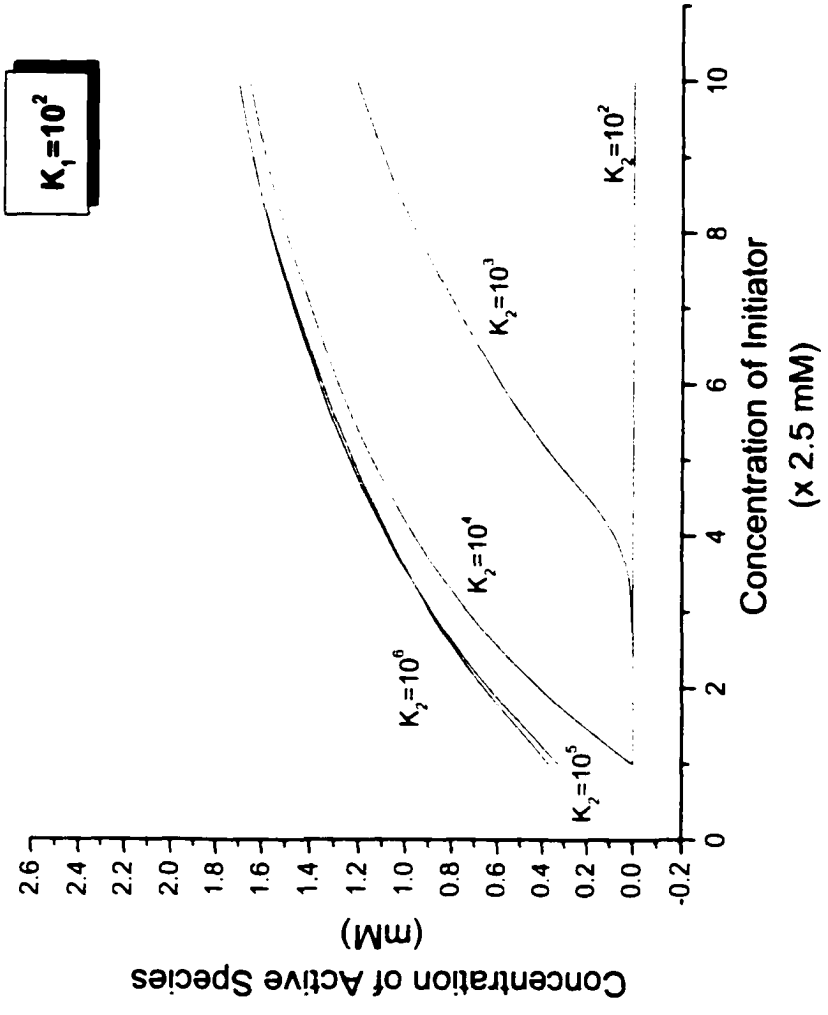

98

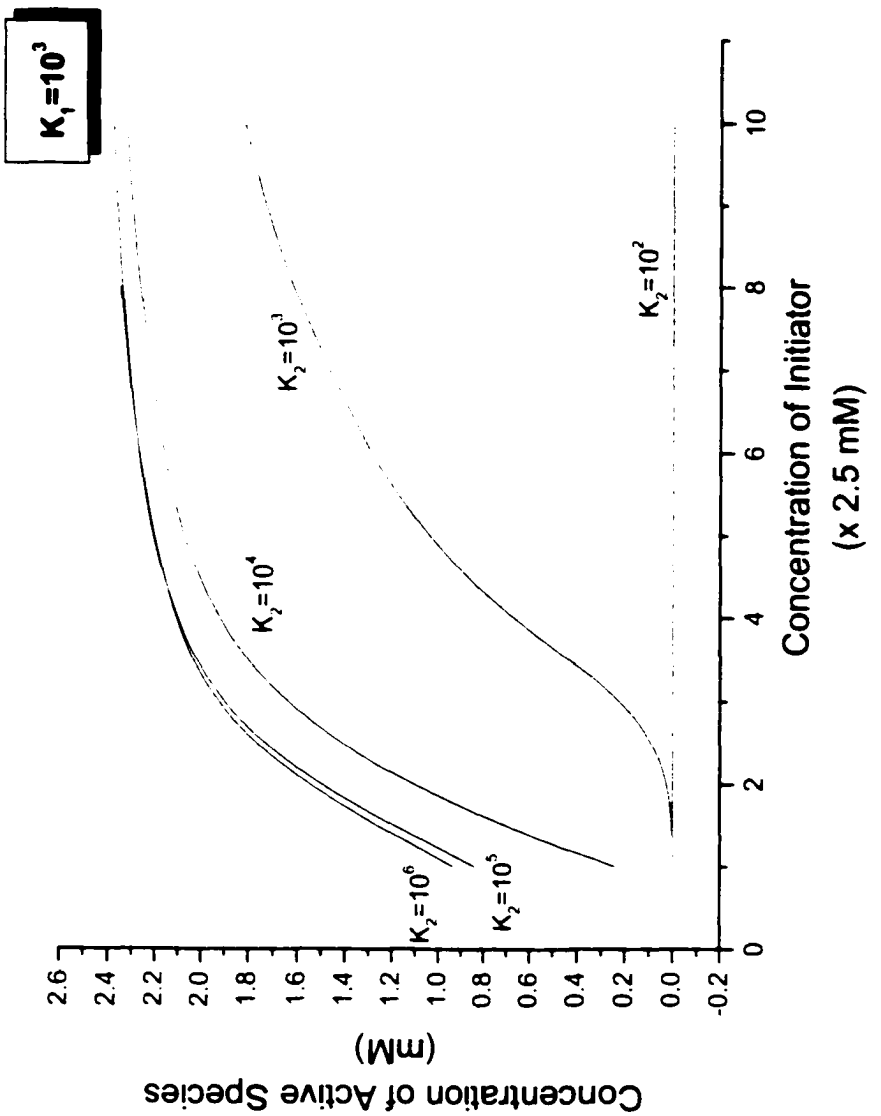

100

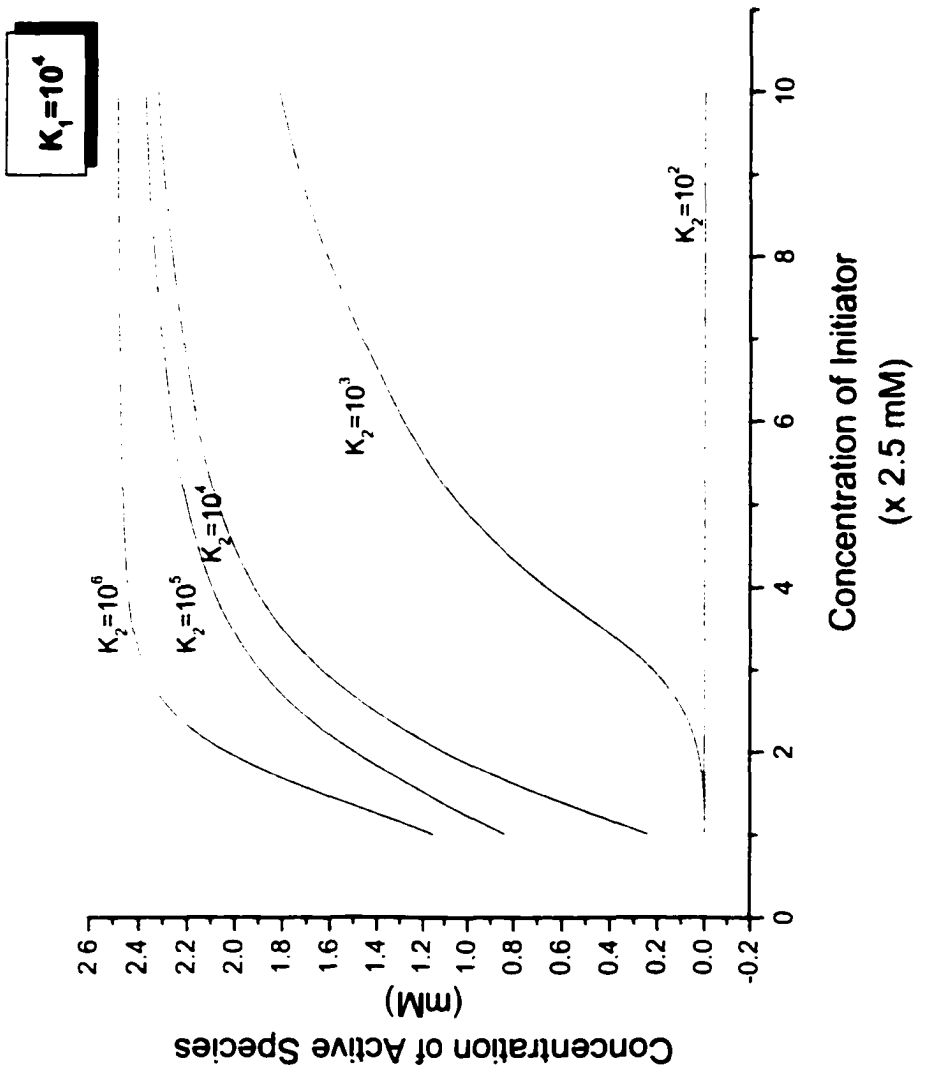

101

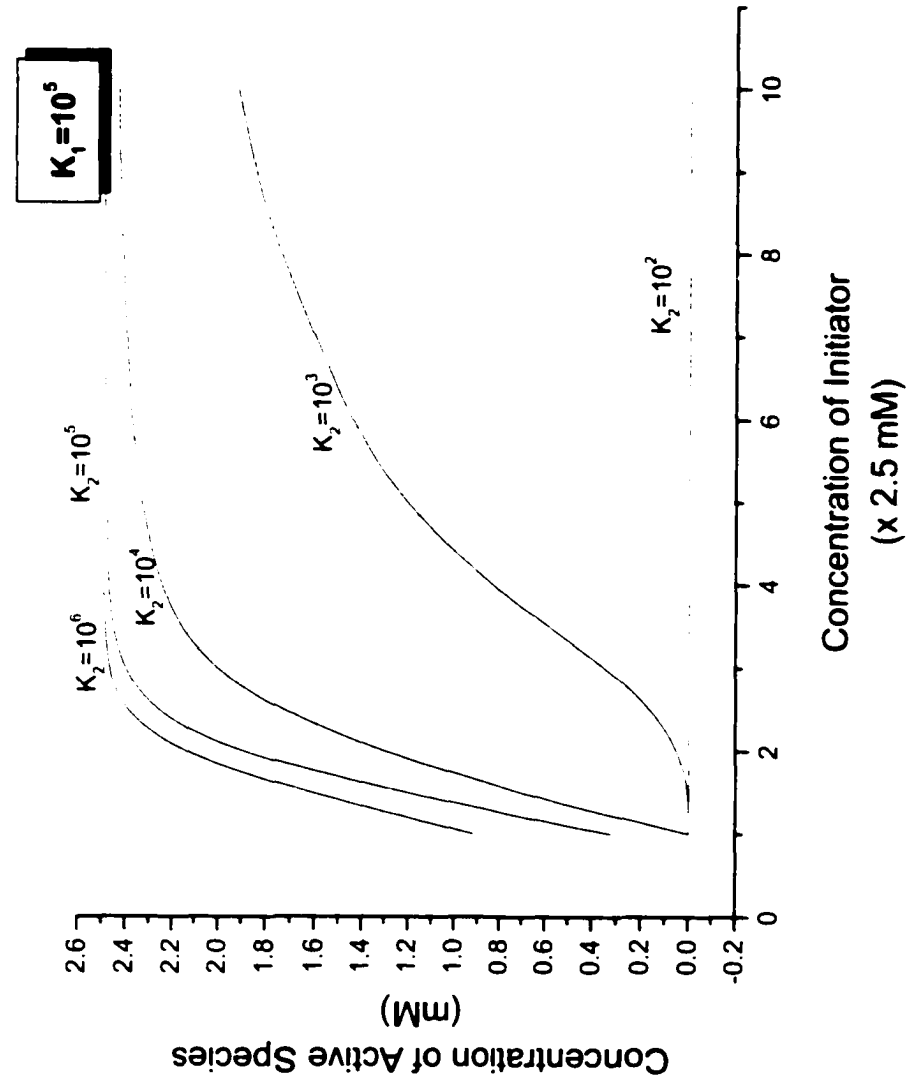

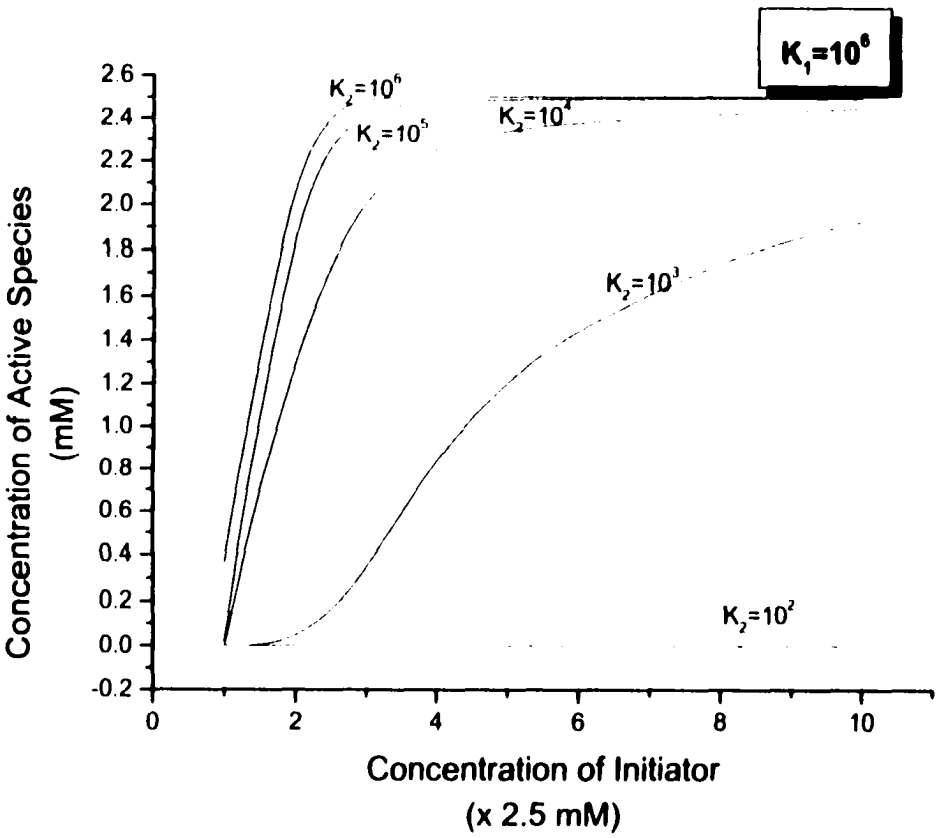

Figure 24. Calculated relationship between [A] and [I] based on the mechanism in Scheme 16.The initial concentration of coinitiator [C] = 2.5 mM.

102

also that a 1:1 ratio of initiator/coinitiator may generate a low concentration of active species, which explains why some 1:1 systems are reported to be active.

Based on the above results, an optimum method for preparing an active initiation system for the polymerization of polar monomers included an initiator/coinitiator ratio of 2:1 and rapid mixing of MMA with both initiation components. All of the following work was performed according to this method, if not otherwise stated.

3.2.2 Efficient MMA Polymerization Systems

Two efficient polymerization systems, System 1 and System 2, were made according to the above method, i.e., using the molar ratio of initiator/coinitiator to be 2:1 and the feeding sequence as MMA followed by initiator solution followed by coinitiator solution without any time delay. Polymerizations in these two systems were fast (about 1 h) with quantitative conversion of monomer.

3.2.2.1 Kinetics

The kinetic details of the two systems were studied, which included the kinetic order with respect to the concentrations of monomer and the initiation system, and the apparent activation energy for the polymerizations.

3.2.2.1.1 System 1

A typical polymerization of MMA for System 1 is shown in Figure 25. After a induction period of about 14 min, the quantitative conversion of MMA was reached within 35 min in toluene at 0 °C. A linear relationship between $[MMA]/[MMA]_0$ versus reaction time during the polymerization process was obtained, which indicated that the polymerization rate had a zero dependence on the concentration of monomer. Because for any reaction (polymerization in this case), the reaction rate has the following relationship with the concentration of reactants (monomer in this case):

$$\text{Rate} = -d[M]/dt = k_{app}[M]^n \qquad (6)$$

Where k_{app} is the apparent rate constant of the reaction, [M] is the concentration of the reactant, i.e. monomer in this case. If the Rate is zero order in [M], i.e., n=0, Equation 6 becomes:

$$-d[M]/dt = k_{app} \qquad (7)$$

Multiplying both sides of the Equation 7 by *dt* and integrating the resultant equation, yield

$$[M]_0 - [M] = k_{app}\, t \qquad (8)$$

Dividing both sides of Equation 8 by $[M]_0$ and rearranging the equation, yield

$$[M]/[M]_0 = 1 - k_{app}/[M]_0 \cdot t \qquad (9)$$

Equation 9 shows that for a reaction that is zero order in the concentration of reactant (monomer), a linear relationship between $[M]/[M]_0$ and the reaction time should hold, which was observed in the polymerization of System 1. From the slope of the regression line, the rate constant of $4.22\text{x}10^{-2}$ mol L^{-1} min^{-1} was obtained. The polymerization rate was comparable to those reported by Collins et al.[25,28,29]

High molecular weight PMMA ($\bar{M}_n = 2.1\text{x}10^5$) with narrow MWD ($\bar{M}_w/\bar{M}_n = 1.2$) was obtained. This high molecular weight is hard to obtain by group transfer polymerization (GTP), in which a normal limit for molecular weight is $3\text{x}10^4$, an order of magnitude lower than what was obtained in the polymerization via the present initiation systems.[42,43] In addition, the polymerization was carried out at 0 °C, which is advantageous over the anionic polymerization of MMA, in which the polymerization temperature is well below 0 °C.[44]

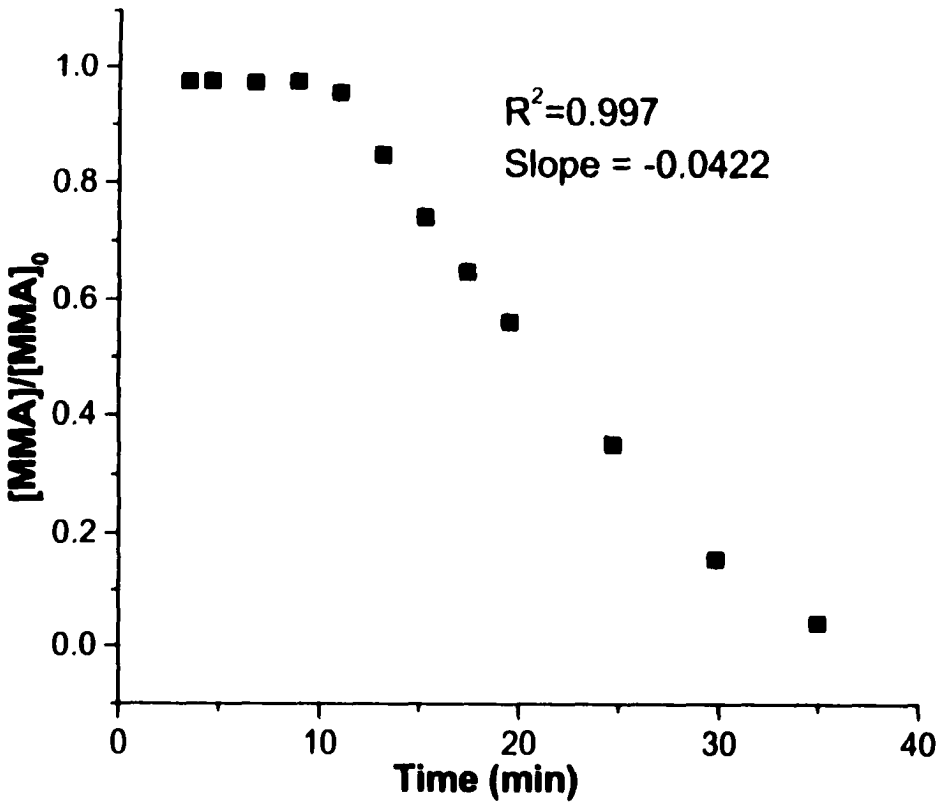

Figure 25. Polymerization of MMA by **1**/$B(C_6F_5)_3$ (2:1) initiation systems.

$[\mathbf{1}]_0$ = 5.0 mM, $[B(C_6F_5)_3]_0$ = 2.5 mM, $[MMA]_0$ = 1.0 M, toluene as solvent, temp = 0 °C.

The dependence of the polymerization rates on the concentrations of the initiation components was also studied (Figure 26). From the slope of a double logarithm plot of apparent rate constant versus coinitiator concentration (Figure 27), the rate orders were estimated. Note that in each experiment, the initiator/coinitiator ratio was kept to be 2:1, hence the concentration of only one initiation component varied independently. The concentration of coinitiator was chosen as the independent variable. The rate orders obtained from Figure 27 were combined rate orders[145] with respect to the concentrations of initiation systems, which was about 3 (2.9±0.1).

The dependence of the polymerization rates on temperature for System 1 is shown in Figure 28. The Arrhenius plot is shown in Figure 29. The plot of the logarithm of the apparent rate constants versus the reciprocal of the absolute temperature were linear, which demonstrated that an Arrhenius behavior was followed. From the slope of the plot, activation energy of 39±2 kJ/mole in the temperature range shown in the plot was estimated, which falls into the range of the activation energies of Ziegler-type polymerizations, which is 20 -70 kJ/mole.[146] This value is higher than an anionic polymerization of MMA initiated by $M^+[Al_2R_6X]^-$ (X = Cl) when $M^+ = Li^+$ or K^+ [147] (with activation energies of 21 and 26 kJ/mole, respectively), but is very close to that of the similar anionic polymerization when $M^+ = NR_4^+$ (with the activation energy of 40 kJ mole).[144]

3.2.2.1.2 System 2

For System 2, a fast polymerization of MMA was also obtained by using a 2:1 ratio of 2 $B(C_6F_5)_3$, although the rate was slower than that for System 1. When the same concentration of initiator (dimethyl zirconocene) and coinitiator ($B(C_6F_5)_3$) as those used

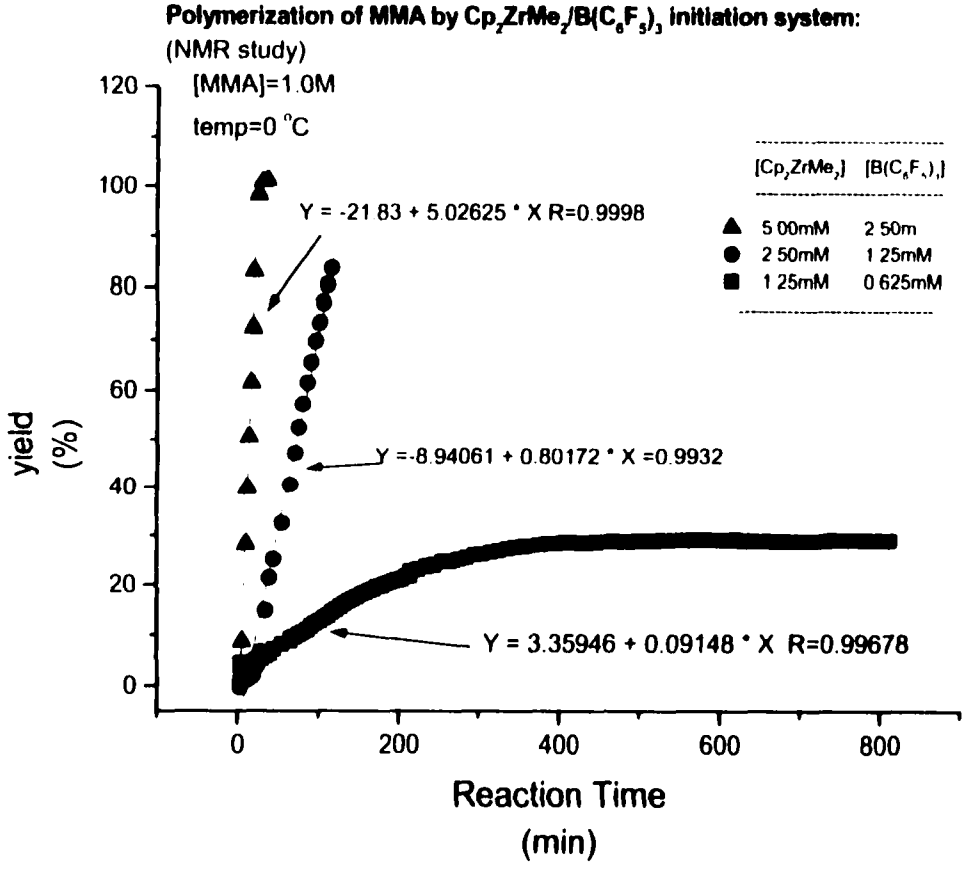

Figure 26. Polymerization of MMA by **1**/$B(C_6F_5)_3$ (2:1) initiation systems at different concentrations of initiator.

$[MMA]_0$ = 1.0 M, toluene as solvent, temp = 0 °C.

107

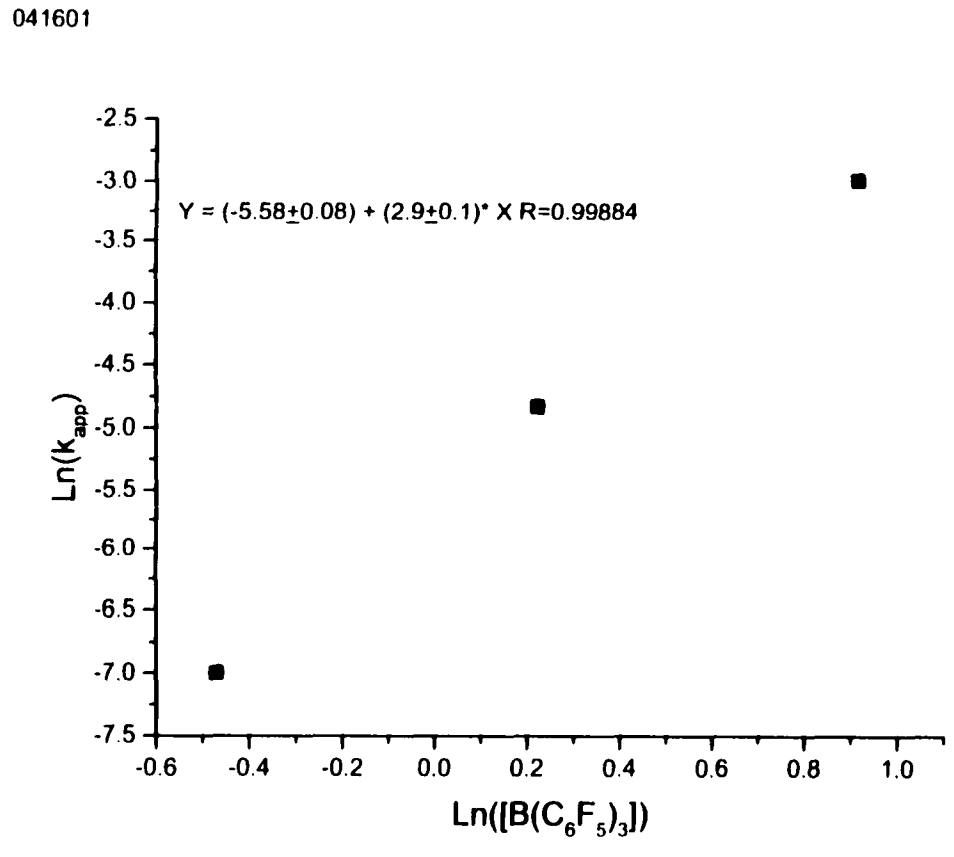

Figure 27. Relationship between the polymerization rate and $[B(C_6F_5)_3]_0$ in System 1

The molar ratio of $I/B(C_6F_5)_3$ was kept at 2:1, $[MMA]_0$ =1.0 M, toluene as solvent, temp = 0 °C.

108

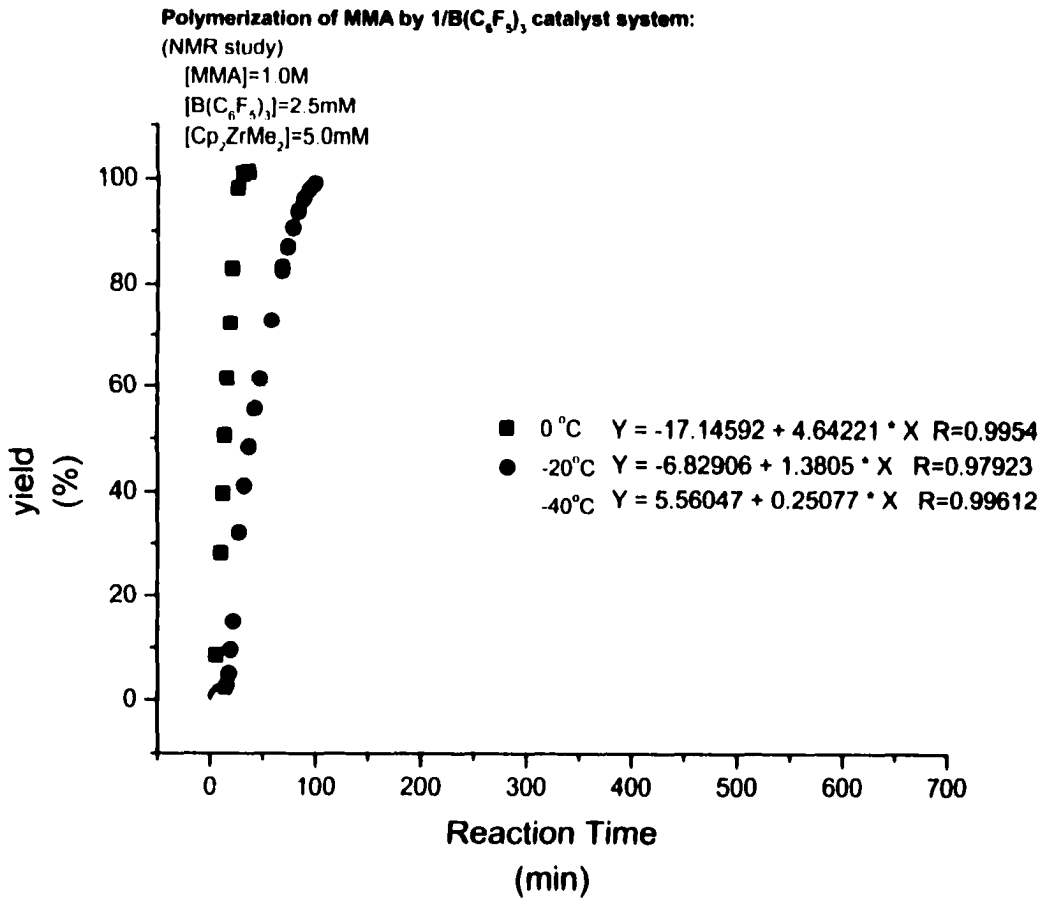

Figure 28. Polymerization of MMA by 1/$B(C_6F_5)_3$ (2:1) initiation systems at different temperature

$[1]_0$ = 5.0 mM, $[B(C_6F_5)_3]_0$ = 2.5 mM, $[MMA]_0$ =1.0 M, toluene as solvent.(Fitting lines are not shown)

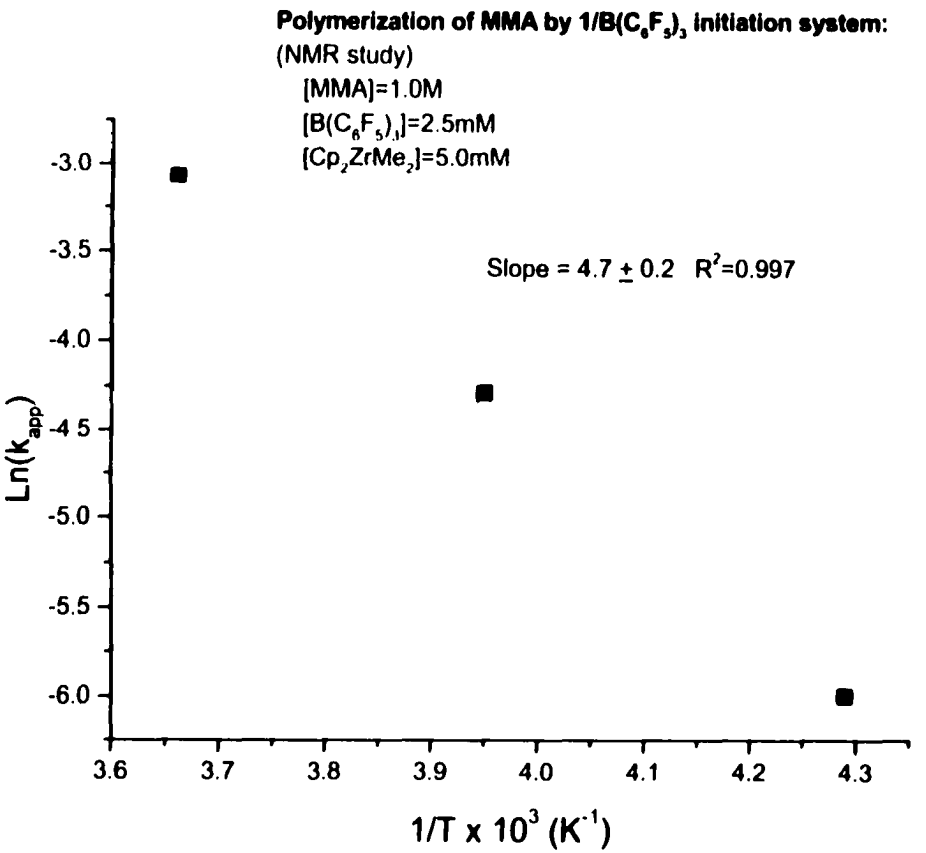

Figure 29. Arrhenius plot of System 1.

$[\mathbf{1}]_0$ = 5.0 mM, $[B(C_6F_5)_3]_0$ = 2.5 mM, $[MMA]_0$ =1.0 M, toluene as solvent.

in System 1 were applied. System 2 gave a quantitative conversion in about 65 min at 22 °C (Figure 30). The polymer obtained from System 2 had a $\bar{M}_n$ of 5.3 x10^4 and $\bar{M}_w/\bar{M}_n$ = 1.2. However, in System 2, the polymerization rate was first order in [MMA], which was shown by a linear relationship between ln([MMA]/[MMA]$_0$) versus reaction time (Figure 31). The apparent polymerization rate constants were calculated from the slopes of the corresponding regression lines.

The dependence of the polymerization rates on the concentrations of the initiation components was shown in Figure 32. From the slope of a double logarithm plot of apparent rate constant versus coinitiator concentration (Figure 33), the rate orders were estimated to be close to 2 (1.7±0.2).

The dependence of the polymerization rates on temperature is shown in Figure 34. The Arrhenius plot is shown in Figure 35. The plot of the logarithm of the apparent rate constants versus the reciprocal of the absolute temperature were linear, which demonstrated that an Arrhenius behavior was followed. From the slope of the plot, activation energies of 47±7 kJ/mole in the temperature range shown in the plot was estimated, which is higher than that of System 1, but also falls into the range of the activation energies of Ziegler-type polymerizations. The higher activation energy may be ascribed to the more sterically hindered structure of **2** than that of **1**.

3.2.2.2 Stereochemistry of PMMA and Stereoregularity Control Mechanism

The tacticity of the polymer obtained from the two systems was measured by ^{13}C NMR. Totally different tacticities were obtained from the two systems.

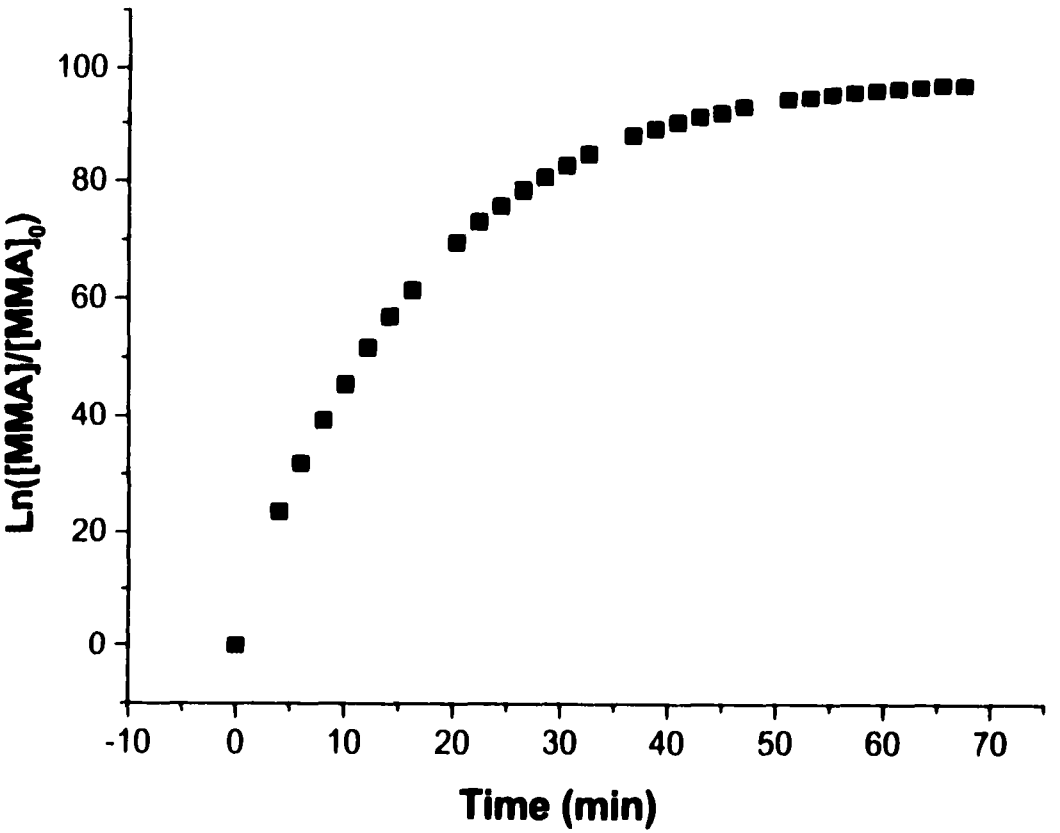

Figure 30. Polymerization of MMA by **2**/$B(C_6F_5)_3$ (2:1) initiation systems.

$[\mathbf{2}]_0$ = 5.0 mM, $[B(C_6F_5)_3]_0$ = 2.5 mM, $[MMA]_0$ =1.0 M, toluene as solvent, temp = 22 °C.

112

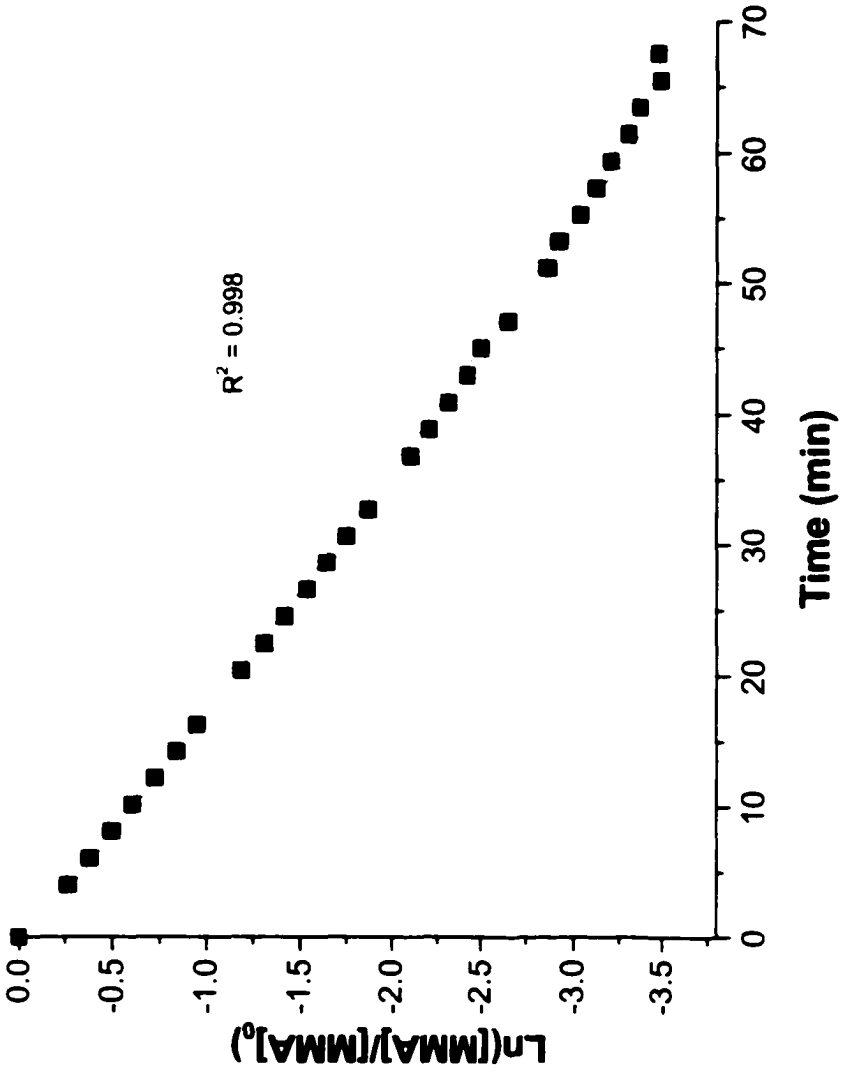

Figure 31. ln([MMA]/[MMA]$_0$ vs. reaction time for System 2.

[2]$_0$ = 5.0 mM, [B(C_6F_5)$_3$]$_0$ = 2.5 mM, [MMA]$_0$ = 1.0 M, toluene as solvent, temp = 22 °C.

113

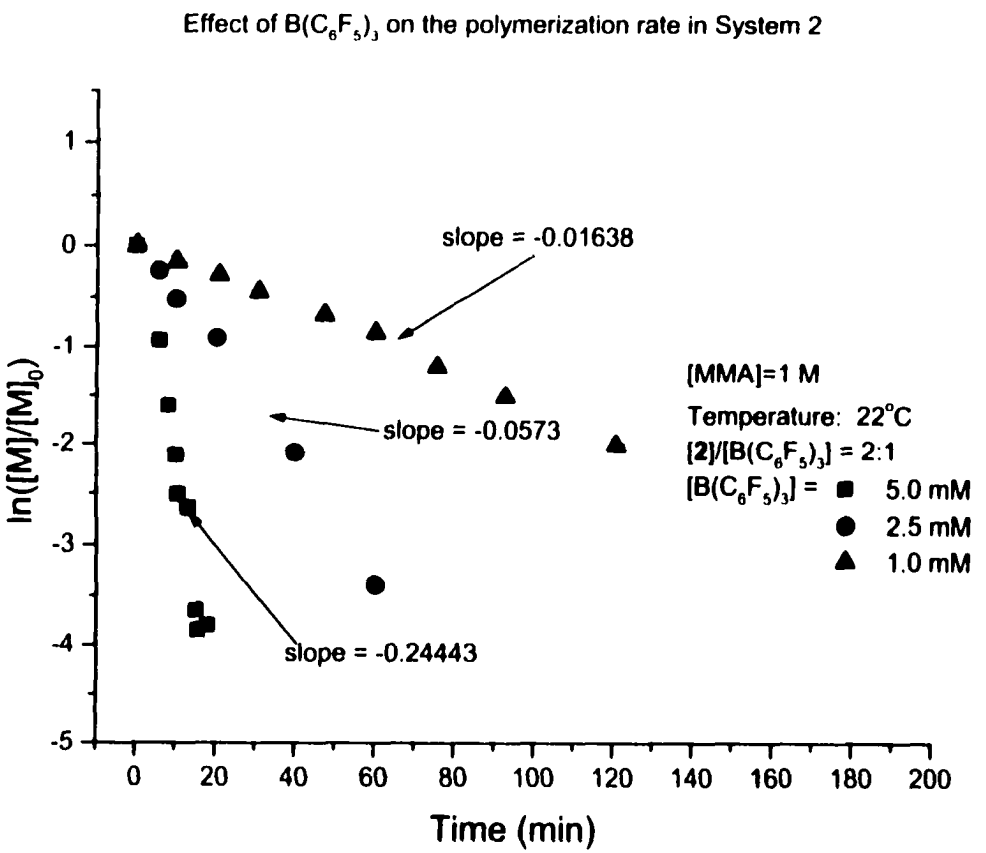

Figure 32. Polymerization of MMA by **2**/$B(C_6F_5)_3$ (2:1) initiation systems at different concentrations of initiator.

$[MMA]_0$ = 1.0 M, toluene as solvent, temp = 22 °C

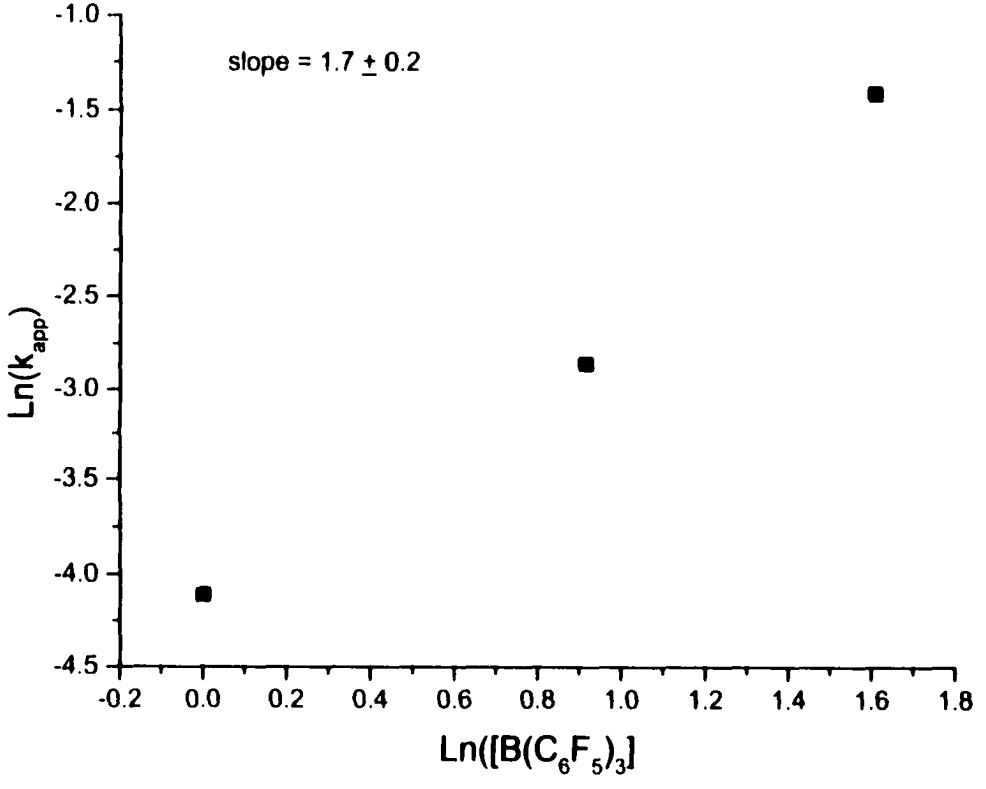

Figure 33. Relationship between the polymerization rate and $[B(C_6F_5)_3]_0$ in System 2

The molar ratio of **2**/$B(C_6F_5)_3$ was kept at 2:1, $[MMA]_0$ = 1.0 M, toluene as solvent, temp = 22°C.

115

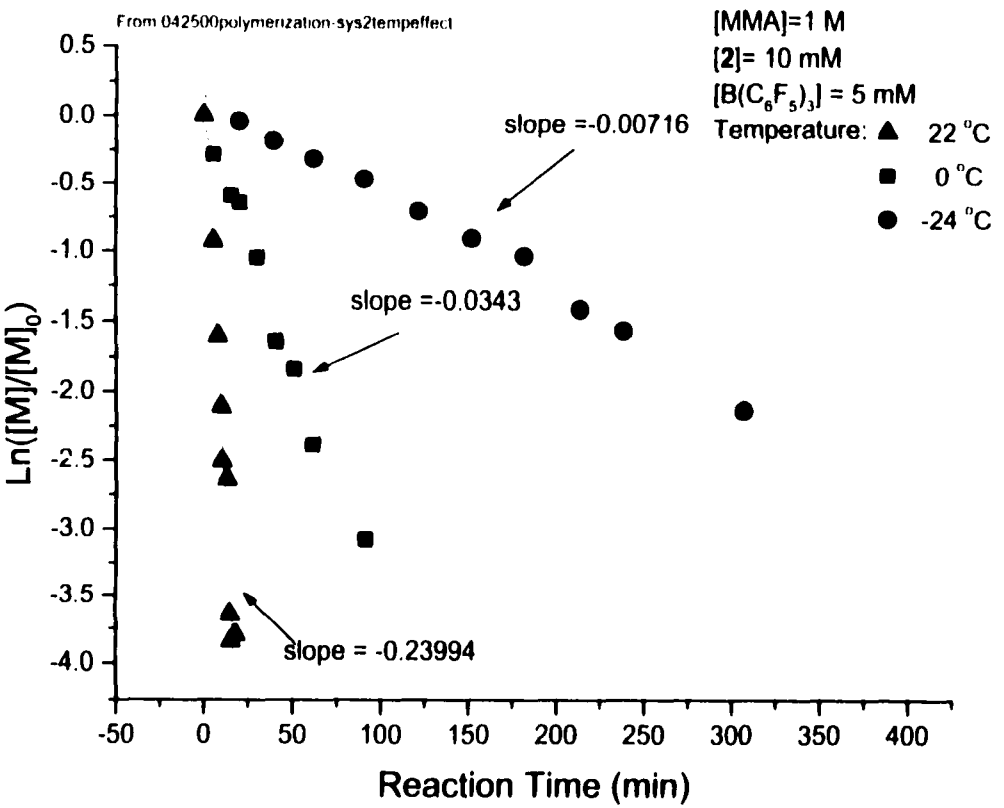

Figure 34. Polymerization of MMA by **2**/$B(C_6F_5)_3$ (2:1) initiation systems at different temperature

$[\mathbf{1}]_0$ = 10 mM, $[B(C_6F_5)_3]_0$ = 5.0 mM, $[MMA]_0$ =1.0 M, toluene as solvent.

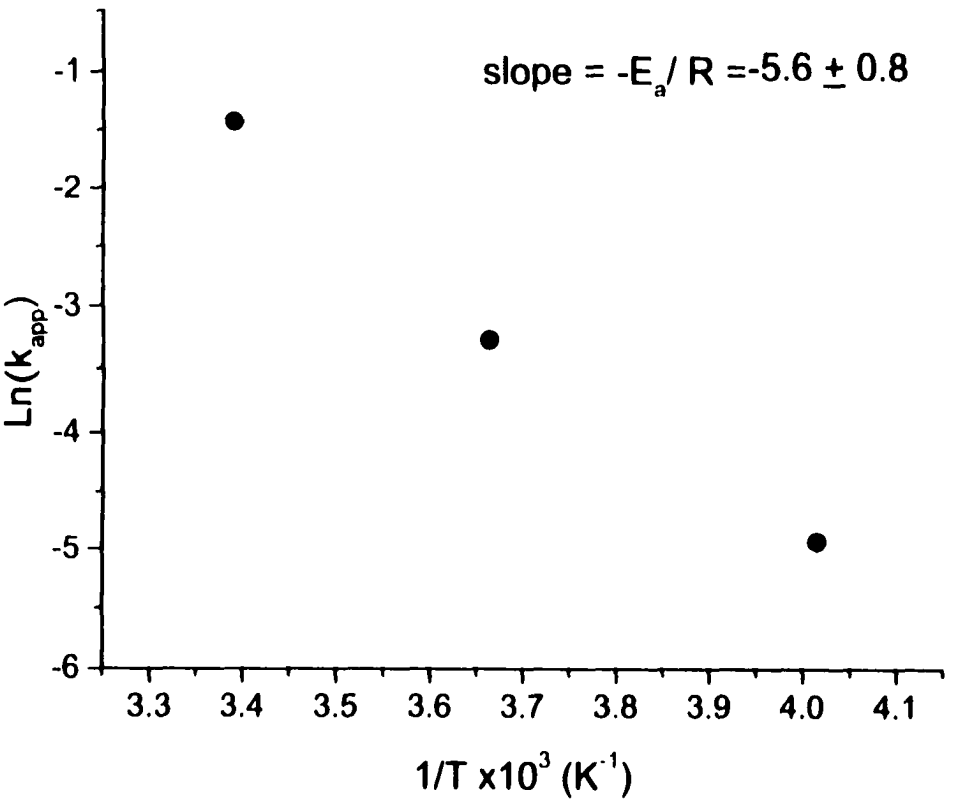

Figure 35. Arrhenius plot of System 2.

$[2]_0$ = 10 mM, $[B(C_6F_5)_3]_0$ = 5 mM, $[MMA]_0$ = 1.0 M, toluene as solvent

117

3.2.2.2.1 System 1

For System 1, in which an achiral initiator **1** with C_{2v}-symmetry was used, moderately syndiotactic-rich polymer ([rr] = 55%) was obtained. (Figure 36) The error pentad distribution of the polymer was analyzed based on ^{13}C NMR of carbonyl resonances of PMMA (Table 4). In this system, measurements of [mrrm] = 4.2 and [mmmr]+[rmmr] = 1.2 were obtained. These results did not match the expected ratio of [mmmr]:[mrrm] = 2:1 for enantiomorphic site-control mechanism.[11] They did not match the pentad ratio of [mmmr]:[mrrm] = 1:0 either, which is expected for the chain-end control mechanism.[11] Therefore, the chain growth in System 1 followed neither pure enantiomorphic site-control nor pure chain-end control mechanism.

To further investigate the propagation statistics of the polymerization, the syndiotactic ([rr]), heterotatctic ([mr]), and isotactic ([mm]) triad fractions obtained from ^{13}C-NMR were used to test the Bernoulli model.

The fractions of [rr], [mr] and [mm] and various tetrad fractions from the main chain can be calculated from:

$$[rr] = [mrrm] + [rrrm] + [rrrr] \quad (10)$$

$$[mr] = [mrmr] + [mrmm] + [mmrr] + [rrmr] \quad (11)$$

$$[mm] = [mmmm] + [mmmr] + [rmmr] \quad (12)$$

$$[mmm] = [mmmm] + 0.5[mmmr] \quad (13)$$

$$[mmr] = [mmmr] + 2[rmmr] \quad (14)$$

$$[rmr] = 0.5[mrmr] + 0.5[rmrr] \quad (15)$$

$$[rrm] = 2[mrrm] + [mrrr] \quad (16)$$

$$[rrr] = [rrrr] + 0.5[mrrr] \quad (17)$$

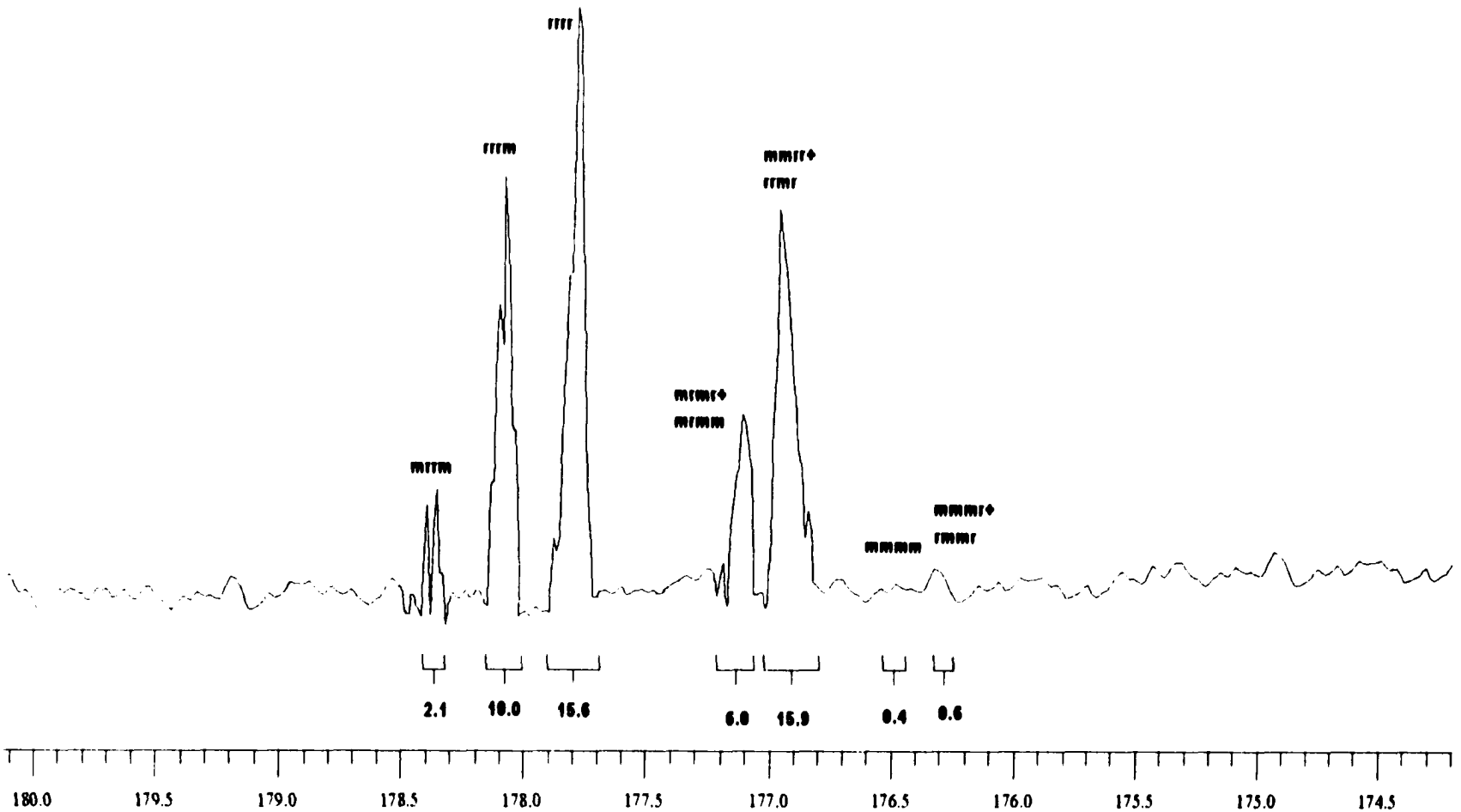

Figure 36 Representative C-13 NMR spectrum of PMMA obtained from System 1.
(Polymerization was carried out at 22 °C)

Table 4 Tacticity and molecular weight of PMMA[a]

System	Pentad fraction (%)[b]										$\bar{M}_n$[d] x 10^{-3}	$\bar{M}_w$[d] / $\bar{M}_n$
	[mrrm]	[rrrm]	[rrrr]	[mrmr]	[mrmm]	[mmrr]	[rrmr]	[mmmm]	[mmmr]	[rmmr]		
1	4.2	19.8	30.8	←11.9[c]→		←31.4[c]→		0.8	←1.2[c]→		210	1.2
2	4.0	0.0	0.0	0.0	0.0	8.3	0.0	79	8.5	0.0	53.2	1.2

[a] For the polymerization conditions, refer to Figure 25.

[b] Observed in ^{13}C NMR of carbonyl resonances of PMMA.

[c] Signals from the two pentads overlapped and the percentage for each one could not be resolved.

[d] Measured by GPC, calibrated by PMMA standards.

120

The fractions of racemic [r] and meso diads [m] from the main chain can be calculated from:

$$[r] = [rr] + 0.5[mr] \quad (18)$$

$$[m] = [mm] + 0.5[mr] \quad (19)$$

The persistence ratio, ρ, defined as:

$$\rho = 2[m][r]/[mr] \quad (20)$$

should be unity for a Bernoullian process. The first-order Markoff probabilities P_{mr}, and P_{rm} can be calculated from:

$$P_{mr} = [mr]/(2[mm] + [mr]) \quad (21)$$

$$P_{rm} = [mr]/(2[rr] + [mr]) \quad (22)$$

For a Bernoullian process, $\Sigma P = P_{mr} + P_{rm}$, should be equal to one.

To test the first-order Markov model, the following equations should be satisfied:

$$4[mmm][rmr]/[mmr]^2 = 1 \quad (23)$$

$$4[mrm][rrr]/[mrr]^2 = 1 \quad (24)$$

The Bernoulli model assumes that only the last monomer unit in the propagating chain end is important in determining polymer stereochemistry. Polymer stereochemistry is not affected by the penultimate unit or units further back. The first-order Markov model describes a polymerization where the penultimate unit is important in determining subsequent stereochemistry.

From the present ^{13}C-NMR results, the following was obtained:

$$[rr] = 0.042 + 0.198 + 0.308 = 0.548$$

$$[mr] = 0.119 + 0.314 = 0.433$$

$$[mm] = 0.008 + 0.012 = 0.020$$

$$[r] = 0.548 + 0.5*0.433 = 0.765$$

$$[m] = 0.02 + 0.5*0.433 = 0.237$$

$$\rho = 2*0.237*0.765/0.433 = 0.837$$

$$P_{mr} = 0.433/(2*0.02+0.433) = 0.915$$

$$P_{rm} = 0.433/(2*0.548 + 0.433) = 0.283$$

$$\Sigma P = 0.085 + 0.717 = 0.802$$

The persistence ratio, ρ, is not equal to 1 and ΣP is not equal to 1 either, both of which show that the propagation in this polymerization does not follow the Bernoullian process. Combining all the above stereochemistry analysis, it can be seen that the propagation in System 1 was not a simple case, multiple propagation modes may exist in this system.

Due to insufficient resolution of the ^{13}C NMR spectrum, some pentads overlapped, e.g., mmmr overlapped with rmmr, which made it impossible to calculate some tetrad fractions (Equation 13-17), which, however, are needed for Markov model testing (Equation 23, 24). Therefore, the first-order Markov testing was not performed.

3.2.2.2.2 System 2

For System 2, a highly isotactic polymer was obtained (Figure 37, [mm] = 88%). It can be seen that the stereochemistry of PMMA was controlled by the symmetry of the dimethyl zirconocene, i.e., an achiral initiator (**1**) with C_{2v} symmetry led to moderately syndiotactic PMMA, while a chiral initiator (**2**) with C_2 symmetry led to isotactic PMMA. This stereochemical control of the final polymer is the same as that discovered in metallocene-initiated α-olefin polymerizations. As mentioned in the introduction,

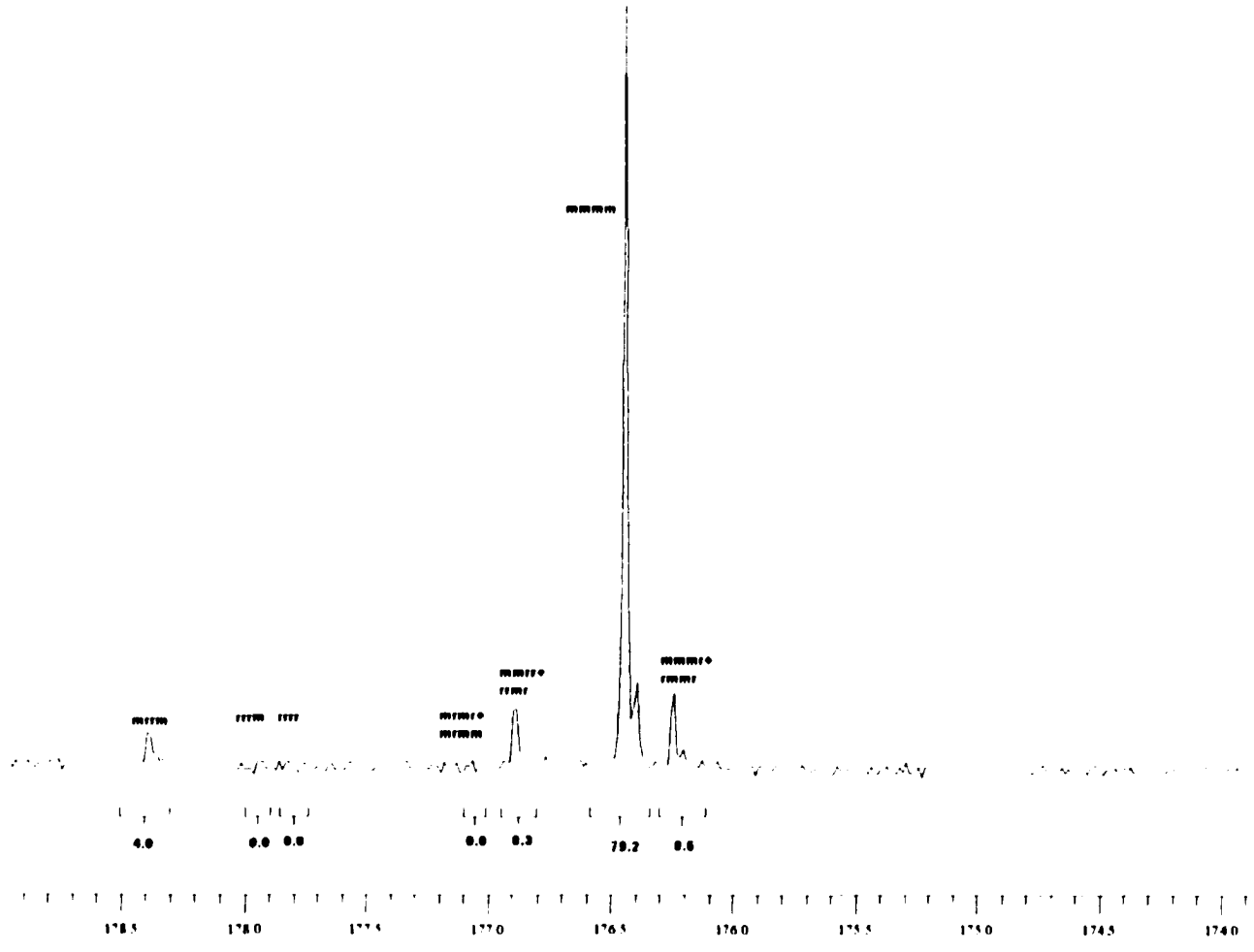

Figure 37. Representative C-13 NMR spectrum of PMMA obtained from System 2.
(Polymerization was carried out at 22 °C)

123

other Group 4 metallocene initiation systems also demonstrate such stereochemical control of PMMA.[15-17,28,30,38].

In System 2, an error pentad distribution of [mmmr]:[mmrr]:[mmrm]:[mrrm] = 8.5:8.3:0.0:4.0 was obtained (Table 4), which was, within experimental error, equal to the theoretical distribution of [mmmr]:[mmrr]:[mmrm]:[mrrm] = 2:2:0:1 for the enantiomorphic site-control mechanism.[1,14,15] Therefore, the stereoregularity of the polymer in System 2 was controlled by an enantiomorphic site-control mechanism.

The enantiomorphic site control statistical model was also tested for the propagation in System 2. The model is described in terms of the single parameter σ. Parameter σ is the probability of an R monomer unit adding at the R site, or the probability of an S monomer unit adding at the S site. The relationship between pentad distribution and σ are:

$$[mmmm] = 5\sigma^4 - 10\sigma^3 + 10\sigma^2 - 5\sigma + 1 \qquad (25)$$

$$[mrrm] = -3\sigma^4 - 6\sigma^3 - 4\sigma^2 + \sigma \qquad (26)$$

$$[mmmr] = [mmrr] = -6\sigma^4 + 12\sigma^3 - 8\sigma^2 + 2\sigma \qquad (27)$$

$$[rmmr] = [rrrr] = \sigma^4 - 2\sigma^3 + \sigma^2 \qquad (28)$$

$$[mmrm] = [rmrr] = [rmrm] = [mrrr] = 2\sigma^4 - 4\sigma^3 + 2\sigma^2 \qquad (29)$$

From Table 4, [mmmm] = 0.79, [mrrm] = 0.04, [mmmr] = [mmrr] = 0.084 (average of the two measured values is used here), [rmmr] = [rrrr] = 0, and [mmrm] = [rmrr] = [rmrm] = [mrrr] = 0. To test the enantiomorphic site control statistical model, the experimental data were plugged into Equations 25-29 and the following was obtained:

$$[mmmm] - 0.79 = 5\sigma^4 - 10\sigma^3 + 10\sigma^2 - 5\sigma + 0.21 \; (= 0)$$

$$[mrrm] - 0.04 = -3\sigma^4 - 6\sigma^3 - 4\sigma^2 + \sigma - 0.04 \ (= 0)$$

$$[mmmr] - 0.084 = -6\sigma^4 + 12\sigma^3 - 8\sigma^2 + 2\sigma - 0.084 \ (= 0)$$

$$[rmmr] = \sigma^4 - 2\sigma^3 + \sigma^2 \ (= 0)$$

$$[mmrm] = 2\sigma^4 - 4\sigma^3 + 2\sigma^2 \ (= 0)$$

Drawing the above functions in the same graph, Figure 38 was obtained, which shows that all five curves pass through a common point within the experimental error. The σ value of this common point is 0.048. Figure 38 indicates that the propagation of the polymer chain in System 2 followed the enantiomorphic site control model and the probability of an R monomer unit adding at the R site (or the probability of an S monomer unit adding at the S site) is only 0.048. In other words, about 95% of the R monomer added to the S site of the active center (or S monomer added to R site).

The factors that may influence the isotacticity of the PMMAs in this system were investigated. Figure 39 shows the temperature effect on the isotacticity of the final polymers. In the entire temperature range in which the polymerization was carried out, high isotacticity was obtained ([mm] ~ 90%). However, the isotacticity increased with decreasing temperature, which is also observed in the olefin polymerization systems. The [mm] changed from 94% at -24 °C to 89% at 22 °C. This phenomenon can be ascribed to greater restrictions on the conformation changes in the active centers at lower temperature, which formed a more static template that allowed only one orientation of the monomer molecule to grow onto the polymer chain. This observation is consistent with the enantiomorphic site-control mechanism obtained from the above NMR analysis.

126

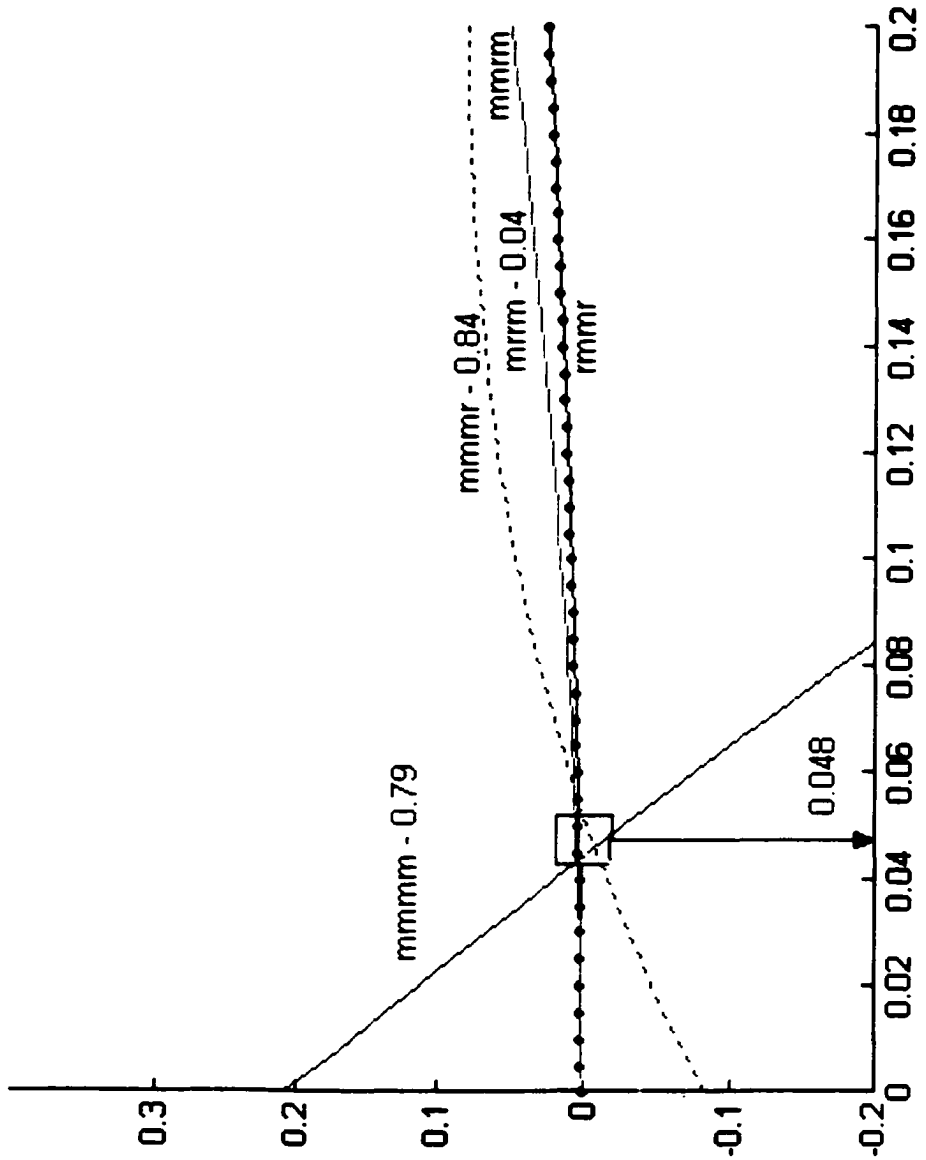

Figure 38. Enantiomorphic site control model test in System 2

127

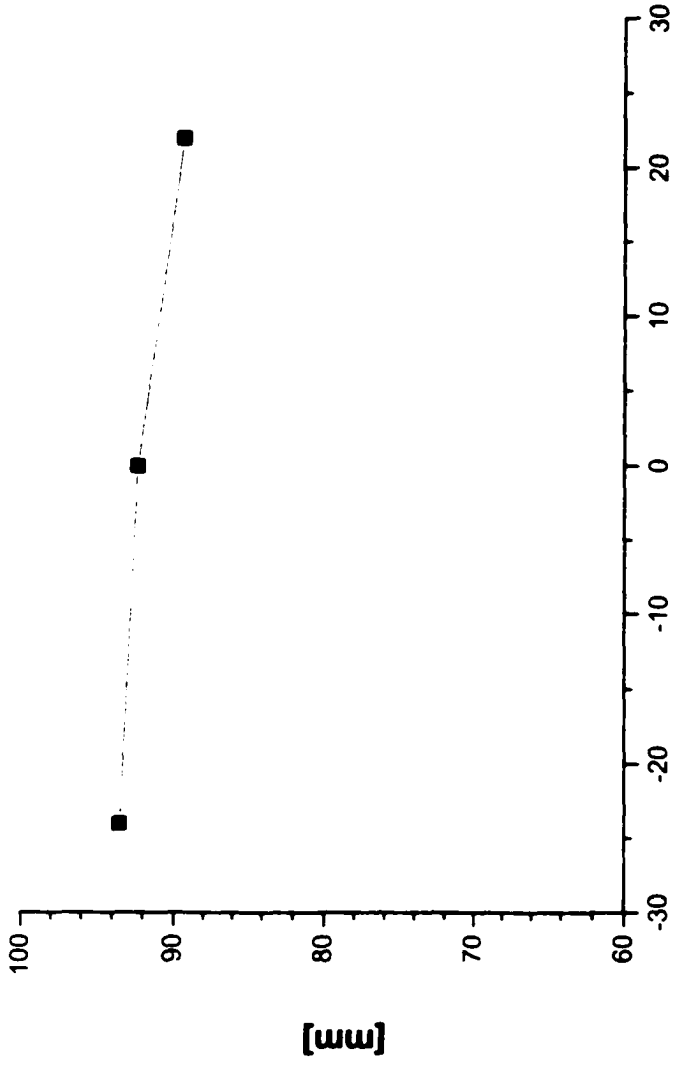

Figure 39. Temperature effect on the isotacticity of the PMMA obtained in System 2. [MMA] = 1 M, [2] = 10 mM, [$B(C_6F_5)_3$] = 5 mM.

Figure 40 shows the changes of tacticity with conversion. To avoid the interference of other factors that may change the tacticity, the polymerizations were carried out at low temperature. The decrease of the isotacticity occurred mainly at the early stage of the polymerization. A 6% decrease of [mm], from 100% to 94%, was observed before 30% conversion of the monomer in this case. From then on, the isotacticity ([mm]) stayed almost the same up to the quantitative conversion.

The effect of excess initiator on the tacticity was also tested. Two polymerizations with the same conditions ([MMA] = 1 M, $[B(C_6F_5)_3]$ = 2.5 mM, temperature = 22 °C) but different [**2**] (10 and 5 mM respectively) were performed. The polymers obtained showed the same isotacticity, i.e., [mm] = 91.3% and 91.1% respectively. Therefore, the excess initiator has no effect on the tacticity of the final polymers.

The effect of monomer concentration on the tacticity was also tested. Two polymerizations with the same conditions ([**2**] = 10 m M, $[B(C_6F_5)_3]$ = 5 mM, temperature = 0 °C) but different [MMA] (0.5 and 2 M respectively) were performed. The polymers obtained showed almost the same isotacticity, i.e., [mm] = 90.3% and 93.4% respectively. Therefore, the monomer concentration has no effect on the tacticity of the final polymers either.

3.2.2.3 Living Characteristics of the Polymerization Systems

Sequential monomer-addition experiments were performed for both systems. After the completion of the polymerization, judged by the disappearance of vinyl signals of MMA in

the ^{1}H NMR spectra, a new batch of MMA was added to the reaction mixture. A second-batch polymerization occurred in both systems.

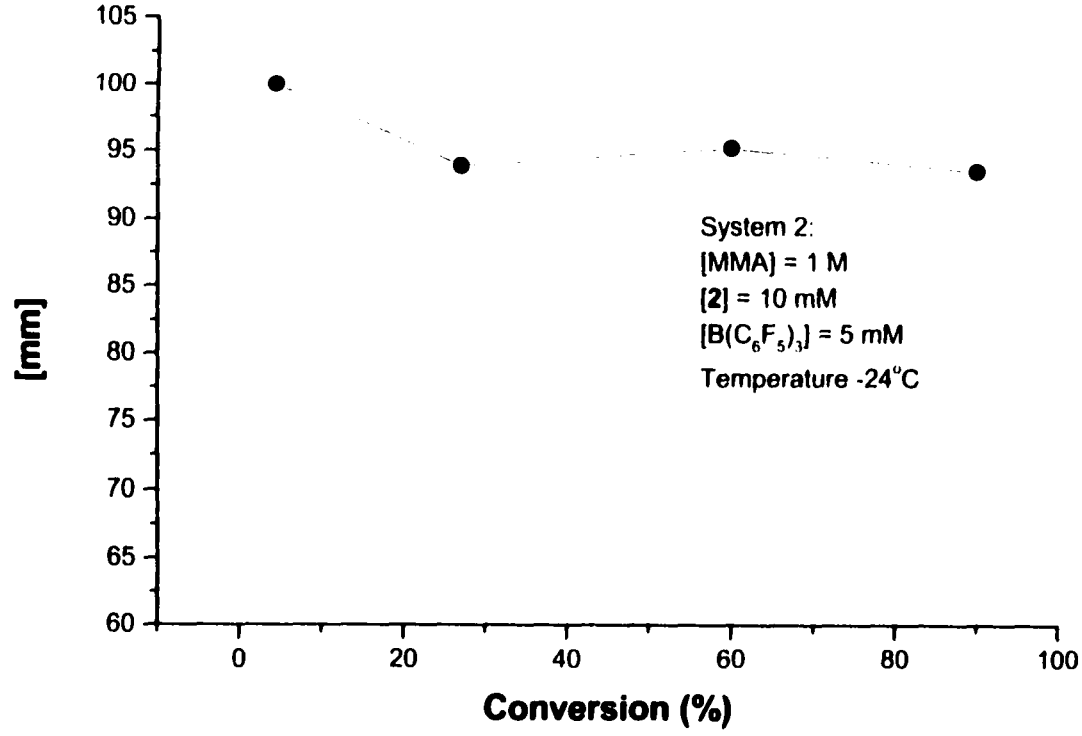

Figure 40. Changes of isotacticity along the progress of polymerization in System 2.

[MMA] = 1 M, [**2**] = 10 mM, $[B(C_6F_5)_3]$ = 5 mM, Temperature -24 °C

129

Several criteria have been well established for a living polymerization system[49], which include:

1. Polymerization proceeds until all of the monomer has been consumed. Further addition of monomer results in continued polymerization.

   However, this is a loose criterion. A tight criterion would be stated that all of the chains continue to grow when additional monomer has been added. Both chain termination and chain transfer reactions will produce dead polymer chains that will not increase in molecular weight upon addition of more monomer.

2. The number average molecular weight, $\bar{M}_n$ is a linear function of conversion.

   This is not a rigorous criterion. For example, if termination occurs only at the end of the polymerization, the number of chains will be a constant throughout the polymerization and the above required linear relationship between $\bar{M}_n$ and conversion will apply. However, this type of plot will detect chain transfer reactions: a linear plot is obtained only when there is no chain transfer.

3. The number of polymer molecules (and active centers) is a constant, which is sensibly independent of conversion.

   This criterion is especially sensitive to the occurrence of chain transfer, since this will increase the number of polymer molecules. However, it is not in itself a good diagnostic test for termination reactions, because termination reactions will not change the total number of molecules. Both Criteria 2 and 3 can be regarded as necessary but not sufficient criteria for a living polymerization.

4. The molecular weight can be controlled by the stoichiometry of the reaction.

This criterion depends on the quantitative utilization of the initiator before all of the monomer has been consumed, i.e., the initiator efficiency.

When chain transfer exists, since new chains grow from zero length, the total average molecular weight will decrease relative to the stoichiometric value.

5. Narrow-molecular-weight distribution polymers are produced.

   In general, it is possible to prepare a polymer with a narrow molecular weight distribution using a living polymerization when the rate of initiation is competitive with the rate of propagation and all of the active chain termini are equally susceptible to reaction with monomer.

6. Block copolymers can be prepared by sequential monomer addition.
7. Chain-end functionalized polymers can be prepared in quantitative yield.

The living nature of System 1 and System 2 will be discussed against the above criteria.

3.2.2.3.1 System 1

Figure 41 shows the living polymerizations in system 1. Two runs with time intervals of 2 min and 17 min, respectively, between the completion of the first batch polymerization and the addition of the second batch of MMA are shown. For both runs, the initial monomer concentration for the second batch polymerization was the same as that for the first batch polymerization, i.e., 1.0 M. With a 2 min interval, the second batch polymerization occurred at a polymerization rate almost the same as that of the first batch polymerization, while with a longer interval (17min), the polymerization rate of the second batch was a little bit slower. Both second batch polymerizations went to quantitative conversion of the second batch monomer smoothly. These results indicated that on the addition of the second batch of MMA, the active species for polymerization

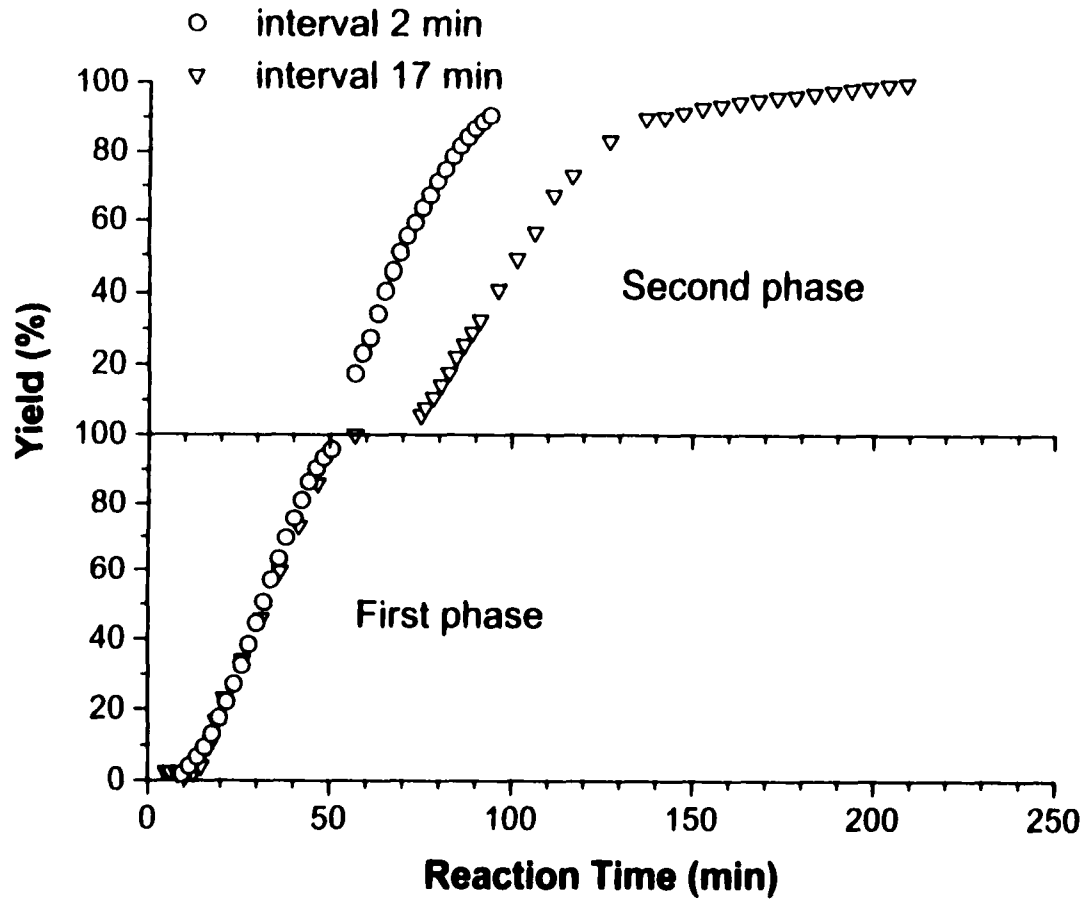

Figure 41. Living characteristics of the System 1. $[1]_0$ = 5.0 mM, $[B(C_6F_5)_3]_0$ = 2.5 mM, $[MMA]_0$ = 1.0 M, (both first and second batches), toluene as solvent, temperature = 0 °C. The time interval between the completion of the first batch polymerization and the start of the second batch MMA was: o 2 min; ∇ 17 min.

132

existed in System 1. Another experiment with a time interval as long as 120 min was also performed by the gravimetry method. The second batch polymerization occurred and quantitative conversion of the second batch of MMA was accomplished as well, which implied that the active centers in this system either have a long life time after the completion of the first batch polymerization, or can be generated when new monomer was added to the system. Criterion 1 for living polymerization system was loosely satisfied in System 1. However, the above experiments can not determine whether the second batch of MMA was grown onto the living polymer chains from the first batch polymerization or onto the newly generated active species when the second batch of monomer was added.

Figure 42 depicts the GPC traces of the polymer obtained at full conversion of the first- and the second-batch polymerizations with different time intervals. With a short time interval (2 min), only 20% of the increment of $\bar{M}_n$ (from 2.21 x 10^5 to 2.66 x 10^5) was obtained after the second-batch polymerization. The $\bar{M}_w/\bar{M}_n$ broadened from 1.22 to 1.39 (Figure 42a). With a longer time interval (17 min, Figure 42b), $\bar{M}_n$ of the final polymer showed almost no change from the first batch polymerization, i.e., 2.25 x 10^5 of the final polymer versus 2.19 x 10^5 of the polymer obtained from the first batch polymerization. $\bar{M}_w/\bar{M}_n$ however, increased from 1.22 to 1.58 with the MWD of the final polymer totally enveloped that of the first-batch polymer. When a time interval of 120 min was used, dramatically, the GPC trace (Figure 42c) of the final polymer shifted to the lower molecular weight side of the first-batch polymer and an even broader MWD ($\bar{M}_w/\bar{M}_n$ = 1.93) was obtained. Clearly, these results do not support a scheme where all polymer chains kept growing on the addition of new monomer in this system. On the

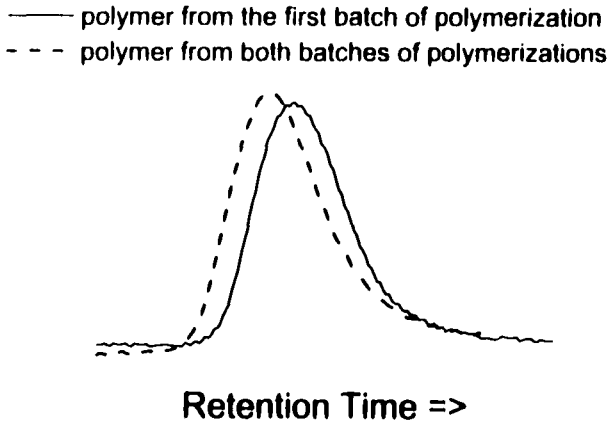

a

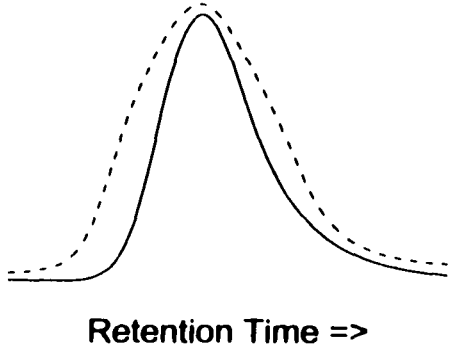

b

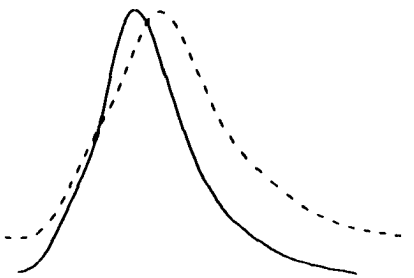

c

Figure 42. GPC traces of polymers from sequential addtion experiments.

Experimental conditions are the same as those of Figure 41

with time interval of a) 2 min; b) of 17 min; c) 120 min.

135

contrary, they revealed two facts about the living characteristics in System 1: 1) The active chains were deactivated during the polymerization process, especially in the time interval between the two batches when no MMA was present. 2) New active species were generated on the addition of the second batch of MMA. Therefore, the longer the time interval, the smaller the fraction of the previous polymer chains that was left active, which resulted in a smaller fraction of high molecular weight polymer chains in the final polymer, assuming they grew from the previous active chains. In addition, with a longer time interval, more second batch monomer was consumed on the newly generated active species and lower molecular weight polymer chains were produced in the final polymer. Therefore, Criterion 1 of a living polymerization was not rigorously satisfied with System 1. In addition, from the above results, Criterion 5 was not well satisfied. Although the MWD of the first batch polymer was not broad ($\bar{M}_w/\bar{M}_n$ = 1.22), which is the upper limit of MWD that can be considered as a "narrow" molecular weight distribution, the MWD after the second batch of polymerization broadened, and therefore can not be considered as "narrow". A chain breaking process (either termination or transfer) existed in System 1.

To further investigate the characteristics of System 1, polymer samples at various conversions in both polymerization batches (with a time interval of 2 min) were obtained and their molecular weights and MWDs were measured. (Figure 43) At low conversions, bimodal GPC traces were obtained, which indicated the existence of two propagating centers with different chain lengths. With the progression of the polymerization, both propagating chains grew longer, therefore, the bimodal GPC trace shifted to lower retention time. However, the area fraction of the right side of the GPC traces increased,

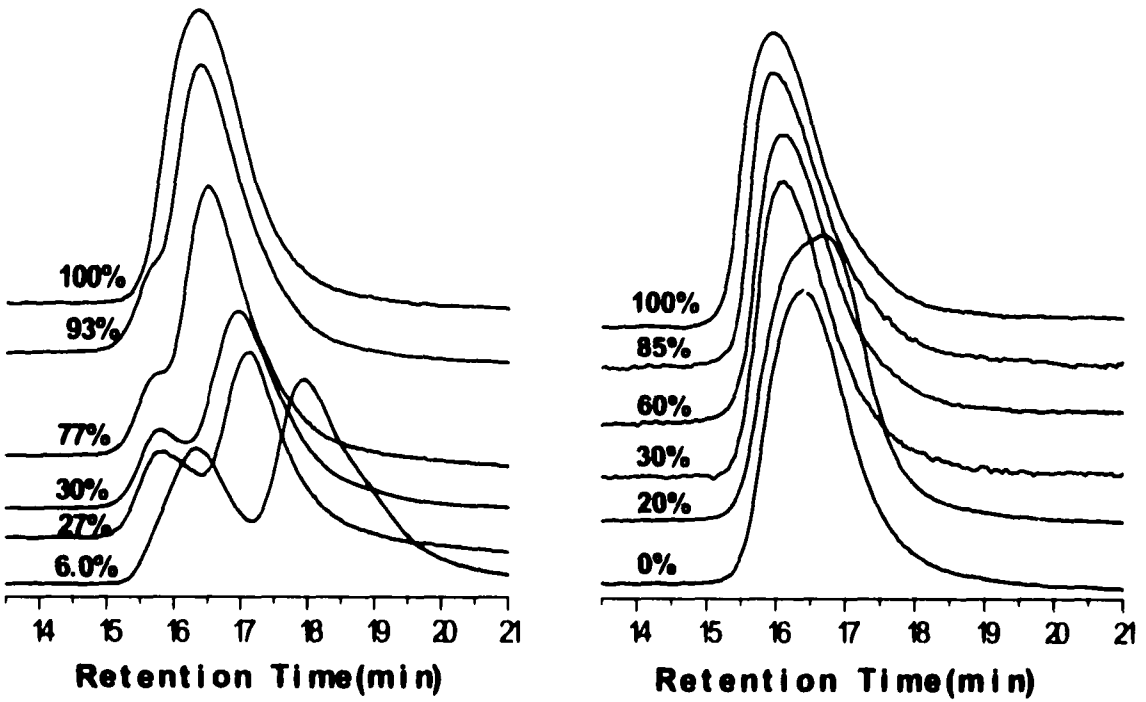

Figure 43. GPC traces of PMMA from **1**/$B(C_6F_5)_3$ initiation system: $[B(C_6F_5)_3]_0$ = 2.5 mM, $[\mathbf{1}]_0$ = 5.0 mM, $[MMA]_0$ = 1.0 M, temp = 0 °C, numbers indicate the conversion of the monomer. a) first batch polymerization; b) second batch polymerization. With time interval between the two batches of polymerization of 2 min.

suggesting that more monomer was grown onto the propagating centers with shorter chain length. Gradually, the two fractions moved closer and finally the MWD looked more like a monomodal distribution. In the second batch polymerization, at an early stage, $\bar{M}_n$ decreased to a value lower than that of the first batch polymer. This is solid evidence that new active species were generated on the addtion of the second batch of MMA, which grew lower molecular weight polymer chains. With increasing conversion, GPC traces of the polymer shifted to higher molecular weights and approached a monomodal distribution again.

The bimodal GPC traces of the first batch polymerization were deconvoluted into two peaks (Figure 44) and the measured and deconvoluted molecular weights at various conversion were listed in Table 5. Plotting the meaured and deconvoluted $\bar{M}_n$'s against conversion, Figure 45 was obtained.

As far as the molecular weights of the total samples are concerned, the number average molecular weight is not a linear function of conversion, which excludes System1 from a living polymerization according to Criterion 2. However, the relationship between the deconvoluted $\bar{M}_n$'s and conversion shows an interesting observation. One fraction (the left side fraction) of the polymer in System 1 increased the chain length linearly with the conversion, while the other fraction first increased with the conversion and then levelled off. The polymers corresponding to the left fraction in the GPC traces also showed a relatively narrow MWD, ~1.1, which, combined with the above linear $\bar{M}_n$ – conversion relationshop, indicates that this portion of the polymerization was living. However, chain breaking processes occurred in the other polymer fraction which corresponded to the right fraction of the GPC traces.

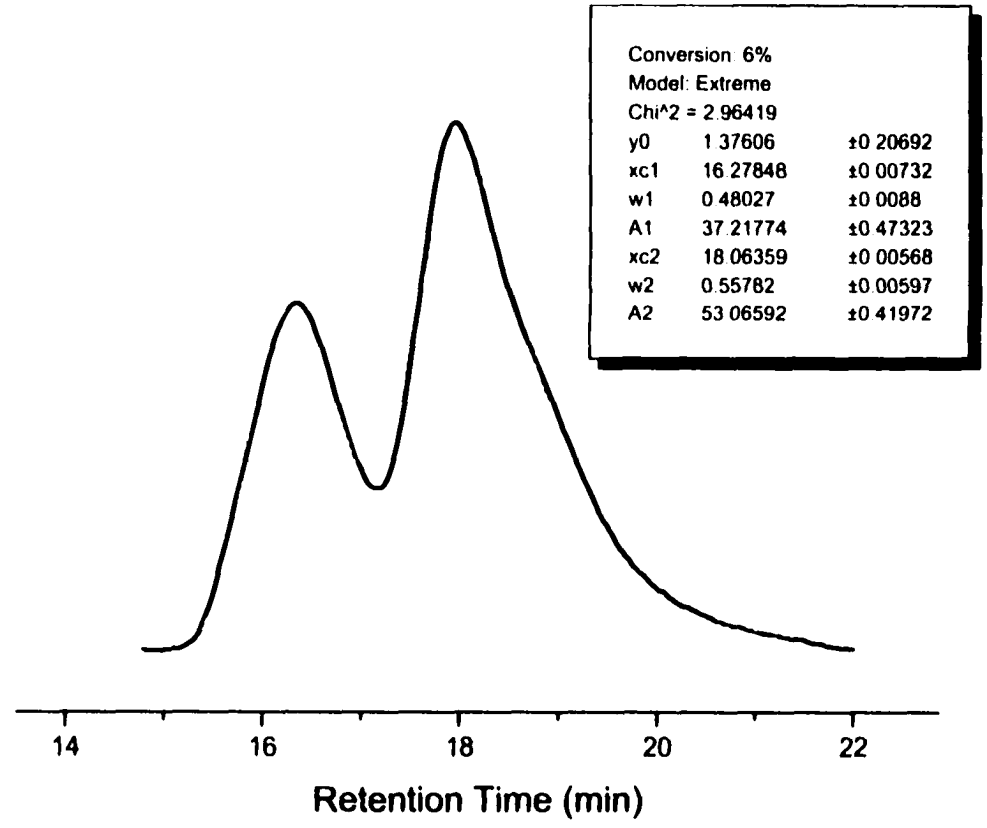

Conversion = 6%

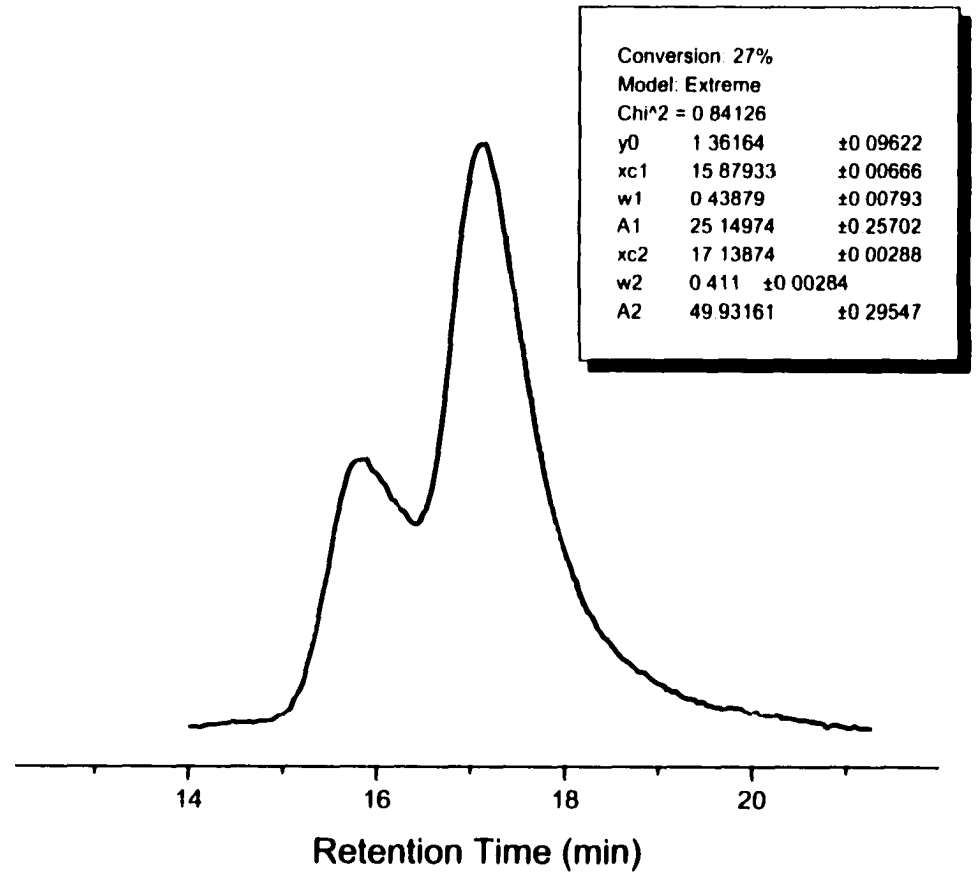

Conversion = 27%

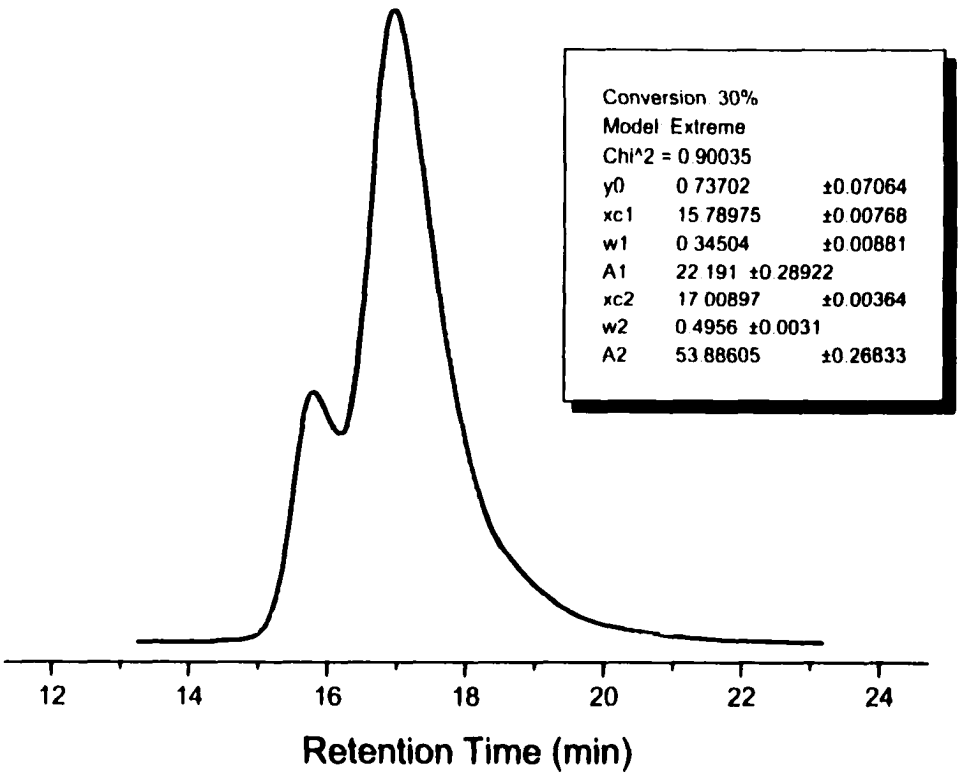

Conversion = 30%

141

142

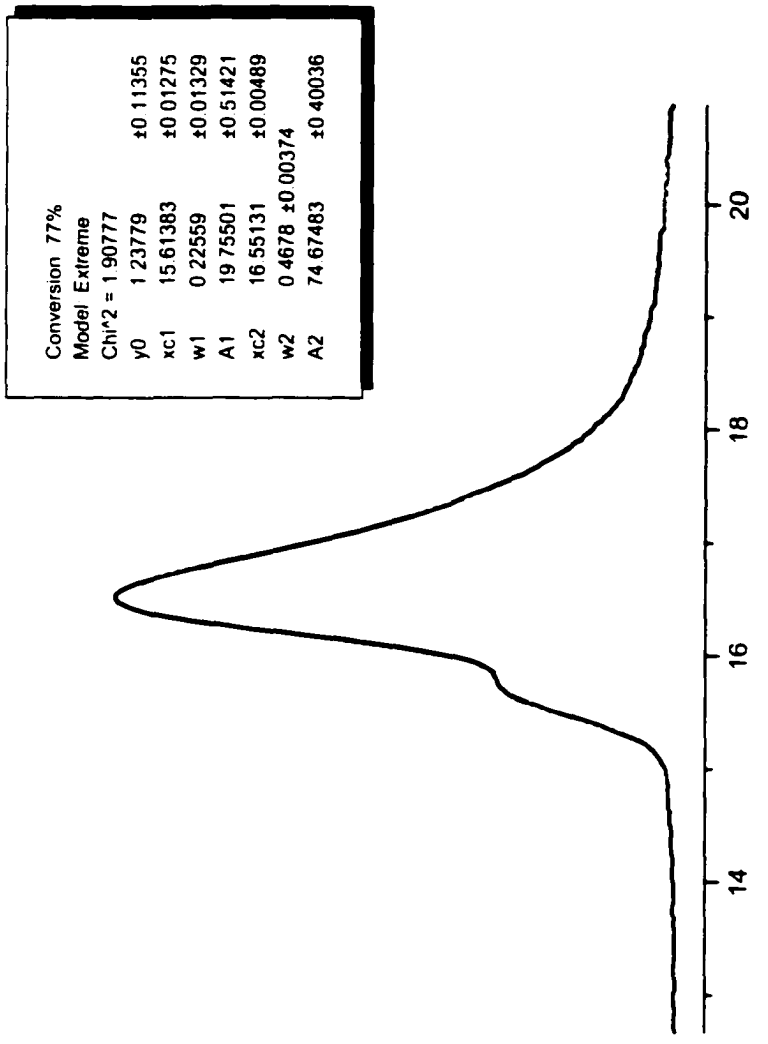

Conversion = 77%

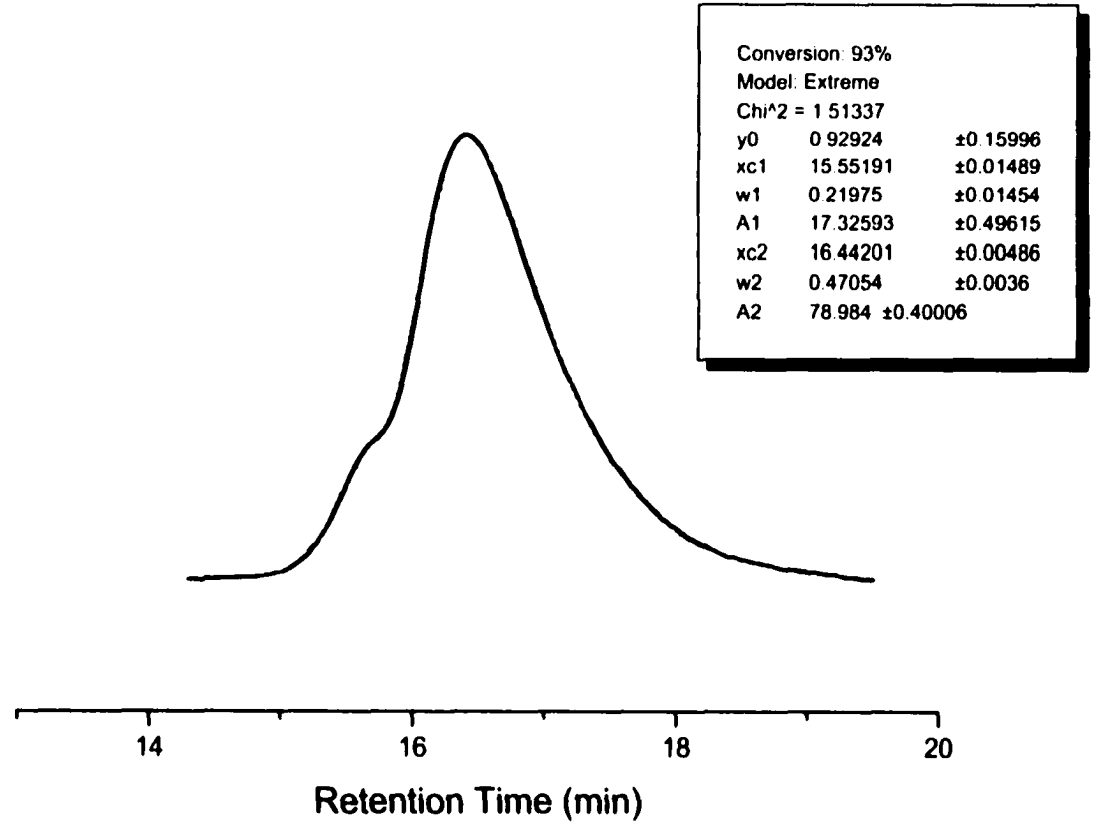

Conversion = 93%

Figure 44 Deconvolution of GPC traces.

143

Table 5. Molecular weights in System 1[a]

Yield %	$\bar{M}_n$			$\bar{M}_w$			$\bar{M}_w/\bar{M}_n$			Area Fraction[c]	
	Total[b] x10^{-5}	Left[c] x10^{-5}	Right[c] x10^{-5}	Total[b] x10^{-5}	Left[c] x10^{-5}	Right[c] x10^{-5}	Total[b]	Left[c]	Right[c]	Left	Right
6	0.85	3.36	0.58	1.80	3.73	0.72	2.1	1.1	1.2	0.41	0.59
27	1.65	4.33	1.28	2.69	5.64	1.55	1.6	1.3	1.2	0.33	0.67
30	1.79	4.89	1.31	2.92	6.16	1.74	1.6	1.3	1.3	0.29	0.71
77	2.40	6.87	2.03	3.27	7.67	2.72	1.4	1.1	1.3	0.21	0.79
93	2.57	7.47	2.33	3.54	8.28	3.07	1.4	1.1	1.3	0.18	0.82

[a] $[\mathbf{1}]_0$ = 5.0 mM, $[B(C_6F_5)_3]_0$ = 2.5 mM, $[MMA]_0$ = 1.0 M, toluene as solvent, temperature = 0 °C.

[b] Measured from GPC, calibrated by PMMA standard

[c] Mathematically deconvoluted by two peaks, as shown in Figure 43.

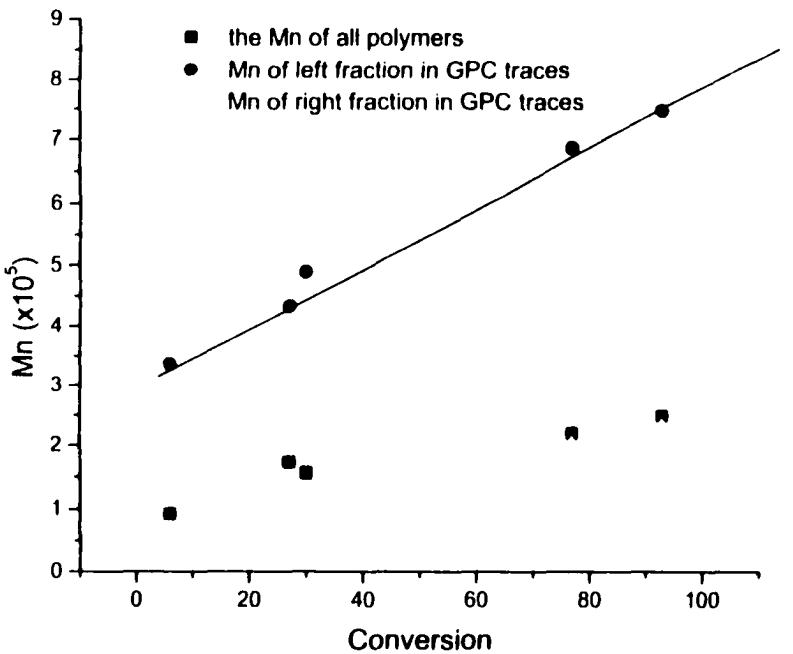

Figure 45 $\bar{M}_n$ vs. conversion in System 1.

$[\mathbf{1}]_0$ = 5.0 mM, $[B(C_6F_5)_3]_0$ = 2.5 mM, $[MMA]_0$ = 1.0 M, toluene as solvent, temperature = 0 °C

The same observations was also obtained in System 1 when a **1**/$B(C_6F_5)_3$ of 4:1 was used (Figure 46). Deconvoluting the measured GPC traces into two peaks, the similar relationship of $\bar{M}_n$ vs. conversion in this 4:1 system was also obtained (Figure 47). The bimodal distribution was also observed at the early stage of the polymeizations with **1**/$B(C_6F_5)_3$ of 10:1 and 1.5:1, respectively, as shown in Figure 48 and Figure 49. An interesting observation is that with the increase of the ratio (**1**/$B(C_6F_5)_3$), the fraction of the left side of the GPC traces increased, which shows another effect of excess intiator on the polymerization, i.e., excess of initiator increases the amount of the active species that corrsponds to the left side peak of the GPC traces, whatever that species really is.

3.2.2.3.2 System 2

In contrast to System 1, System 2 possesses a much clearer living nature. Figure 50 and Figure 51, respectively, show the plots of conversion versus reaction time and the GPC traces of the first-batch and final polymers in System 2. The second batch polymerization continued and progressed to full conversion after the addition of the second batch of MMA. The GPC trace of the final polymer (Figure 51) showed a continuous growth of the polymer chains during the second batch polymerization, although a bimodal distribution was obtained. In this bimodal distribution, a large fraction of the signal moved to higher molecular weight and a small fraction of it remained at the same retention time where the signal of the first batch polymer is located. From deconvolution of this GPC trace, two signals with $\bar{M}_n$ of 1.34×10^5 and 0.59×10^5 respectively were obtained. The latter fits very well with the measured $\bar{M}_n$ of the first batch polymer, which was 0.60×10^5, showing that this fraction of polymer chains was the terminated chains at the completed conversion of the first batch polymerization. From

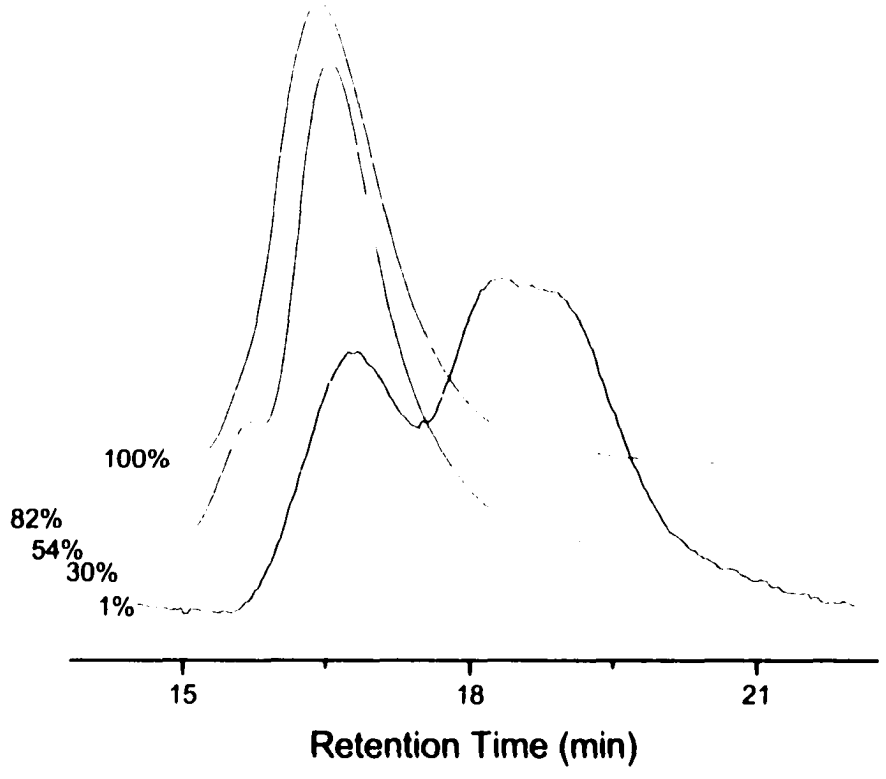

Figure 46. GPC traces of PMMA from **1**/$B(C_6F_5)_3$ initiation system: $[B(C_6F_5)_3]_0$ = 2.5 mM, $[\mathbf{1}]_0$ = 5.0 mM, $[MMA]_0$ = 1.0 M, temp = 0 °C, numbers indicate the conversion of the monomer.

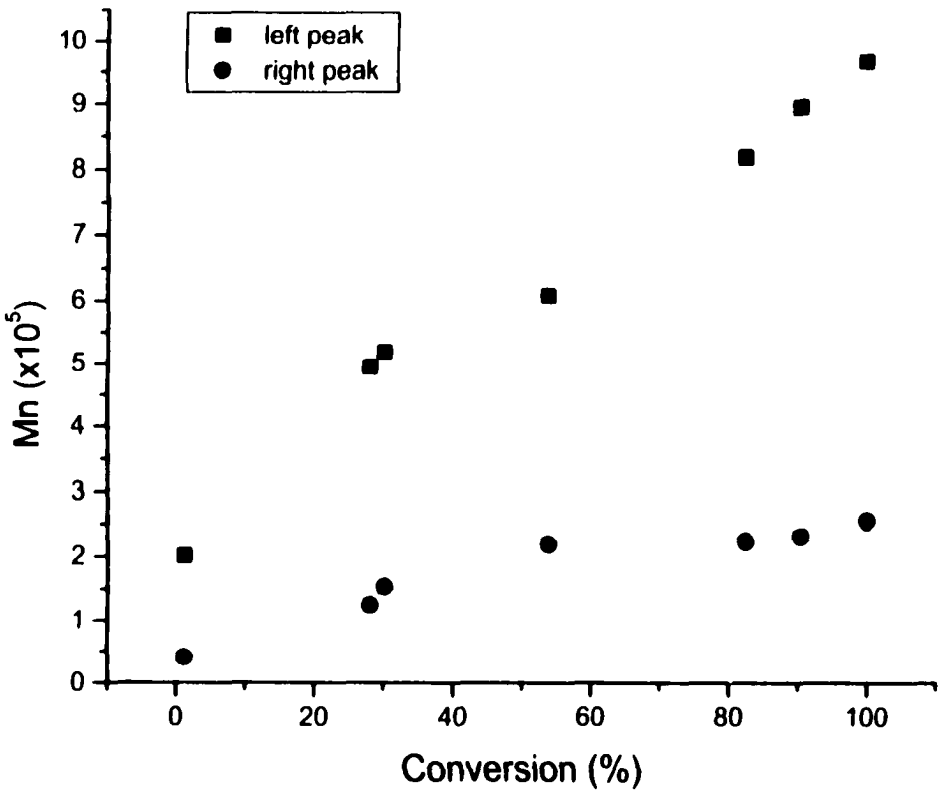

Figure 47. $\bar{M}_n$ vs. conversion in System 1.

$[1]_0$ = 10.0 mM, $[B(C_6F_5)_3]_0$ = 2.5 mM, $[MMA]_0$ = 1.0 M, toluene as solvent, temperature = 0 °C.

148

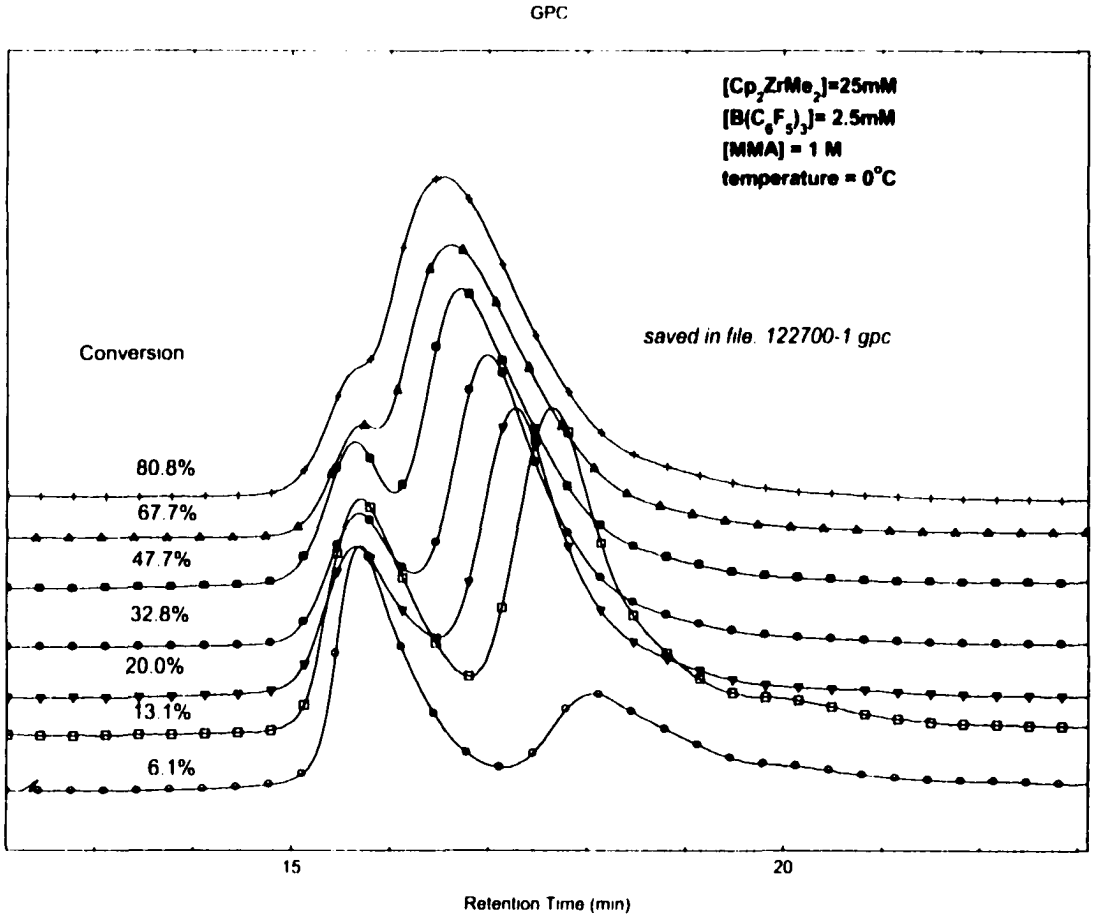

Figure 48. GPC traces of PMMA from **1**/$B(C_6F_5)_3$ initiation system: $[B(C_6F_5)_3]_0$ = 2.5 mM, $[\mathbf{1}]_0$ = 25 mM, $[MMA]_0$ = 1.0 M, temp = 0 °C, numbers indicate the conversion of the monomer.

149

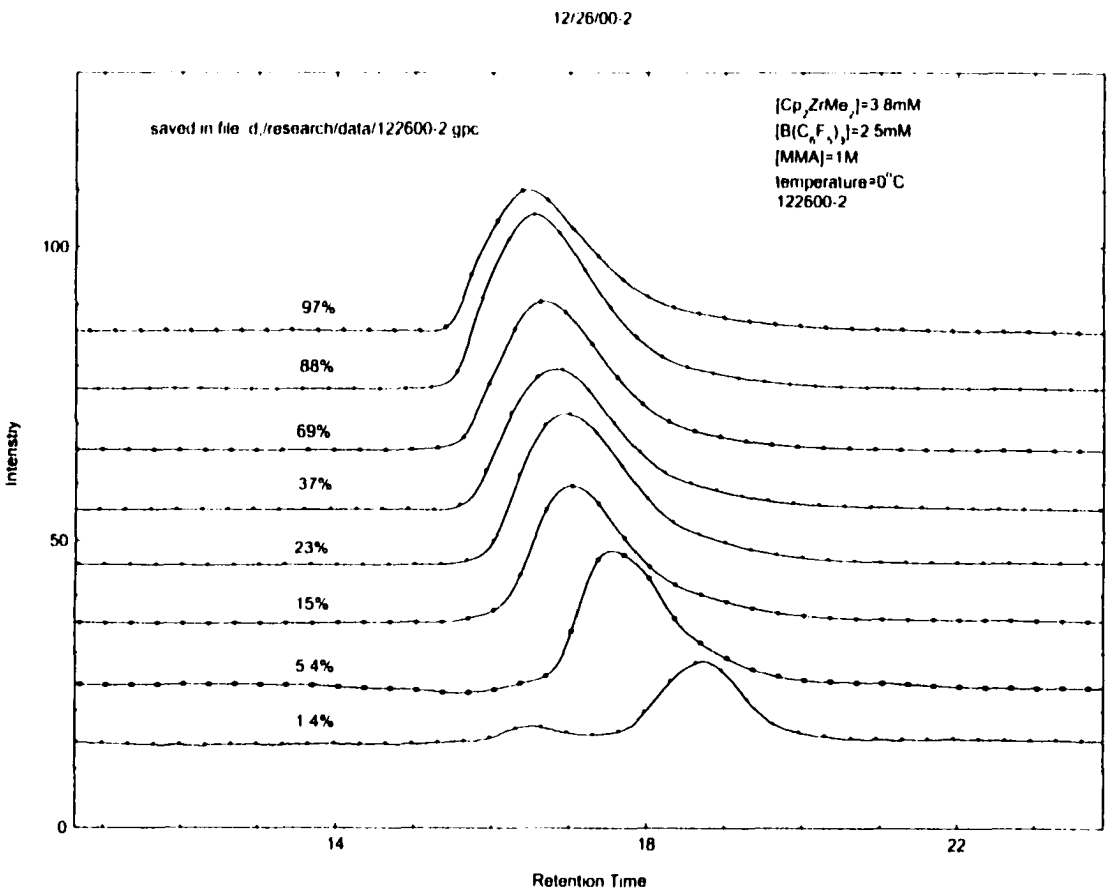

Figure 49. GPC traces of PMMA from **1**/$B(C_6F_5)_3$ initiation system:

$[B(C_6F_5)_3]_0$ = 2.5 mM, $[\mathbf{1}]_0$ = 25 mM, $[MMA]_0$ = 1.0 M, temp = 0 °C, numbers indicate the conversion of the monomer.

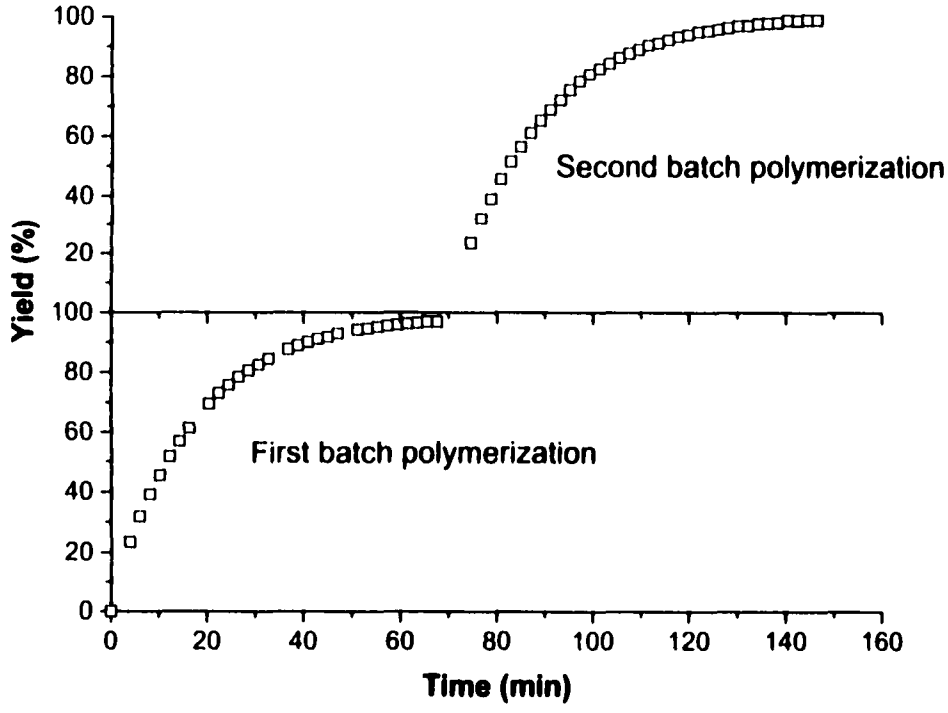

Figure 50. Living characteristics of the System 2.

$[2]_0$ = 5.0 mM, $[B(C_6F_5)_3]_0$ = 2.5 mM, $[MMA]_0$ = 1.0 M, (both first and second batches), toluene as solvent, temperature = 22 °C, time interval between two batches was 0 min.

151

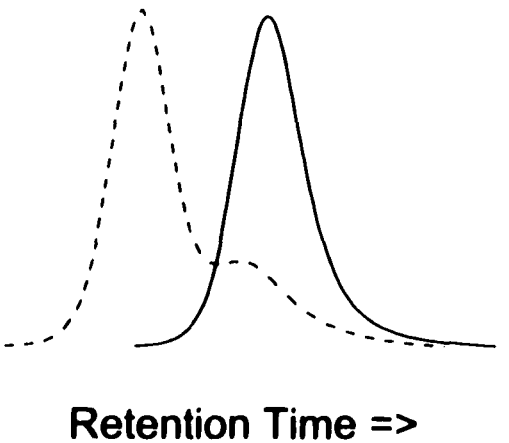

Figure 51. GPC traces of polymer from sequential addtion experiments.

Experimental conditions are the same as those of Figure 50.

152

the areas of these two fitted signals, their mole fractions were calculated to be 0.72 and 0.28 respectively. Considering that the initial concentrations of MMA used in the two batches were 1.0 and 0.91 M respectively and assuming no new active species were generated during the second batch, i.e., the second batch of MMA (0.91M) was all grown on the 72% of the polymer chains generated from the first batch (with 28% of chains terminated), the final $\bar{M}_n$ of the continuously growing chains was calculated as 1.36×10^5, which was consistent with the above deconvoluted value of 1.34×10^5. Therefore, System 2 complied well with the Criterion 1 of the living polymerization, i.e., the polymer chains continue to grow when additional monomer has been added. No new active species were generated and the chains number of the polymer in the system was constant, which met with the Criterion 3. To further confirm the above conclusion and to further investigate the living character of System 2, polymers at various conversions for both batches were also obtained by the gravimetry method (Figure 52, 53). It should be noted that because the polymerization in System 2 was first order in [MMA], at a late stage, the polymerization occurred slowly due to a low concentration of MMA. In order to obtain 100% conversion, a long time was spent at this late stage of polymerization, during which [MMA] was virtually zero and chain termination or chain transfer probably would occur. In fact, this is the reason why a bimodal distribution is seen in Figure 51. In order to prevent this from happening, in the gravimetry method for the sequential monomer-addition experiment, the second batch of MMA was added at 51 min, which corresponded to 95% conversion of the first batch polymerization. The polymer at various conversions in both batches (Figure 52) shows that in this system, only one single active species existed over the whole polymerization, which resulted in the monomodal

molecular weight distribution in Figure 52. In both batches of polymerization, $\bar{M}_n$ increased linearly with conversion and a narrow MWD (Criterion 5) was obtained throughout the whole polymerization (Figure 53, $\bar{M}_w/\bar{M}_n$ < 1.2). Criterion 2 was satisfied.

In addition, since there is no decrease of $\bar{M}_n$ at low conversion of the second batch (Figure 52, contrast to that in System 1), the final $\bar{M}_n$ was almost twice as much as that of the first batch polymerization (1.08×10^5 vs. 0.532×10^5 in Figure 53), and the narrow MWD throughout both of the polymerizations implied that the polymer chains did not undergo termination or transfer and no new polymer chains were generated during the polymerization. In other words, the number of polymer molecules was a constant in Sysetm 2, which fits exactly Criterion 3 of a living polymerization system. All these results indicated that System 2 was a pure living system.

More study was performed on System 2 because of its clearly living characteristics. The different polymerization conditions are listed in Table 6 and the corresponding $\bar{M}_n$ vs. conversion and initiation efficiency vs. conversion plots for each entry in Table 6 are shown in Figure 54. The initiation efficiency (I_{eff})[29] was calculated by the following equation:

$$I_{eff} = \frac{\bar{M}_n(\text{theoretical})}{\bar{M}_n(\text{observed})} = \frac{[M]_0 / [B(C_6F_5)_3]_0}{[M]_0 / [\text{polymer chain}]} = \frac{[\text{polymer chain}]}{[B(C_6F_5)_3]_0} \qquad (30)$$

assuming that each $B(C_6F_5)_3$ molecule ends up in one active polymer chain for an initiation efficiency of 100%. The concentration of polymer chains, i.e., [polymer chain]

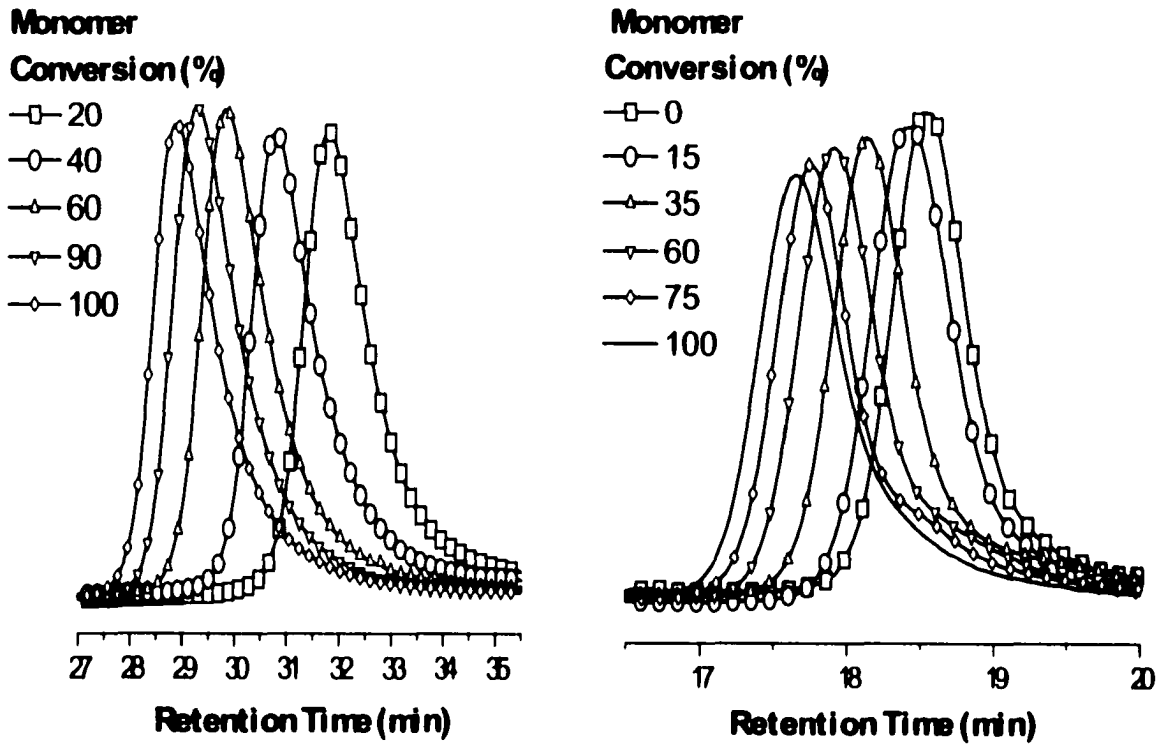

a b

Figure 52. GPC traces of PMMA's from **2**/$B(C_6F_5)_3$ initiation system:

$[B(C_6F_5)_3]_0$ = 2.5 mM, $[\mathbf{2}]_0$ = 5.0 mM, $[MMA]_0$ = 1.0 M, temp = 22 °C.

a) first batch polymerization; b) second batch polymerization.

155

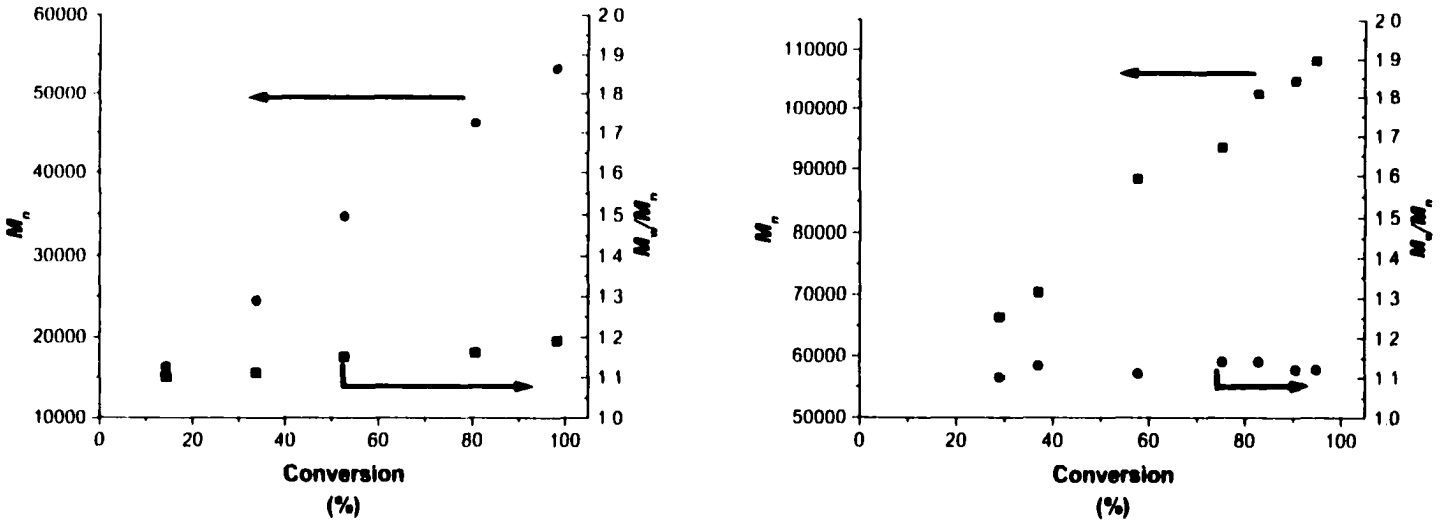

Figure 53. $\bar{M}_n$ and $\bar{M}_w/\bar{M}_n$ vs. monomer conversion of MMA polymerization by **2**/$B(C_6F_5)_3$ initiation system: $[B(C_6F_5)_3]_0$ = 2.5 mM, $[\mathbf{2}]_0$ = 5.0 mM, $[MMA]_0$ = 1.0 M, temp = 22 °C. a) first batch polymerization; b) second batch polymer

156

le 6. Various polymerizations of MMA by using 2/B(C_6F_5)$_3$ initiation system [a]

Entries	[2] (mM)	[B(C_6F_5)$_3$] (mM)	$[MMA]_0$ (M)	T_p [b] (°C)	Yield (%)	$\bar{M}_n$ [c] (x10^4)	$\bar{M}_w/\bar{M}_n$ [c]	I_{eff} [d]	k_{app} [e] (min^{-1})
1	10	5.0	1.0	22	100	2.03	1.19	0.99	0.24
2	10	5.0	1.0	0	96	2.76	1.08	0.70	0.038
3	10	2.5	1.0	22	96	3.24	1.37	1.19	0.053
4	10	1.0	1.0	22	98	5.27	1.72	1.85	0.017
5	10	5.0	1.0	-24	88	2.50	1.11	0.70	0.0072
6	5.0	2.5	1.0	22	100	5.32	1.19	0.75	0.057
7	2.0	1.0	1.0	22	22	6.72	1.21	0.33	0.0063
8	10	5.0	2.0	0	96	11.35	1.13	0.34	0.021
9	10	5.0	0.5	0	100	1.77	1.08	0.57	0.029

[a] All polymerizations were carried out in toluene solution.
[b] Polymerization temperature.
[c] Measured by GPC, calibrated by PMMA standards.
[d] Initiation efficiency, calculated from Equation 34.
[e] Apparent polymerization rate constant.

157

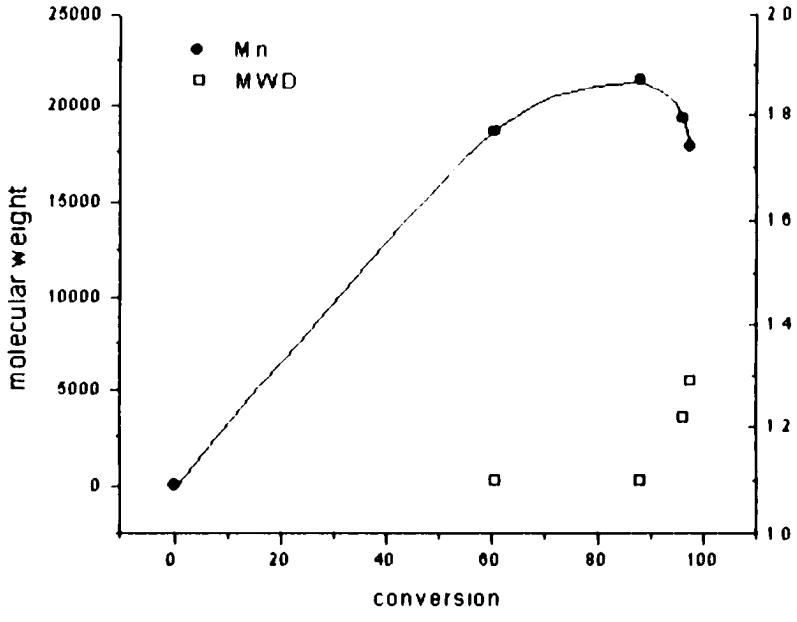

a

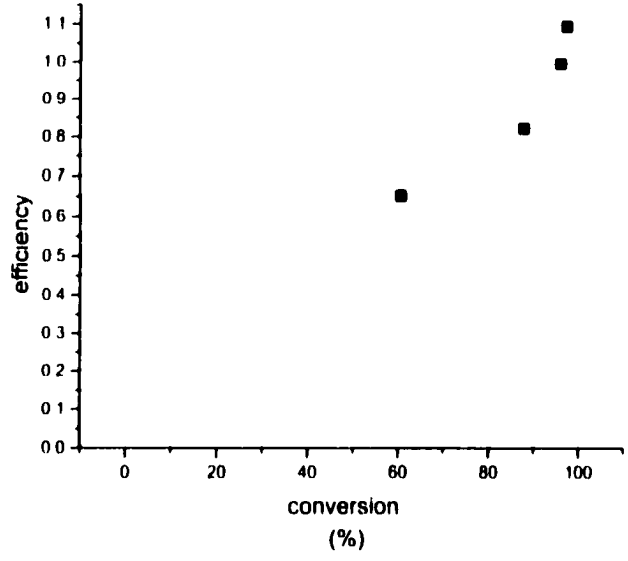

b

Entry 1 of Table 6

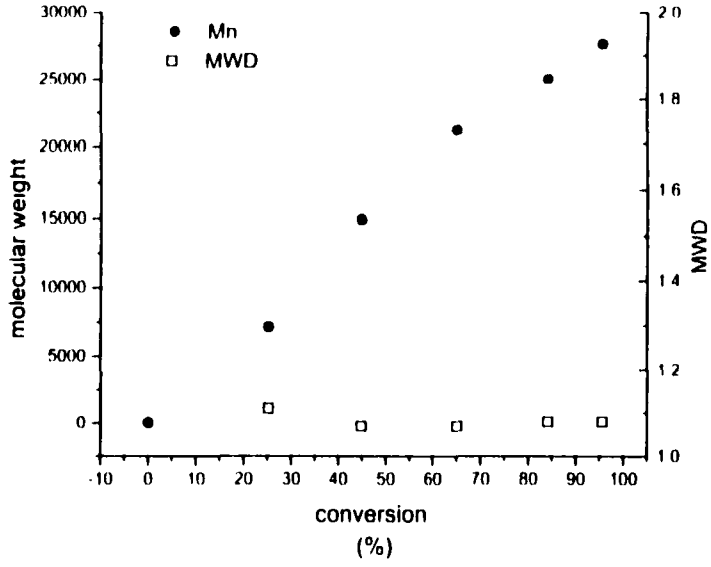

a

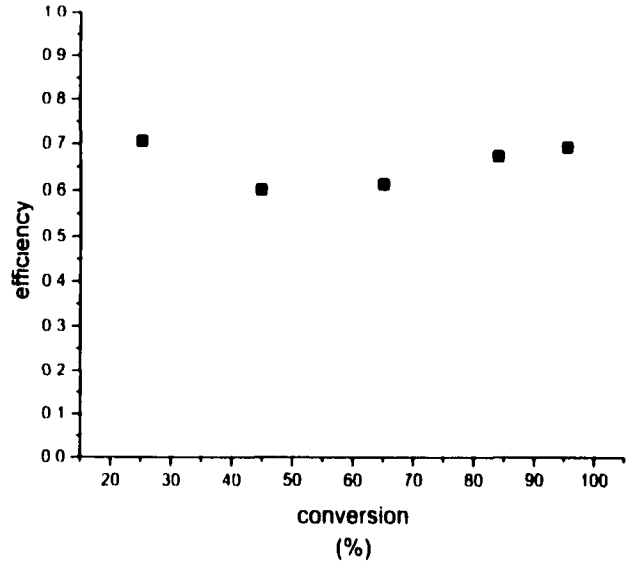

b

Entry 2 of Table 6

159

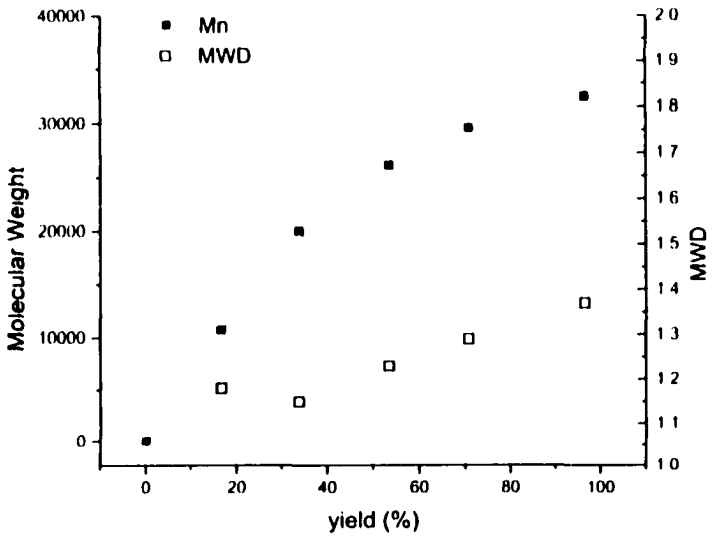

a

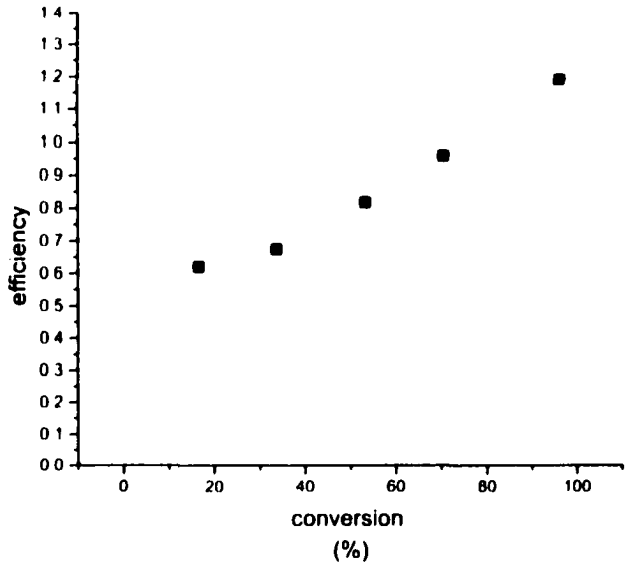

b

Entry 3 of Table 6

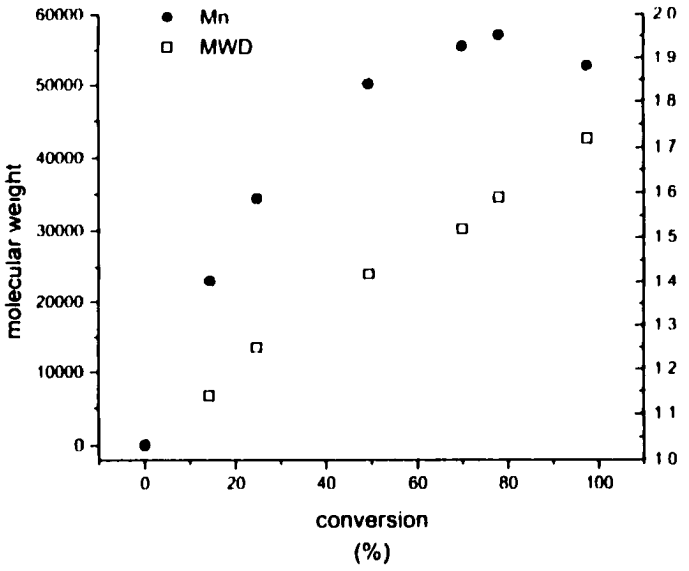

a

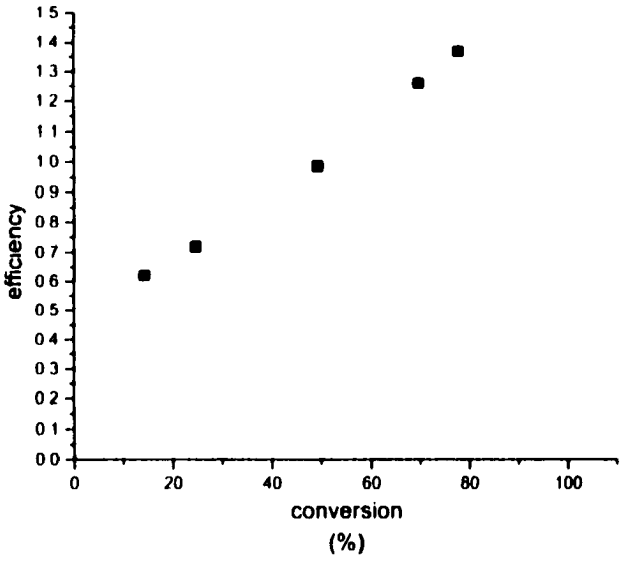

b

Entry 4 of Table 6

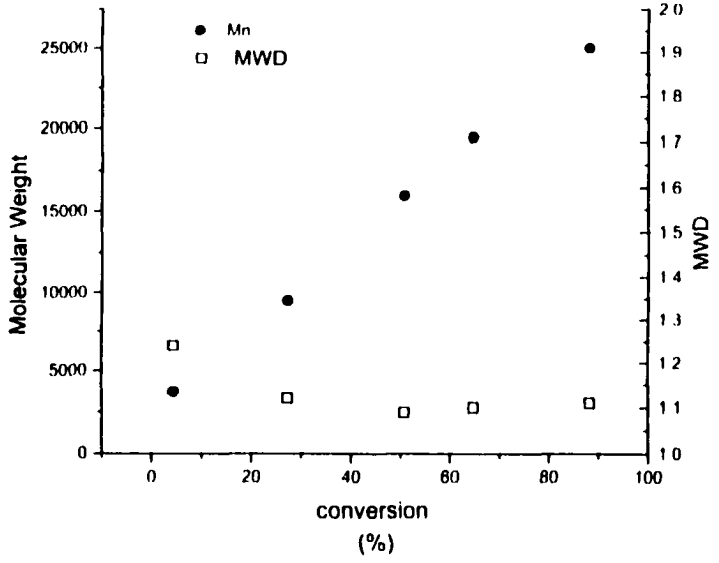

a

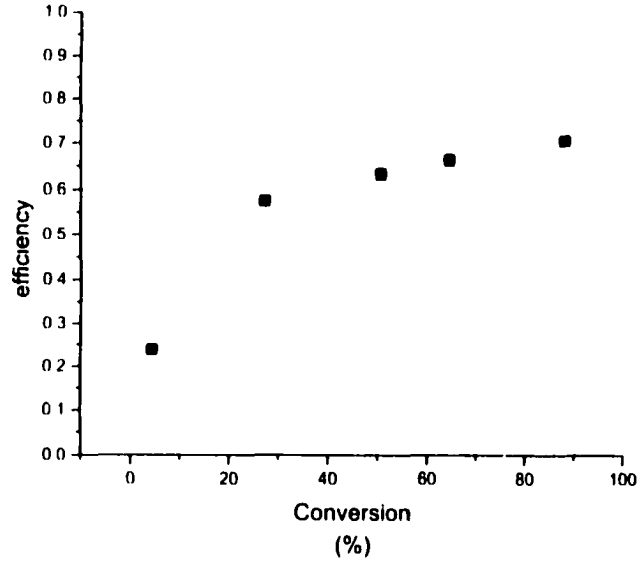

b

Entry 5 of Table 6

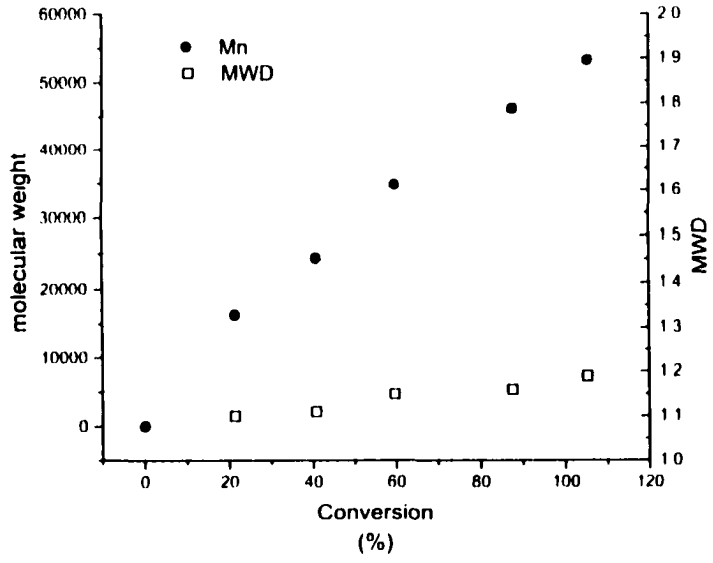

a

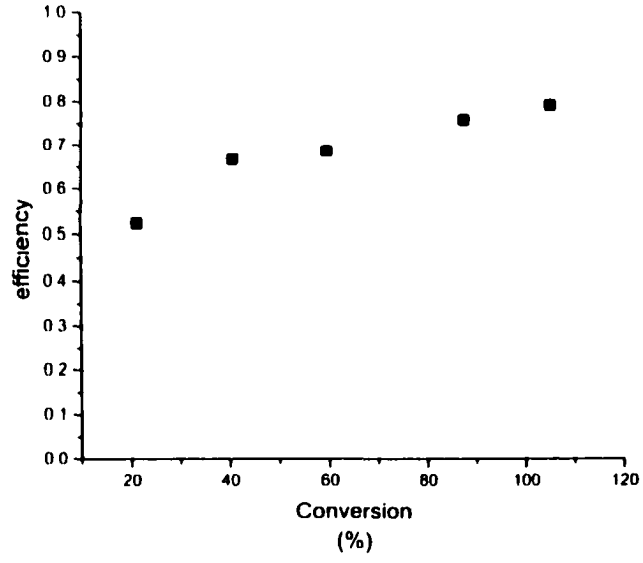

b

Entry 6 of Table 6

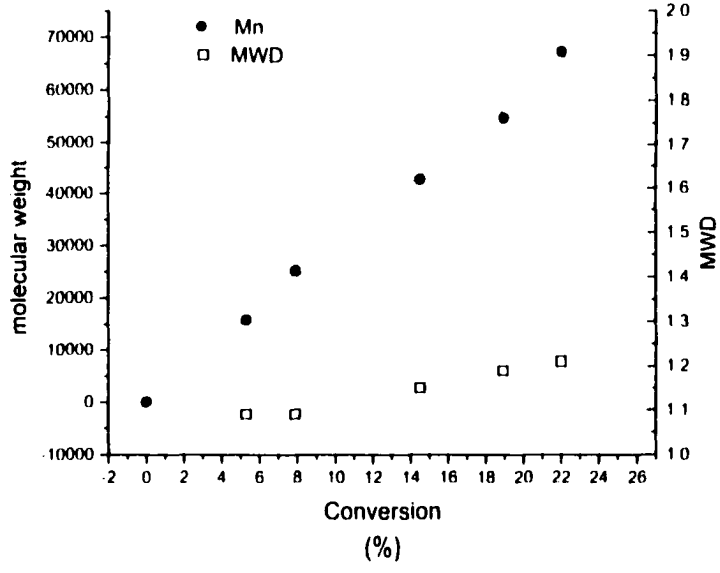

a

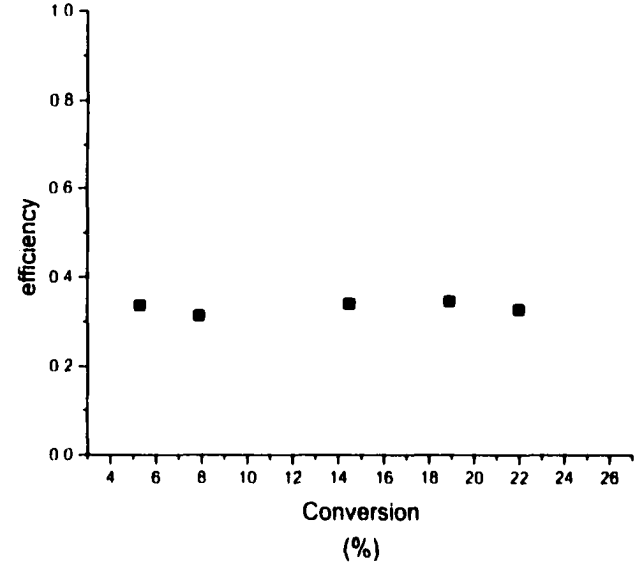

b

Entry 7 of Table 6

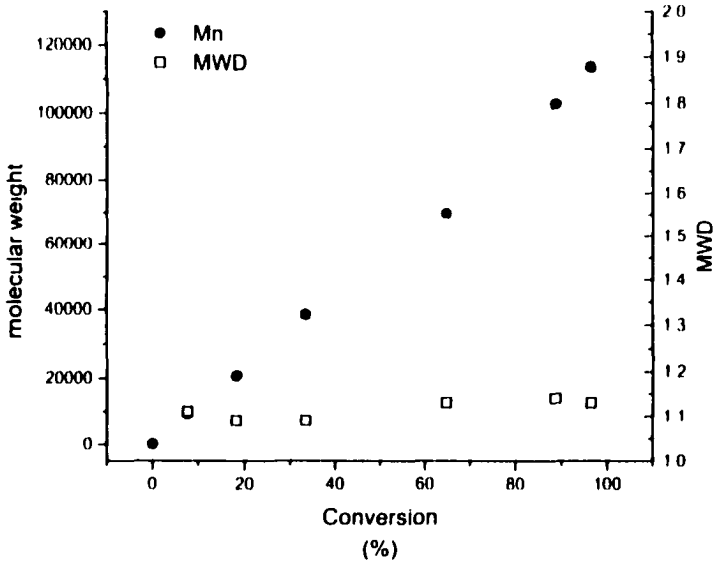

a

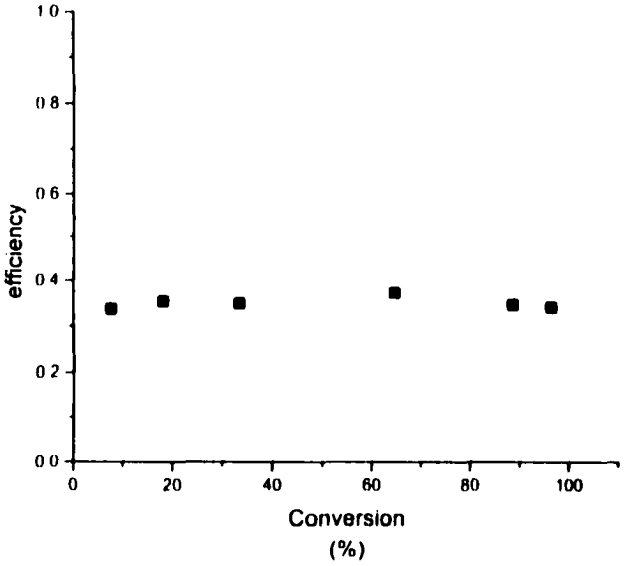

b

Entry 8 of Table 6

165

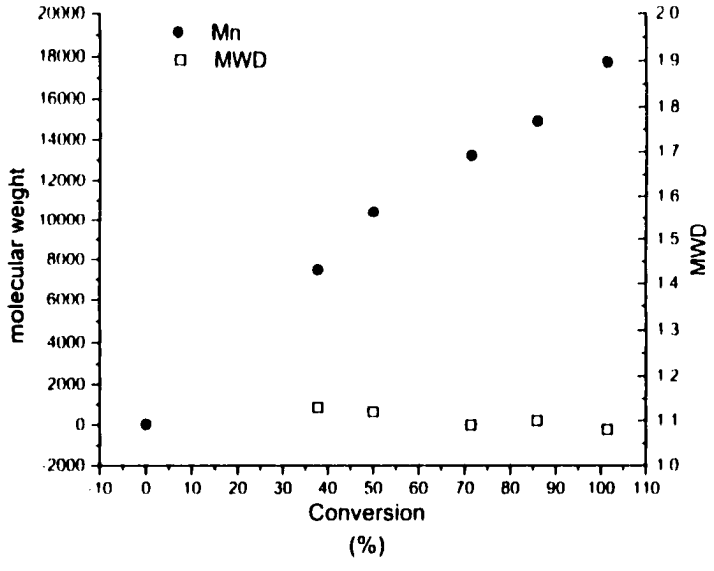

a

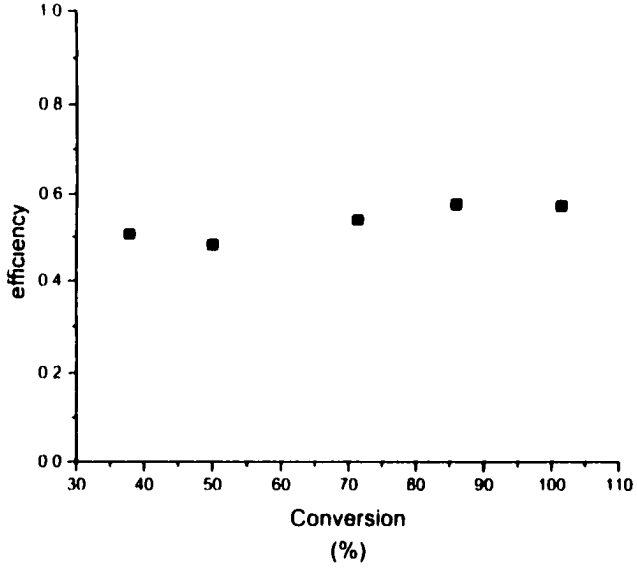

b

Entry 9 of Table 6

Figure 54 Various polymerization systems using **2**/$B(C_6F_5)_3$ initiation system.

in Equation 30 can be calculated by:

$$[\text{polymer chain}] = \frac{[\text{monomer consumed}]}{\overline{DP}_n} \qquad (31)$$

The monomer consumed and the average degree of polymerization can be calculated as follows:

$$[\text{monomer consumed}] = [\text{MMA}]_0 \cdot \text{conversion} \qquad (32)$$

$$\overline{DP}_n = \bar{M}_n / FW \qquad (33)$$

The FW in Equation 33 is the molecular weight of the repeat unit, which is 100 in the case of PMMA, therefore the I_{eff} can be finally expressed by:

$$I_{eff} = \frac{[MMA]_0 \cdot conversion \cdot 100}{[B(C_6F_5)_3]_0 \cdot \bar{M}_n} \qquad (34)$$

I_{eff} is a parameter that represents the percentage of the $B(C_6F_5)_3$ molecules that are converted to the active polymer chains in the polymerization systems. Since $[B(C_6F_5)_3]_0$ is a constant, I_{eff} is proportional to the concentration of the active polymer chains in the systems (according to Equation 30), therefore the change of I_{eff} reflects the change of the active polymer chains in the polymerization system.

From Figure 54, it is seen that most of the polymerization systems were living systems, which are represented by linear $\bar{M}_n$ vs. conversion, low $\bar{M}_w/\bar{M}_n$ and constant I_{eff}, in other words constant active polymer chains, throughout the whole conversion (Entries 2, 5, 6, 7, 8, 9). All of these polymerization occurred either at a relative low temperature (≤ 0 °C), such as Entries 2,4,8,9, or at relatively low concentrations of initiator and coinitiator ($[B(C_6F_5)_3] \leq 2.5$ mM, **2**/$B(C_6F_5)_3$ =2), such as Entries 6 and 7. When a

polymerization occurring at room temperature and high concentrations of initiator and coinitiator, it normally resulted in a too fast reaction, i.e., a quantitative conversion in less than 30 min, which resulted in a hard-to-control polymerization as in Entry 1. (This is perhaps why System 1 was not very well controlled, since most of the polymerization in System 1 finished in less than 30 min). Another interesting observation in polymerization of System 2 is that the excess initiator seemed to have a negative effect on the living polymerization. In both Entries 3 and 4, in which **2**/$B(C_6F_5)_3$ are 4:1 and 10:1, respectively, poor living systems were observed. The $\bar{M}_n$ leveled off with an increase of $\bar{M}_w/\bar{M}_n$ and increase of I_{eff}, all of which indicates the generation of new active species at the late stage of polymerization. Therefore, the high excess of initiator enables the new species to be generated in the systems. However, compared with the polymerization rate, this process is a slow one because all the above "nonlivingness" occurred only at the late stage of the polymerization, which means it needs a relatively long time for the new active centers to be generated. All these results strongly indicated that the generation of the active centers is an equilibrium reaction that involves the participation of the initiator, and its reaction rate is low.

Another observation is that when $[MMA]_0$ was increased, the $\bar{M}_n$ of the final polymer increased, Entries 2,8,9. However, the increase of $\bar{M}_n$ was not proportional to the increase of $[MMA]_0$, which can not be explained. The observation is that the I_{eff} of Entries 2,8,9 were different. Again it can not be explained why the change of the I_{eff} with $[MMA]_0$ occurred. Therefore, Criterion 4 for the living polymerization was not fully met in System 2.

3.3 Mechanism of the Polymerization

Combining all of the above results, a mechanism (Scheme 17) is presented based on the reported mechanism for similar systems.[17,29] In initiation, an equimolar amount of the initiator,

Scheme 17.

Initiation:

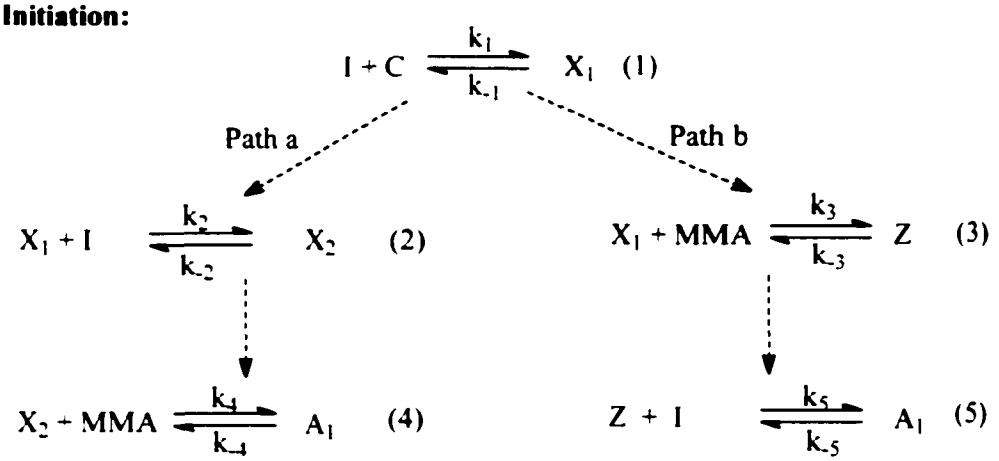

Propagation: (see Scheme 17 for details)

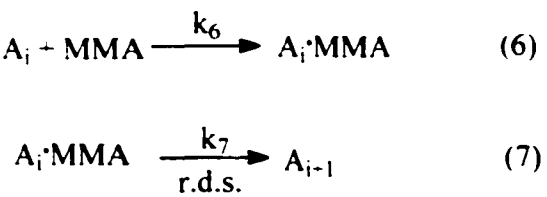

I, and the coinitiator, C, first form a mononuclear cationic zirconocene complex, $L_2ZrMe^{+}\cdots Me^{-}B(C_6F_5)_3$ (L is Cp or its derivatives),[11,41] referred to as X_1. X_1 subsequently reacts with an excess of I and MMA to form the initial propagating center A_1 via two possible paths. In Path a, the excess I first reacts with the coordinatively unsaturated X_1. A dinuclear cationic complex X_2 is therefore formed, whose structure is probably $[(L_2ZrMe)_2(\mu\text{-}Me)]^{+}\cdots Me^{-}B(C_6F_5)_3$.[17,41,51,52] X_2 then reacts with MMA

forming A_1; In Path b, MMA first coordinates with X_1. An adduct Z is formed,[25,28,29] which then reacts with I to produce A_1. After the formation of A_1, propagation starts, which includes two steps: 1) a fast coordination of MMA to the propagating center A_i (i = 1, 2, ..., stands for the number of MMA units in the propagating chain) that forms an intermediate A_i·MMA; and 2) an insertion of the coordinated MMA into the polymer chains via a polymer transfer mechanism reported by Collins.[29] The later step (Step 7) is the rate determining step for the propagation.

Considering the feature that in the polymer transfer mechanism[29], two metal centers in the propagating center are interchanged with the addition of one monomer unit; (Scheme 18) and the initial propagating center can be generated from the dinuclear cationic complex (X_2)[17], it is suggested that the propagating center should contain two

Scheme 18.

Proposed "cage" structure of the Propagation center A_i:

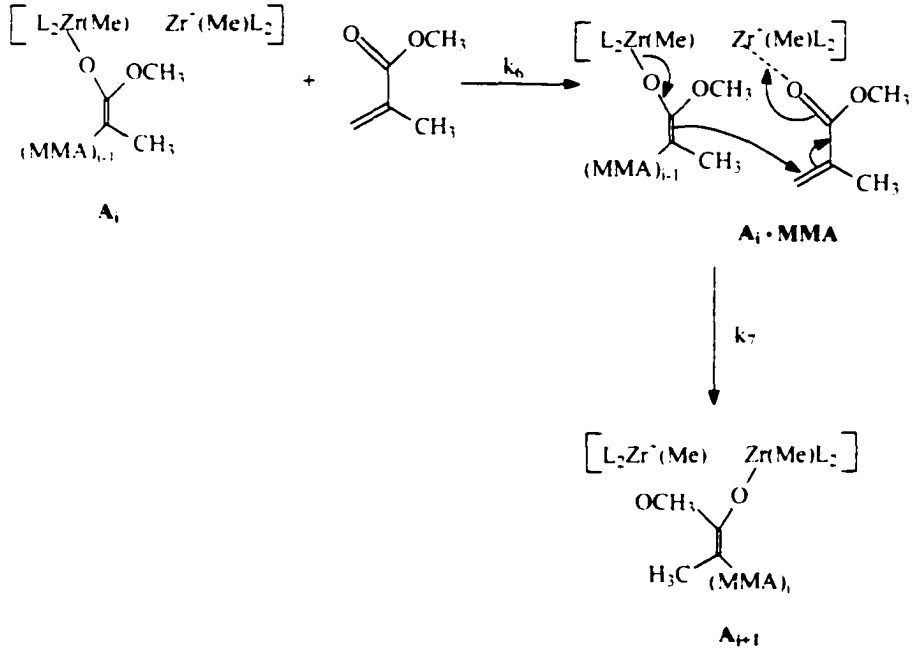

metals that are trapped in adjacent space, in which the two metal centers may be confined together by the respective connection to the common counterion. This structure is referred to as a "cage" (Scheme 18) and its concentration, i.e., $[A_i]$, is assumed constant throughout the polymerization.

This mechanism provides an explanation for the observations in the two systems. From Step 7, the polymerization rate can be expressed as:

$$R_p = k_7 \cdot [A_i \cdot MMA] \qquad (35)$$

When Step 6 is irreversible and fast (i.e., $[A_i] = [A_i \cdot MMA]$), R_p is

$$R_p = k_7 \cdot [A_i] = k_7 \cdot [A_1] \qquad (36)$$

R_p depends on the concentration of the initial propagating center formed in the initialization step.

In System 1, the bimodal MWD implied that both Path a and Path b were involved in the formation of A_1 and the features of the MWD can be ascribed to the kinetic and thermodynamic attributes of these two paths. In Step 1, when initiator **1** first reacted with the coinitiator $B(C_6F_5)_3$, forming X_1,[111] which subsequently reacted through both Path a and Path b to form A_1. In Path b, since MMA has a smaller size and stronger nucleophilicity than **1**, it attacked the cationic center of X_1 easily. Therefore, Path b was the kinetically favorable path. However, in Path a, the formation of X_2 distributed the positive charge to two zirconocene centers, which made it relatively stable, therefore, Path a was the thermodynamically favorable path. Most of A_1 was produced through Path a while a small amount of A_1 was formed quickly through Path b. This scenario explained the changes of the MWD observed in System 1. In Path a, since Step 4 is a fast step[13] and $[MMA] >> [X_2]$, which results in

$$[A_1] = [X_2] \quad (37)$$

From the two equilibria, Step 2 and Step 1,

$$[X_2] = k_2/k_{-2}\,[X_1][I] \quad (38)$$

and

$$[X_1] = k_1/k_{-1}[I][C] \quad (39)$$

therefore,

$$[A_1] = k_2/k_{-2}\,(k_1/k_{-1}[I][C])\,[I] \quad (40)$$

Combining Equation (36) and (40) gives R_p as

$$R_p = k_7 \cdot k_2/k_{-2}\,(k_1/k_{-1}[I][C])[I] = k_{app}\,c^3 \quad (41)$$

where c is the concentration of coinitiator [C] and [I] = 2c. Equation 41 fits well with the experimental observations in System 1, i.e., the polymerization rate was zero order with respect to [MMA] and third order (combined rate order[145]) in the concentration of the initiation components.

Initiator **2** differed significantly from **1** in the large size of its π-ligands ($IndH_4$ versus Cp) and the constraint on its configuration due to the -$Si(CH_3)_2$- bridge, both of which introduced steric hindrance to the reactions in which **2** participated. Therefore, Path b is more favorable because it involves a nucleophilic attack from a small molecule, MMA, in Step 3 rather than from a much more sterically hindered molecule, the initiator **2** itself, in Step 2. Consequently, all the reactions go through Path b and Step 3 is the rate determining step. Only monomodal MWD was observed for polymer in System 2. When Step 5 is irreversible and fast (i.e., $[A_1] = [M]$), R_p is

$$R_p = k_7[A_1] = k_7[M] \quad (42)$$

From the two equilibria, Step 3 and Step 1,

$$[M] = k_3/k_{-3}\,[X_1][MMA] \qquad (43)$$

and

$$[X_1] = k_1/k_{-1}[I][C] \qquad (44)$$

therefore,

$$R_p = k_7\, k_3/k_{-3}\, k_1/k_{-1}[I][C][MMA]$$

$$= k_{app}c^2[MMA] \qquad (45)$$

Equation (45) agrees well with the kinetic results of System 2

3.4 Polymerization of Other Monomers via These Initiation Systems

3.4.1 Homopolymerization

3.4.1.1 Methyl Acrylate (MA)

Comparing the polymerization of MA, carried out by the 2/$B(C_6F_5)_3$ initiation system with a ratio of 2:1, with the polymerization of MMA using the same experimental conditions, poly(methyl acrylate) (PMA) shows a broader MWD and a similar $\bar{M}_n$ to that of the PMMA. When 2 mL of **2** solution (35 mM) and 1 mL of $B(C_6F_5)_3$ solution (35 mM) as the initiation system was used with 4 mL of MA or MMA, $\bar{M}_n$ = 1.53x10^5 and 1.31 x10^5, respectively, were obtained. The MWD's are shown in Figure 55. Although β-H exists in the MA (CH_2=C<u>H</u>$COOCH_3$), high molecular weight PMA was obtained by System 2, which indicates that this initiation system can prevent the β-H termination or transfer from occurring. This may be caused by the steric template formed by **2**, which impeded the access of the β-H from the metal center. However, the more bimodal-shaped MWD of PMA than that of PMMA shows more chain breaking occurred in MA polymerization.

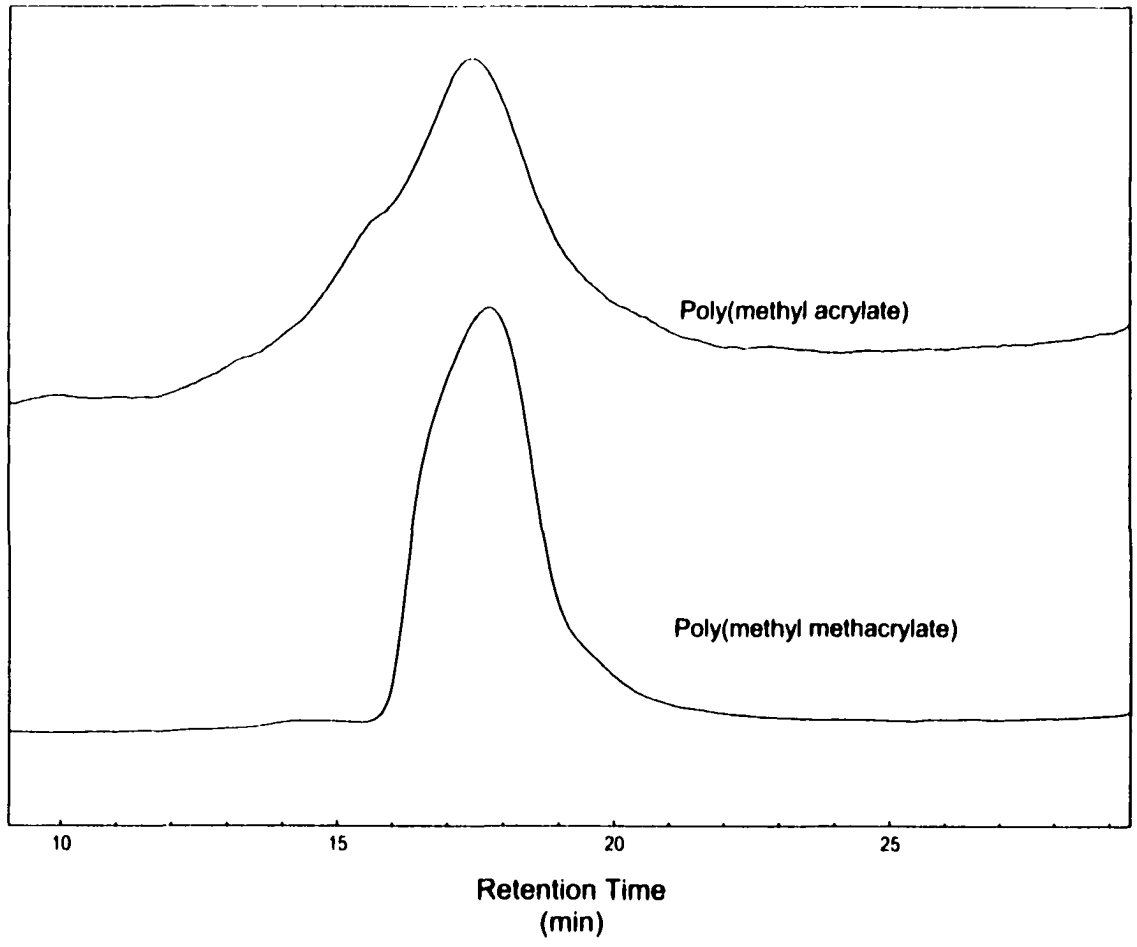

Figure 55. GPC traces of PMMA and PMA obtained from 2:1 of **2**/$B(C_6F_5)_3$ initiation system.

2 mL of **2** (35 mM) and 1 mL of $B(C_6F_5)_3$ (35 mM) and 4 mL of monomer.

174

3.4.1.2 1-Hexene

Polymerizations of 1-hexene using the **2**/$B(C_6F_5)_3$ initiation system were performed in 2:1 and 1:1 ratios, respectively. The 1:1 ratio of dimethyl zirconocene and $B(C_6F_5)_3$ is widely reported[1-5] as an active initiation system for the polymerization of olefins, therefore it was used as a comparison to study the polymerization of 1-hexene by 2:1 system. Figure 56 shows the MWD of the polymers obtained by both 1:1 and 2:1 of **2**/$B(C_6F_5)_3$ initiation systems. The $\bar{M}_n$ and $\bar{M}_w/\bar{M}_n$ for 1:1 system are 770, 1.95 and for for the 2:1 system are 900, and 1.91. It is interesting to note that the 2:1 system gave almost the same poly(1-hexene) as the 1:1 system did, which indicates that the 2:1 system has the same activity toward polymerization of 1-hexene as that of 1:1 system. Two important inspirations from this observation are: 1) in the polymerization of olefin using dimethyl zirconocene/$B(C_6F_5)_3$ system, half of the $B(C_6F_5)_3$ is unnecessary and can be saved. 2) the same 2:1 ratio system can be both used to polymerize polar monomers, e.g. MMA, and nonpolar monomers, therefore, the copolymerization of these two kinds of monomers are possible.

The capability of polymerization of olefins by 2:1 of dimethyl zirconocene/$B(C_6F_5)_3$ systems was also observed by Waymouth et al.[52] In their study, Waymouth reported that the poly(1-hexene) obtained from $Cp_2^*ZrMe_2$ or $(EtIndH_4)_2ZrMe_2$ with $B(C_6F_5)_3$ in a 2:1 ratio had $\bar{M}_n$ of 670 and 500 respectively, close to what was obtained in this laboratory. However, at that time (1992), the application of metallocene initiation systems to the polymerization of polar monomers had just begun,[24,25] the capability of polymerization of polar monomers by these 2:1 ratio initiation systems had not been realized, therefore the potential of copolymerization of polar monomers with olefins by them was not studied.

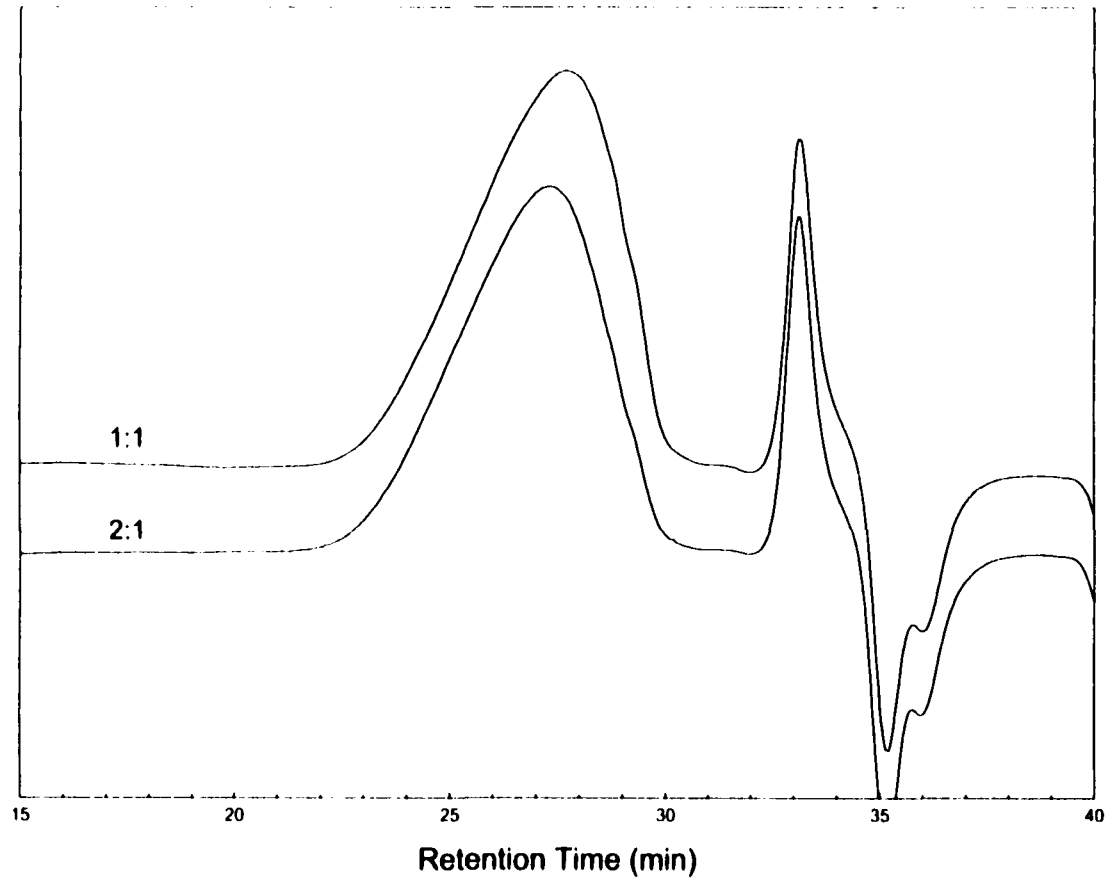

Figure 56. GPC traces of poly(1-hexene) obtained from 2:1 and 1:1 of **2**/$B(C_6F_5)_3$ initiation system. 2 mL of **2** (35 mM), 2 mL of toluene, 2 mL of 1-hexene and 2 mL or 1 mL of $B(C_6F_5)_3$ (35 mM)

176

Another observation of the 1-hexene polymerization by these 2:1 initiation system is that the final polymers have a low $\bar{M}_n$, less than 1000, which is much lower than the $\bar{M}_n$ obtained from polar monomers. This may indicate that such initiation systems are not highly active toward the 1-hexene polymerization, which is similar to the 1:1 initiation systems used for the α-olefin polymerizations: the activity of polymerization drops dramatically with the changing from ethylene, propylene to 1-butene, 1-pentene, 1-hexene and other higher α-olefins. Only low molecular weight homopolymers are obtained for such high α-olefins.

3.4.1.3 ε-Caprolactone

Polymerization of ε-caprolactone was performed by using the initiation system of **1**/$B(C_6F_5)_3$. Both 1:1 and 2:1 initiation systems were tested. When the 2:1 ratio was used, i.e., 2.5 mL of **1** (144 mM in toluene), 2.5 mL of $B(C_6F_5)_3$ (72 mM in toluene) and 2 mL of ε-caprolactone, slow polymerization was observed, and a viscous reaction mixture was obtained in 2 h. However, when a 1:1 ratio initiation system was used, i.e., 0.63 mL of **1** (144 mM in toluene), 1.25 mL of $B(C_6F_5)_3$ (72 mM in toluene) and 2 mL of ε-caprolactone, relatively faster polymerization was observed, and the reaction mixture could not flow after 2 hour's polymerization. After precipitation, 2.15 g of polymer were collected after precipitation and dried under vacuum, corresponding to 100% conversion of monomer. In order to rule out the possibility that the above polymerization occurred via a cationic ring opening mechanism by $B(C_6F_5)_3$, the $B(C_6F_5)_3$ was mixed with ε-caprolactone; after 2 h, no obvious polymerization was observed. Therefore the polymerization of ε-caprolactone was caused by the **1**/$B(C_6F_5)_3$ initiation system, not by only $B(C_6F_5)_3$.

3.4.1.4 Propylene oxide (PO)

Polymerization of PO by **2**/$B(C_6F_5)_3$ was also observed. However, since polymerization of PO was also caused by $B(C_6F_5)_3$ alone, the above polymerization can not be ascribed to the function of the **2**/$B(C_6F_5)_3$ initiation system. It may be caused by a simple cationic ring opening polymerization by $B(C_6F_5)_3$.

3.4.1.5 Vinyl Acetate (VA)

Polymerization of VA by **2**/$B(C_6F_5)_3$ was attemted, but no polymerization was observed.

3.4.2 Copolymerization

3.4.2.1 MMA and ε-Caprolactone

After polymerization of MMA using a 1:1 ratio of **1**/$B(C_6F_5)_3$, ε-caprolactone was charged into the reaction vessel. The polymerization of ε-caprolactone started and continued until the quantitative conversion of ε-caprolactone was reached. The GPC traces of the final polymer and PMMA from the first batch polymerization are shown in Figure 57. After 20 h of polymerization of MMA, the active species were still alive, and could continue polymerizing ε-caprolactone. However, the second batch polymerization did not occurred on the existing polymer chains. It seemed that new active centers were generated and the polymerization took place on these new active centers. This observation is similar to the sequential monomer-addition experiments of System 1 with long time intevals in 3.2.2.3.1, which again showed that the active species had a long living span, because of the continuous regeneration of the new active centers. The regeneration of new active centers was so slow compared with the polymerization rate,

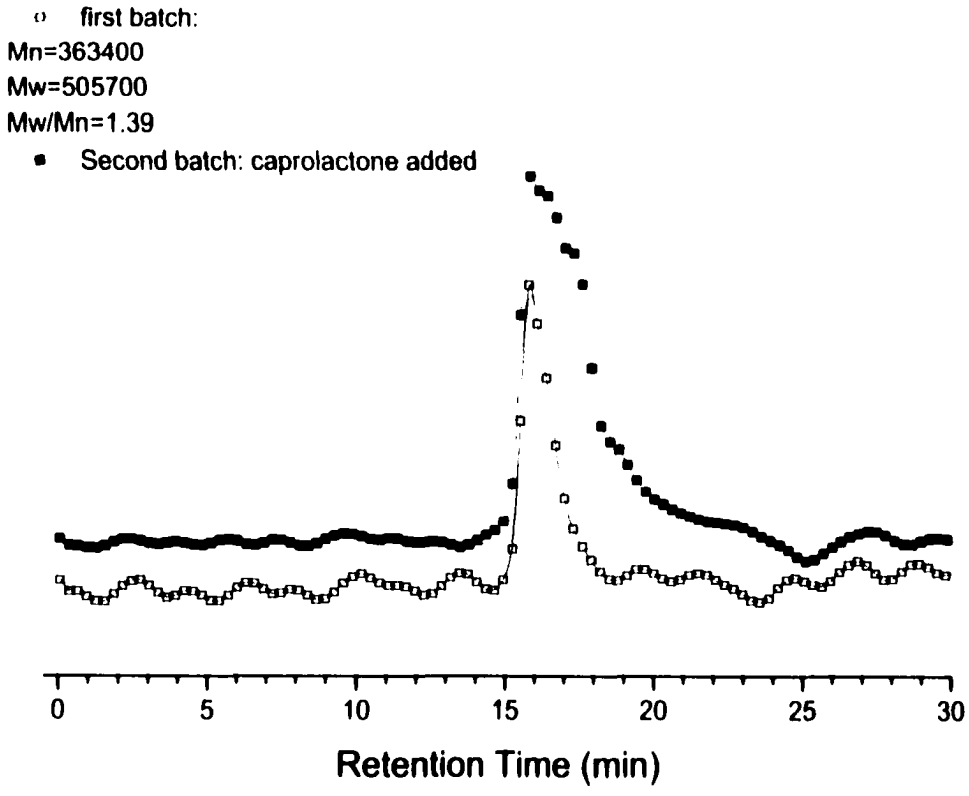

Figure 57. Copolymerization of MMA with ε-caprolactone by 1:1 ratio of **1**/$B(C_6F_5)_3$

therefore, relative narrow ($\bar{M}_w/\bar{M}_n \leq 1.4$) PMMA and poly(ε-caprolactone) could be obtained.

3.4.2.3 MMA and 1-Pentene

Copolymerization of an α-olefin with MMA was studied. 1-Pentene was chosen as the representative α-olefin since it is the smallest α-olefin that is in the liquid state at room temperature, and it can be used in the present experimental equipment without using gas phase reaction apparatus, also the smaller the α-olefin, the higher the activity will be obtained using the dimethyl zirconocene/$B(C_6F_5)_3$ initiation system.[1-5]

To get the polymerization of both monomers, the methods of mixing monomers with the initiation systems are important. It was found that when the 1-pentene and MMA were first mixed and then the initiation system (System 2) was charged to these comonomers, polymerization of MMA started and continued until quantitative conversion was reached with the same polymerization rate as that without 1-pentene present (Figure 58). This result showed that in the competition of coordination to the active centers, MMA was much more favorable than 1-pentene, quite likely because MMA coordinated with the cationic active center using a lone-pair on oxygen. After the complete polymerization of MMA, no polymerization of 1-pentene started (in 16 min). Another equivalent of $B(C_6F_5)_3$ was then added to the reaction mixture to bring the virtual ratio of **2**/$B(C_6F_5)_3$ from 2:1 to 1:1. There was still no polymerization of 1-pentene in the next 10 h. Therefore, mixing comonomers together can not produce the copolymer by **2**/$B(C_6F_5)_3$ initiation system, which implies that the random copolymer can not be produced by this kind of initiation system.

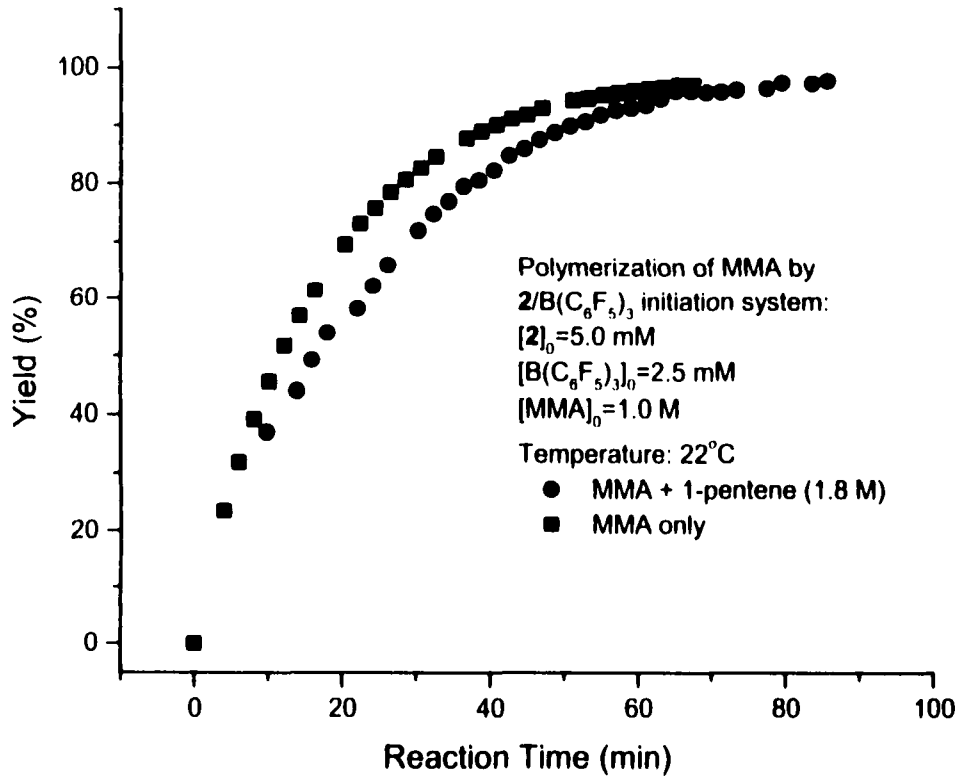

Figure 58. Polymerization of MMA with 1-pentene present comparing with homopolymerization of MMA.

Another method of mixing the comonomer with the initiation system was to first add **2** to 1-pentene followed by $B(C_6F_5)_3$ in a 2:1 ratio of **2**/$B(C_6F_5)_3$. Polymerization of 1-pentene occurred fast. The NMR tube containing the above reaction mixture became warm and the polymerization finished in 3 min, as was shown by the disappearance of the vinyl signals in of 1-pentene (Figure 59). The small signal at about 4.8 ppm was probably the vinyl end group in the poly(1-pentene) chain. After the complete polymerization of 1-pentene, MMA was added to the reaction vessel. Polymerization of MMA occurred soon, and progressed with almost the same polymerization rate as that of homopolymerization of MMA using the same experimental conditions (Figure 60). The reaction mixture separated into two layers, with the bottom layer yellow in color and the top layer lighter yellow in color. The GPC traces of the poly(1-pentene) from the first batch polymerization and the final polymers from both layers after the complete polymerization of MMA are shown in Figure 61. The top layer of the final reaction mixture contained the two homopolymers of PMMA and poly(1-pentene). The bottom layer, however, contained a polymer that was very likely the copolymer of MMA and 1-pentene, the GPC trace of which shows no signal of poly(1-pentene) and a higher molecular weight than the homopolymer of MMA obtained in the top layer. The results indicate that the **2**/$B(C_6F_5)_3$ initiation system with a molar ratio of 2:1 is an active system that can copolymerize polar monomers with olefins. However, due to the low activity to the polymerization of 1-pentene from this initiation system, the copolymerization results were not magnificent, only a little increase of molecular weight of copolymer comparing with homopolymer was obtained. Further copolymerization study is worth doing. To make the future results more impressive, it is suggested that ethylene or propylene be chosen as the olefin

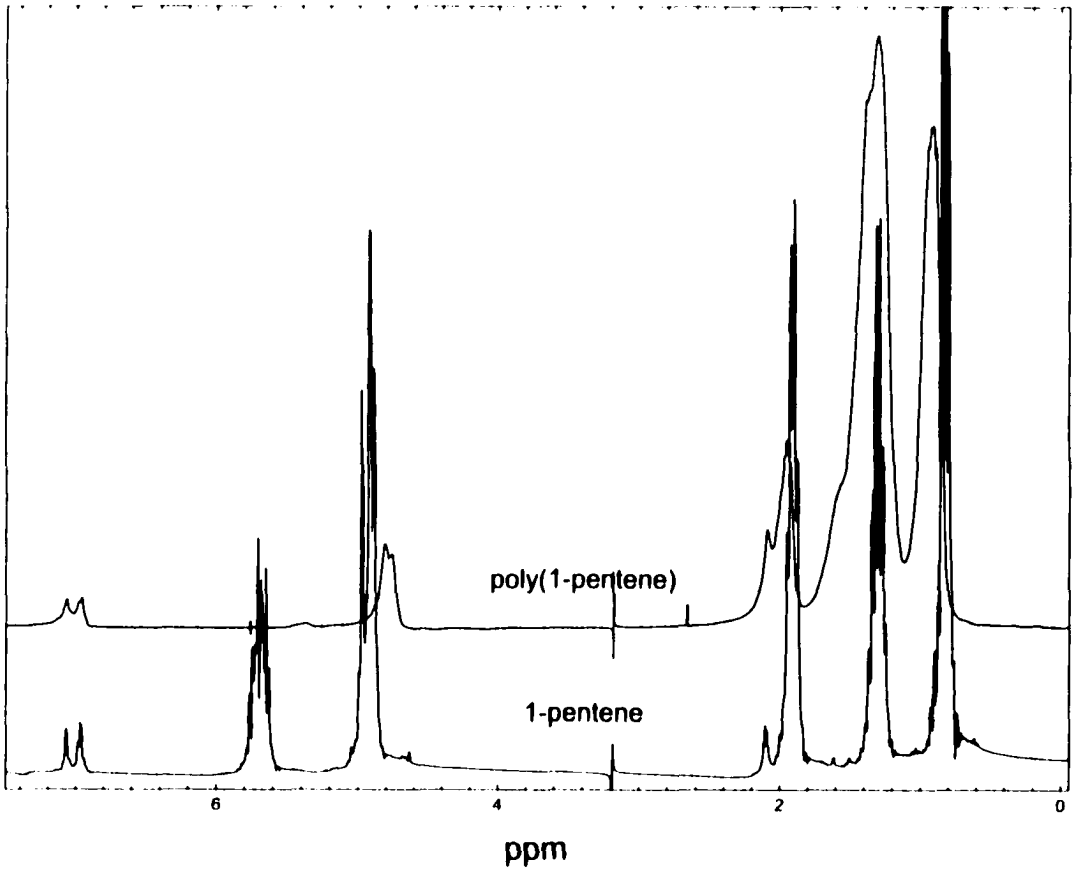

Figure 59. Polymerization of 1-pentene with **2**/$B(C_6F_5)_3$ initiation system.

$[\mathbf{2}]_0$ = 5.0 mM, $[B(C_6F_5)_3]_0$ = 2.5 mM, [1-pentene]$_0$ = 2 M, toluene as solvent, room temperature.

183

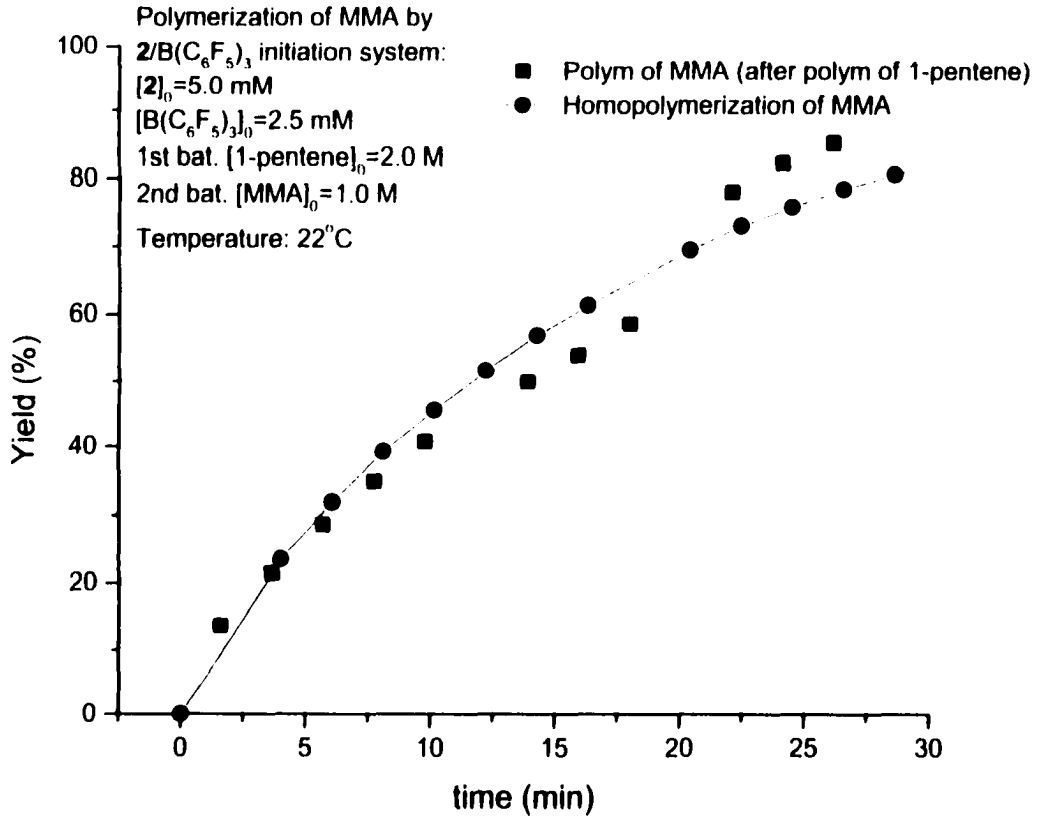

Figure 60. Polymerization of MMA after the polymerization of 1-pentene comparing with homopolymerization of MMA.

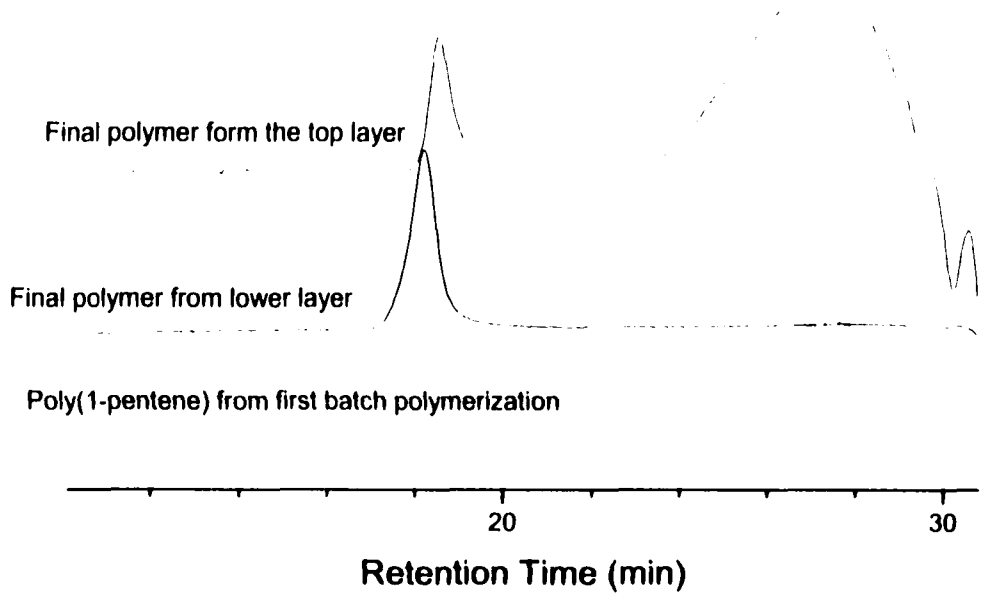

Figure 61 GPC traces of the copolymerization of 1-pentene with MMA.

185

representative, for which the **2**/$B(C_6F_5)_3$ initiation system may have a higher activity and the resulting copolymer may have real industry applications.

4 Summary

A Group 4 metallocene initiation system was discovered for efficient polymerization of methyl methacrylate (MMA). Two methods were used to study this polymerization: gravimetry and ^{1}H NMR. The initiation system consisted of a dimethyl zirconocene as the initiator and $B(C_6F_5)_3$ as the coinitiator. Because of the air sensitivity of the initiators and coinitiator used in the polymerization, proper ways to manipulate them were first studied, these include bench-top inert-atmosphere techniques and glove-box techniques and storage methods. Polymerizations under these carefully controlled manupilations were well reproducible well for both methods.

The parameters that affect the polymerization were then studied. Two representative initiation systems, using Cp_2ZrMe_2 (**1**) or *rac*-$Me_2Si(IndH_4)_2ZrMe_2$ (**2**) as the initiator, were prepared. It was found that the molar ratio of the dimethyl zirconocene to $B(C_6F_5)_3$ was crucial for efficient polymerization. Instead of a slow polymerization (or no polymerization) with a 1:1 molar ratio, a 2:1 molar ratio gave a 20-fold (or more) rate increase and quantitative conversion of MMA to polymer was obtained in less than 1 h. A further increase of the molar ratio did not result in additional acceleration of the polymerization rate. A threshold value of the molar ratio near 2 seemed to exist for both initiation systems. For System 1, in which **1** was used as the initiator, the molar ratio of **1**/$B(C_6F_5)_3$ between 1 and 2 was also studied. For this specific initiation system, the threshold value was found more precisely to be near 1.5. The ratio effect was explained by a two-step equilibration reaction between the initiators and the coinitiator.

The effect of the feeding sequence on polymerization was also studied. In contrast to the reported critical feeding sequence effect on the polymerization with a 1:1 (initiator :

coinitiator) initiation system, the feeding sequence played a less significant role in affecting the polymerization rate for the present 2:1 initiation systems. A fast mixing of three reactants for the polymerization: the initiator, the coinitiator and the monomer, regardless of the order, gave the fastest polymerization rate. An explanation for the difference between the present systems and the reported 1:1 initiation systems was provided with the consideration of the results from the ratio effect's study.

Excess initiator and solvent effects on the polymerization respectively were studied. The excess initiator acted as a scavenger which made it possible to polymerize MMA at a low concentration of $B(C_6F_5)_3$. However, the excess initiator also induced the production of new active centers in the system, which broke the livingness of the polymerization. The polymerization occurred slower in a more polar solvent, which can be ascribed to the competition between MMA and the solvent in coordination with the active center in the polymerization system.

Based on the above results, an optimum method for preparing an active initiation system for the polymerization of polar monomers was found, which included an initiator/coinitiator ratio of 2:1 and rapid mixing of MMA with both initiation components in nonpolar solvents.

After the effective polymerization systems were found, the kinetics, stereochemical control, and living characteristics of them were studied. System 2, in which **2** was used as the initiator, proceeded as a living polymerization. The polymerization continued after the addition of a second batch of monomer, a narrow molecular weight distribution ($\bar{M}_w/\bar{M}_n$ = 1.2) throughout the whole polymerization was obtained, and the $\bar{M}_n$ increased linearly with the monomer conversion in the both first and second batches

polymerizations. Polymer produced by this system was highly isotactic ([rr] ≥ 88%) and the ^{13}C NMR study showed that the chain propagation in System 2 followed an enantiomorphic site-control mechanism. However, for System 1, bimodal GPC traces were obtained for the polymers before quantitative conversion was reached. The two peaks in the bimodal signal moved closer with the increasing of conversion until a monodal distribution was obtained at the full conversion. In addition, the $\bar{M}_n$ decreased at the low conversion of the second batch monomer and the final $\bar{M}_n$ after the second batch polymerization did not increase much from that of the first batch polymerization when initial monomer concentrations for both batches polymerizations were almost the same. All these results showed that the chain termination (or transfer) process existed in System 1 and new active species were generated during the polymerization. Moderately syndiotactic polymer ([rr] = 55%) was obtained and the chain propagation followed neither an enantiomorphic site-control nor a chain-end control mechanism.

The kinetics of these two systems were also different. For System 2, the polymerization rate was in first order to the monomer concentration and second order in the initiation system; while for System 1, the polymerization rate was in zero order to the monomer concentration and third order in the initiation system. A mechanism is proposed to accommodate the experimental kinetic results, in which two path of forming the active center for polymerization was suggested. Primarily due to the steric effect of the two initiators, they picked different paths in forming the active center which led to different kinetics.

Besides the above homopolymerization of MMA by the present initiation systems, preliminary experiments for polymerization of methyl acrylate, 1-hexene, ε-caprolactone,

propylene oxide, vinyl acetate and copolymerization of MMA with ε-caprolactone, and MMA with 1-pentene were also performed. Methyl acrylate, 1-hexene, and ε-caprolactone were all polymerized and copolymerization of MMA with ε-caprolactone, MMA with 1-pentene were obtained as well. Future work of copolymerization of a polar monomer with nonpolar monomer using the initiation systems found in the present work is highly recommended because of these positive results.

5 Appendix

Numerical Solution of Equation (5-1): (Python code)

```
c = 2.5e-3
for k1 in (1e6, 1e5, 1e4, 1e3, 1e2, 1, 1e-2, 1e-2):
  for k2 in (1e6, 1e5, 1e4, 1e3, 1e2, 1, 1e-2, 1e-2):
       print "k1, k2", k1, k2
       print "n,        x"
       for n in (10,9,8,6,5,4,3,2,1):
            for i in range(0,808):
                 x=i*2.5e-5/8
                 y1=x
                 a=k1
                 b=k1*x-k1*c-k1*n*c-1
                 cc=k1*n*c*c-k1*c*x
                 yx=(b*(-1.0)-pow((b*b-a*cc),0.5))/(2*a)
                 y2=k2*(yx-x)*(n*c-x-yx)
                 if (abs(y1-y2)<0.01):
                      print n,'\t',x
                      break
       print "--------------------------------"
```

cc represents C in Equation 5-2, in which only "-" in "±" gives solutions. yx represents y(x) which is derived from Equation 4-1.

6 References

(1) Brintzinger, H. H.; Fischer, D.; Mulhaupt, R.; Rieger, B.; Waymouth, R. M. *Angew. Chem. Int. Ed. Engl.* **1995**, *34*, 1143.

(2) Kaminsky, W. *Macromol. Chem. Phys.* **1996**, *197*, 3907.

(3) Mashima, K.; Nakayama, Y.; Nakamura, A. *Advances in Polymer Science* **1997**, 133, 1.

(4) Kaminsky, W.; Arndt, M. *Advances in Polymer Science* **1997**, *127*, 143.

(5) Olabisi, O.; Atiqullah, M.;Kaminsky, W. *J. M. S. –Rev. Macromol. Chem. Phys.* **1997**, *C37*, 519.

(6) "Metallocenes, Synthesis, Reactivity, Applications", Ed. Togni, A; Halterman, R. L., Wiley-VCH, **1998**.

(7) Yasuda, H.; Ihara, E. *Adv. Polym. Sci.* **1997**, *133*, 53

(8) Chen, E. Y.; Marks, T. J. *Chem. Rev.* **2000**, *100*, 1391.

(9) Luo, L.; Marks, T. J. *Topics in Catalysis* **1999**, *7*, 97.

(10) Massey, A. G.; Park, A. J. J. *Organomet. Chem.* **1964**, *2*, 245.

(11) Yang, X.; Stern, C. L.; Marks, T. J. *J. Am. Chem. Soc.* **1991**, *113*, 3623.

(12) Sinn, H.; Kaminsky, W.; Vollmer, H. J.; Woldt, R. *Angew. Chem. Int. Ed. Engl.* **1980**, *19*, 390.

(13) Tullo, A. H. *C&EN* **2001**, *79(43)*, 35.

(14) Grubbs, R. H.; Coates, G. W. *Acc. Chem. Res* **1996**, *29*, 85

(15) Soga, K.; Deng, H.; Shiono, T. *Macromolecules* **1994**, *27*, 7938.

(16) Deng, H.; Shiono, T.; Soga, K. *Macromolecules* **1995**, *28*, 3607.

(17) Chen, Y.; Metz, M. V.; Li, L.; Stern, C. L.; Marks, T. J. *J. Am. Chem. Soc.* **1998**, *120*, 6287.

(18) Stehling, U. M.; Stein, K. M.; Kesti, M. R.; Waymouth, R. M. *Macromolecules* **1998**, *31*, 2019.

(19) Stehling, U. M.; Stein, K. M.; Fischer, D.; Waymouth, R. M. *Macromolecules* **1999**, *32*, 14.

(20) Aaltonen, P.; Lofgren, B.; Seppala, J. *Macromolecule*, **1995**, *28*, 5353.

(21) Aaltonen, P.; Fink, G.; Lofgren, B.; Seppala, J. *Macromolecule*, **1996**, *29*, 5255.

(22) Bruzaud, S.; Cramail, H.; Duvignac, L.; Deffieux, A. *Macromol. Chem. Phys.* **1997**, *198*, 291.

(23) Schneiger, M. J.; Schafer, R.; Mulhaupt, R. *Polymer* **1997**, *38*, 2455.

(24) Yasuda, H; Yamamoto, H.; Yokota, K.; Miyake, S.; Nakamura, A. *J. Am. Chem. Soc.* **1992**, *114*, 4908.

(25) Collins, S.; Ward, D. G. *J. Am. Chem. Soc.* **1992**, *114*, 5460.

(26) Yasuda, H.; Yamamoto, H.; Yamoshita, M.; Yokota, K.; Nakamura, A. *Macromolecules*, **1993**, *26*, 7134.

(27) Yasuda, H.; Furo, M.; Yamamoto, H.; Nakamra, A.; Miyake, S.; Kibino, N. *Macromolecules*, **1992**, *25*, 5115.

(28) Collins, S.; Ward, D. G.; Suddaby, K. H. *Macromolecules* ***1994***, *27*, 7222.

(29) Li, Y.; Ward, D. G.; Reddy, S. S.; Collins, S. *Macromolecules* **1997**, *30*, 1875.

(30) Deng, H; Soga, K. *Macromolecules* **1996**, *29*, 1847.

(31) Shiono, T.; Saito, T.; Saegusa, N.; Hagihara, H.; Ikada, T.; Deng, H.; Soga, K. *Macromol. Chem. Phys.* **1998**, *199*, 1573.

(32) Boffa, L. S.; Novak, B. M. *Macromolecules* **1997**, *30*, 3494.

(33) Knjahanski, S. Y.; Elizalde, L.; Cadenas, G.; Bulychev, B. M. *J. Polym. Sci. A: Polym. Chem.* **1998**, *36*, 1599.

(34) Mao, L.; Shen, Q. *J. Polym. Sci. A: Polym. Chem.* **1998**, *36*, 1593.

(35) Jiang, G. J.; Hwu, J. M. *J. Polym. Sci. A: Polym. Chem.* **2000**, *38*, 1184.

(36) Karanikolopoulos, G.; Batis, C.; Pitsikalis, M.; Hadjichristidis, N. *Macromolecules* **2001**, *34*, 4697.

(37) Frauenrath, H.; Keul, H.; Hocker, H. *Macromolecules* **2001**, *34*, 14.

(38) Cameron, P. A., Gibson, V. C.; Graham, A. J. *Macromolecules* **2000**, *33*, 4329

(39) Shriver, D. F.; Drezdzon, M. A. *The Manipulation of Air-sensitive Compounds*, John Wiley & Sons: New York, **1986**.

(40) Samuel, E.; Rausch, M. D. *J. Am. Chem. Soc.* **1973**, *95*, 6263.

(41) Bochmann, M.; Lancaster, S. J.; Hursthouse, M. B.; Abbul Malik, K. M. *Organometallics* **1994**, *13*, 2235.

(42) Webster, O. W.; Hertler, D. Y., Sogah, D. Y.; Farnham, W. B.; RajanBabu, T. V. *J . Am. Chem. Soc.* **1983**, *105*, 5706.

(43) Datye, V. K.; Taylor, P. L. *Macromolecules*, **1984**, *17*, 1415.

(44) Schlaad, H.; Muller, A. H. E. *Macromolecules*, **1998**, *31*, 7127.

(45) For all polymerizations, rate = k_{app} $[MMA]^{r}$, $k_{app} = k\ [B(C_6F_5)_3]_0^{x}\ [initiator]_0^{y}$, since the ratio of initiator/coinitiator = 2:1 was always kept, let $[B(C_6F_5)_3]_0 = c$, then $[initiator]_0 = 2c$, so $k_{app} = k \cdot 2^{y} \cdot c^{x+y}$. The slope of $\ln(k_{app})$ vs. $\ln(c)$ gave the value of x+y, which is referred to as the combined rate order.

(46) Odian, G. Principles *of Polymerization*, 3rd ed; Wiley; New York, **1991**.

(47) Schlaad, H.; Schmitt, B.; Muller, A. H. E.; Jungling, S.; Weiss, H. *Macromolecules* **1998**, *31*, 573.

(48) Boevy, F. A. *Polymer Conformation and Configuration*; Academic Press; New York, **1969**.

(49) Hsieh, H. L.; Quirk, R. P. *Anionic Polymerization: Principles and Practical Applications*; Marcel Dekker; New York, **1996.**

(50) Bochmann, M.; Lancaster, S. J. *Angew. Chem., Int. Ed. Engl.* **1994**, *33*, 1634.

(51) Zhou, J.; Lancaster, J.; Walker, D. A.; Beck, S.; Thornton-Pett, M.; Bochmann, M. *J. Am. Chem. Soc.* **2001**, *123*, 223.

(52) Kesti, M. R.; Coates, G. W., Waymouth, R. M. *J. Am. Chem. Soc.* **1992**, *114*, 9679.